Packet CDMA Communication without Preamble

A Thesis Submitted to the College of

Graduate Studies and Research

In Partial Fulfillment of the Requirements

For the Degree of Master of Science

In the Department of Electrical and Computer Engineering

University of Saskatchewan

Saskatoon, Saskatchewan

By

Md. Sajjad Rahaman

December 2006

Permission to Use

In presenting this thesis in partial fulfilment of the requirements for a Postgraduate degree from the University of Saskatchewan, I agree that the Libraries of this University may make it freely available for inspection. I further agree that permission for copying of this thesis in any manner, in whole or in part, for scholarly purposes may be granted by the professor or professors who supervised my thesis work or, in their absence, by the Head of the Department or the Dean of the College in which my thesis work was done. It is understood that any copying or publication or use of this thesis or parts thereof for financial gain shall not be allowed without my written permission. It is also understood that due recognition shall be given to me and to the University of Saskatchewan in any scholarly use which may be made of any material in my thesis.

Requests for permission to copy or to make other use of material in this thesis in whole or part should be addressed to:

Head of the Department of Electrical and Computer Engineering

University of Saskatchewan

Saskatoon, Saskatchewan, Canada

S7N 5A9

ACKNOWLEDGEMENTS

It is with great admiration that I express my gratitude to Professor David E Dodds. I thank him for his support, belief, and patience throughout the course of my M.Sc. program. His insightful help and guidance has made this work possible.

I extend my appreciation to TRLabs, Saskatoon, SK, University of Saskatchewan and Natural Sciences and Engineering Research Council (NSERC) for financial support. I acknowledge Bruce Tang and Dale Liebrecht for the wonderful technical discussions. I am deeply indebted to my friend, Malaika Hosni, for the technical assistance in writing and personal encouragement and support.

Finally, I thank my parents, Md. Khoda Bux, and Begum Samsunnahar, my brothers, Azad, Imran, Farhan, and my sister, Sabiha, for their endless support throughout my life.

University of Saskatchewan

Packet CDMA Communication without Preamble

Candidate: Md. Sajjad Rahaman

Supervisor: D.E. Dodds

M.Sc. Thesis Submitted to the
College of Graduate Studies and Research
December 2006

ABSTRACT

Code-Division Multiple-Access (CDMA) is one of the leading digital wireless communication methods currently employed throughout the world. Third generation (3G) and future wireless CDMA systems are required to provide services to a large number of users where each user sends data burst only occasionally. The preferred approach is packet based CDMA so that many users share the same physical channel simultaneously. In CDMA, each user is assigned a pseudo-random (PN) code sequence. PN codephase synchronization between received signals and a locally generated replica by the receiver is one of the fundamental requirements for successful implementation of any CDMA technique. The customary approach is to start each CDMA packet with a synchronization preamble which consists of PN code without data modulation. Packets with preambles impose overheads for communications in CDMA systems especially for short packets such as mouse-clicks or ATM packets of a few hundred bits. Thus, it becomes desirable

to perform PN codephase synchronization using the information-bearing signal without a preamble.

This work uses a segmented matched filter (SMF) which is capable of acquiring PN codephase in the presence of data modulation. Hence the preamble can be eliminated, reducing the system overhead. Filter segmentation is also shown to increase the tolerance to Doppler shift and local carrier frequency offset.

Computer simulations in MATLAB® were carried out to determine various performance measures of the acquisition system. Substantial improvement in probability of correct codephase detection in the presence of multiple-access interference and data modulation is obtained by accumulating matched filter samples over several code cycles prior to making the codephase decision. Correct detection probabilities exceeding 99% are indicated from simulations with 25 co-users and 10 kHz Doppler shift by accumulating five or more PN code cycles, using maximum selection detection criterion. Analysis and simulation also shows that cyclic accumulation can improve packet throughput by 50% and by as much as 100% under conditions of high offered traffic and Doppler shift for both fixed capacity and infinite capacity systems.

TABLE OF CONTENTS

page

LIST OF TABLES

LIST OF FIGURES

Figure page

LIST OF ABBREVIATIONS

2G	Second Generation of Mobile Communication Systems
3G	Third Generation of Mobile Communication Systems
A/D	Analog to Digital Converter
ASIC	Application-Specific Integrated Circuit
AWGN	Additive White Gaussian Noise
BPF	Bandpass Filter
CDMA	Code-Division Multiple-Access
CMF	Chip Matched Filter
CMOS	Complementary metal-Oxide Semiconductor
DS-SS	Direct-Sequence Spread-Spectrum
FDMA	Frequency Division Multiple Access
FH	Frequency Hopping
GPRS	General Packet Radio system
GSM	Global System for Mobile Communications
IC	Integrated Circuit
IS-95	Interim Standard - 95
LFSR	Linear Feedback Shift Registers
MAI	Multiple-Access Interfernce
ML	Maximum length
MOS	Metal Oxide Semiconductor
PDF	Probability Density Function
P_d	Probability of Correct Codephase Detection
P_f	Probability of False Alarm
PN	Pseudo-noise
PSD	Power Spectral Density
QoS	Quality of Service
SDMA	Space Division Multiple Access

SMF	Segmented Matched Filter
SNR	Signal to Noise Ration
SG	Spreading Gain
TDMA	Time Division Multiple Access
TMF	Transversal Matched Filter
TRLabs	Telecommunications Research Laboratories
XOR	Exclusive OR
WCDMA	Wideband CDMA

1. Introduction

Wireless communication systems are an emerging technology with the potential of high speed and high quality information exchange. Ubiquitous access to information at any time, at any place is the goal of this technology in the 21st century. Spread spectrum is one of the enabling technologies that have achieved explosive growth. The second generation (2G) digital cellular Code-Division Multiple-Access (CDMA) standard and the third generation (3G) or Wideband CDMA are based on spread spectrum technology. CDMA has the advantages of frequency diversity, anti-jamming, immunity to eavesdropping, soft handoff between cells, and simpler frequency management [1].

Second generation (2G) systems use circuit-switched CDMA whereas third generation (3G) CDMA are packet-switched. Packet switching offers more bandwidth sharing efficiency than its circuit-switched counterpart. Circuit-switched CDMA requires dedicated resources from the system regardless of whether connection between the transmitters and the receivers are maintained or not. Thus, it is not possible to achieve full utilization of system resources with circuit-switched CDMA. Packet switching does not require dedicated physical connection. Information is transferred in packets with all connection sharing a common channel. Whenever a transmitter is not sending packets, other transmitters can access the channel. As a result, packet-switched CDMA achieves higher utilization efficiency. Due to the high utilization efficiency, packet switched CDMA has been chosen as candidate for 3G systems [2]. The wireless CDMA channel is considered throughout this thesis.

1.1 Research Objective

In a CDMA system, pseudo-random (PN) codephase synchronization must be acquired prior to data bit demodulation. In order to deliver a packet in a shared communication channel, each packet carries some overhead. This overhead consists of synchronization data bits. In CDMA, the packets use a preamble for codephase synchronization. This preamble consists of a sequence of a spreading code sequence or pseudorandom (PN) code which is known at the receiver.

The required preamble that precedes the data portion of the packet increases excessive overhead. This reduces the channel transmission efficiency for packets. A simplified packet format is shown in Figure 1.1. Here, P, D, and L represent preamble, data and overall packet length. Transmission efficiency for a fixed length packet is given by [3]

$$\text{Transmission Efficiency} = \frac{D}{L} = \frac{L-P}{L} \tag{1.1}$$

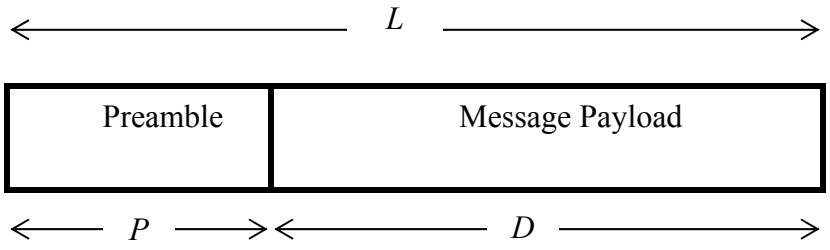

Figure 1.1 A simple packet Format

For a packet CDMA communication, the code sequence used in the preamble continues until the end of the packet because the same code sequence is used to spread the data contained in the message payload. Therefore, useful information for acquisition

is available both in the preamble and in the message payload. The only difference between these codes is that code in the preamble is unmodulated whereas code in the message payload is modulated by the data.

Code phase acquisition in the presence of data modulation would eliminate the necessity of the preamble at the beginning of a packet. Therefore, packet CDMA communication without preambles is possible and 100% efficient transmission is attainable.

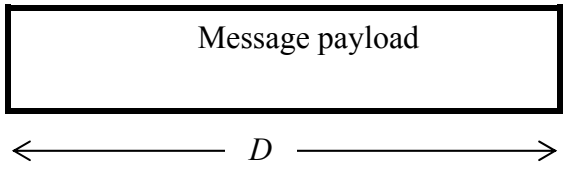

Figure 1.2 A packet format without preamble

This thesis analyzes a segmented matched filter (SMF) acquisition system for packet CDMA systems [4]. The receiver stores the initial part of the packet and demodulation begins after code acquisition is achieved. Based on the stored packet, the SMF can accumulate the results of several code cycles and then select the correct codephase based on the maximum likelihood criteria. As soon as codephase acquisition is achieved, de-spreading and demodulation begin, starting with the stored information and continuing with the remainder of the incoming packets.

1.2 Organization of Thesis

The work presented in this thesis is organized as follows:

In Chapter 1, application of packet CDMA is discussed and the objective of the thesis work is discussed.

Chapter 2 presents a brief introduction to Code-Division Multiple-Access (CDMA) systems and the properties of pseudo-random (PN) code sequence used in a CDMA system. Besides, the role of CDMA in a packet communication system is described.

Chapter 3 describes the various basic PN codephase acquisition methods. Special attention is given to matched filter acquisition procedures and implementations.

In Chapter 4, PN code acquisition using a data modulated received signal is discussed. The structure and properties of the segmented matched filter (SMF) are mentioned.

Chapter 5 contains system models and simulation results. Plots of various acquisition parameters such as probability of correct codephase detection, mean code-acquisition time are shown. Besides, acquisition dependent packet throughput performance for packet CDMA systems is also mentioned.

Summary, conclusion, and suggestions for future research work are mentioned in Chapter 6.

2. Code Division Multiple Access Communication Systems

2.1 Multiple Access Technologies

Emergence of new services and the continuous growth in the number of users have begun to change the design of wireless communication networks. Integration of services, high throughput, and flexibility characterize modern mobile communication systems. To provide these characteristics the available spectrum should be used as efficiently as possible and there should be flexibility in radio resource management [5].

Multiple access (MA) communication refers to a system that enables multiple users to share the same network resources. Telecommunications network resources are usually defined in terms of bandwidth. When more than one user accesses a specific bandwidth, a MA scheme allocates the available bandwidth among multiple users so that everyone can use services provided by the network and to make sure that no single user monopolizes the available resources.

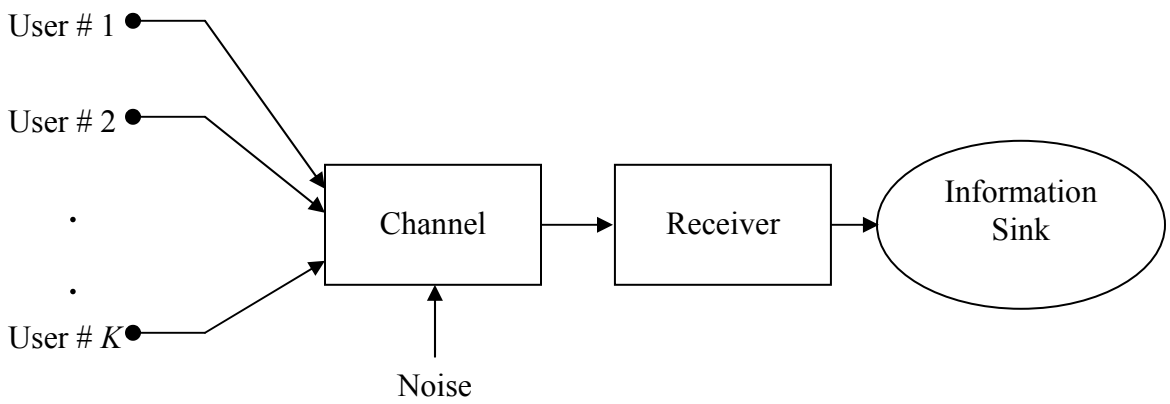

Figure 2.1 Multiple Access Communication System

Four major multiple access techniques are employed to allow users to share bandwidth:

i) Frequency division multiple access (FDMA),

ii) Time division multiple access (TDMA),

iii) Space Division Multiple Access (SDMA),

iv) Code division multiple access (CDMA).

2.1.1 Frequency-Division Multiple-Access

In frequency-division multiple-access (FDMA) communications systems, the available frequency spectrum is divided into a number of small bands. A small portion of total available bandwidth is called a channel and is allocated to a single user. Users of the separate frequency channels can access the system without significant interference from other concurrent users of the system. Stringent radio frequency filtering of the FDMA signal is required to ensure that it remains within its allocated bandwidth. In the absence of filters with ideal cut-off frequency, guard bands are provided in the FDMA spectrum to minimize the adjacent channel interference [1]. Presence of the frequency guard bands imposes additional overhead in the system. This overhead in the FDMA system reduces the amount of bandwidth for information transmissions.

FDMA is applied in applications that require continuous transmissions. It is suitable for analog and limited bandwidth digital applications. In a typical FDMA system, amplifications of several carrier frequencies occur in a single multi-carrier power amplifier. This amplifier has a non-linear response to the received carrier frequencies. Due to this non-linear response of the power amplifier employed in a FDMA system,

intermodulation (IM) distortion happens. IM distortion causes spurious emission or interference to other channels operating in the same frequency range [6].

2.1.2 Time-Division Multiple-Access

In Time-Division Multiple-Access (TDMA) systems, the time axis is partitioned into periodic time-slots and each slot is assigned to a single user to transmit information. TDMA has proven to be an effective way of sharing the available system resources in wireless communication systems. Second-generation (2G) Global System for Mobile Communications (GSM) and the 2.5G General Packet Radio Service (GPRS) use TDMA as their multiple-access scheme [7].

In a TDMA system, the user sends information within successive time slots. Data from a single user always sits in the same time slot position of a frame (Figure 2.2). All information from that portion can be collected and aggregated in the receiver to form the original transmitted information packet.

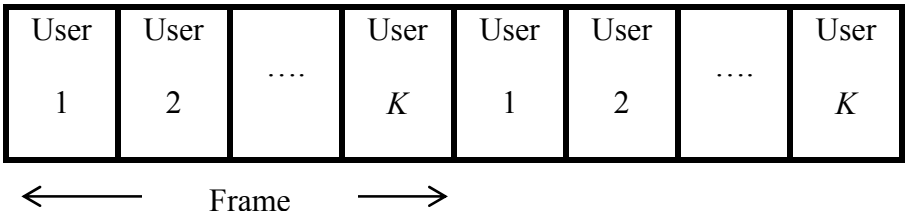

Figure 2.2 TDMA Frame

One of the inherent properties of a TDMA system is strict adherence to timing so as to avoid collision. A TDMA system usually uses guard times between timeslots to allow for small timing errors between different users. Additional overhead is required in TDMA systems for synchronization bits and control information. This has the overall

effect of reducing the time available for the transmission of data and therefore reduces throughput of the TDMA system. Slot synchronization of geographically separated users is a problem.

The number of time slots or channels in a TDMA system is fixed, and a single channel is allocated to a single user for the whole period of information exchange. For real-time and constant-bit-rate voice telephony, a fixed channel or time slot assignment provides good service quality. However, in the case of bursty data transmissions, the fixed channel assignment lacks efficiency in utilizing the spectrum, especially in the case of a large number of users [1][5].

2.1.3 Code-Division Multiple-Access

FDMA and TDMA isolate different transmissions and transform the multi-user access problem into a number of single-user communication links. In a Code-Division Multiple-Access (CDMA) system, each transmission uses all the available bandwidth (Figure 2.3). A CDMA scheme is based on spread spectrum technology to separate the users; so, it is also referred to as Spread-Spectrum Multiple-Access (SSMA) [8]. Spread-spectrum signals have a transmission bandwidth W (Hz) order of magnitude higher than the minimum required bandwidth for the information. If the information symbol rate is R, then we define a bandwidth expansion factor $N = W/R$. So, CDMA is a wideband technology, as compared to FDMA and TDMA which use narrow-band signals.

There are two major types of CDMA systems:

1) Frequency Hopping CDMA (FH-CDMA)

2) Direct sequence CDMA (DS-CDMA).

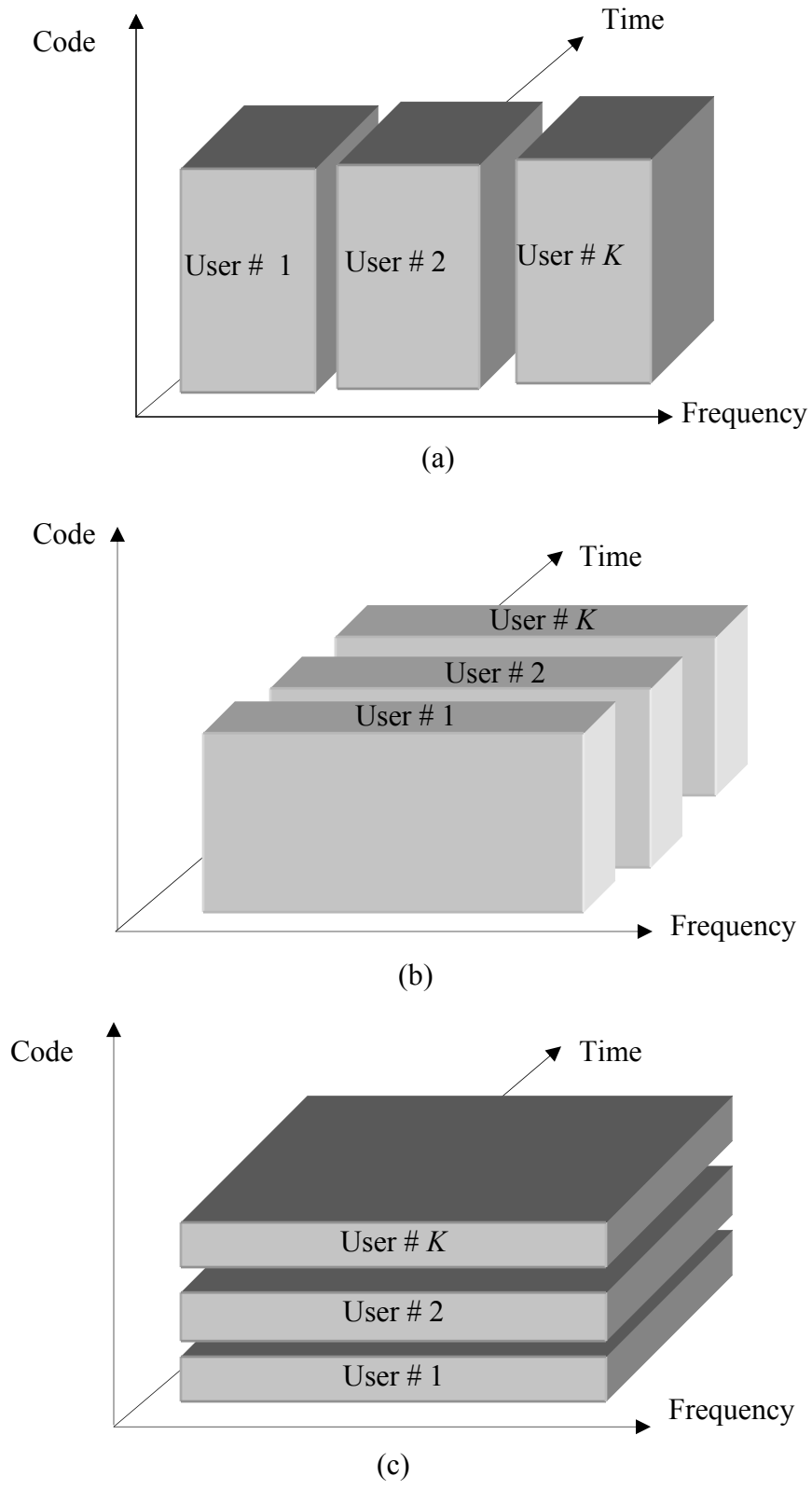

Figure 2.3 Fixed Channel Allocation Strategies: (a) FDMA, (b) TDMA, (c) CDMA

In FH-CDMA, the instantaneous transmission frequency is varied in a pseudo-noise manner (Figure 2.4). The bandwidth at each moment is small, but the total bandwidth over which the carrier frequency varies is large. Bluetooth which is used for short-range robust communication uses frequency hopping-CDMA [9].

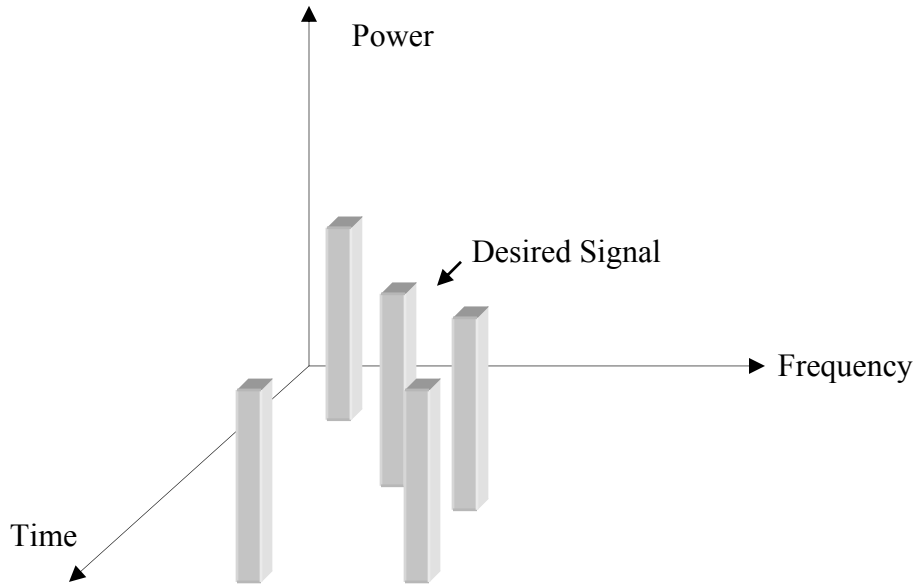

Figure 2.4 FH-CDMA system

Direct sequence-CDMA (DS-CDMA) spreads users' narrowband signals into a much wider spectrum using a high clock (chip) rate signal (spreading sequence) at the transmitter. These spreading sequences are usually a pseudo-noise (PN) code sequence. Due to the nearly orthogonal properties of these sequences, it is possible to accommodate multiple users' information on the same frequency spectrum. Detecting the desired signal at the receiver side is possible when the correct PN sequence and the code phase of that are known to the receiver. Co-user signals are seen as background noise. So, as long as the multiple-user interference is less than a threshold value, it is possible to de-spread the desired signal by using the spreading code used to spread the signal at the transmitter.

Binary DS-CDMA systems employ signals of the form [10]

$$s(t) = \sqrt{2P}d(t)c(t)\cos\omega_0 t \tag{2.1}$$

where P is the average power, $d(t)$ is a binary baseband data signal and $c(t)$ is a baseband spectral-spreading signal, ω_0 is the carrier frequency. The bandwidth of $c(t)$ is much larger than the bandwidth of $d(t)$. For this work, the basic pulse shape is assumed to be rectangular for both $c(t)$ and $d(t)$.

The data signal $d(t)$ consists of a sequence of positive and negative rectangular pulses, so it can be written as

$$d(t) = \sum_{n=-\infty}^{\infty} d_n p_T(t - nT_b) \tag{2.2}$$

where $P_T(t)$ is the rectangular pulse of duration T_b, $\sum_n$ denotes the sum over all integers n that correspond to elements in the data sequence

$$(d_n) = ..., d_{-1}, d_0, d_1, d_2, ... \tag{2.3}$$

The data symbol is a binary digit, either +1 or -1, depending on the data symbols to be sent in the n^{th} time interval and it is assumed that each of which takes the value +1 and -1 with probability 0.5.

The PN sequence consists of a sequence of positive and negative rectangular pulses. Each pulse in the PN sequence is called a chip. If the rectangular chip waveform is denoted by $\psi(t)$, the spreading sequence is written as

$$c(t) = \sum_{n=-\infty}^{\infty} c_n \psi(t - nT_c) \tag{2.4}$$

where the chip waveform $\psi(t)$ is assumed to be a time-limited pulse of duration T_c and c_n is the binary spreading code sequence. The sequence c_n is modeled as a random binary

sequence, which consists of statistically independent symbols, each of which takes the value +1 with probability 1/2 and or the value -1 with probability 1/2. c_n represents chips of a PN sequence and it is given by

$$(c_n) = ..., c_{-1}, c_0, c_1, c_2, ... \tag{2.5}$$

It is convenient to normalize the energy content of the chip waveform according to:

$$T_c^{-1} \int_0^{T_c} |\psi(t)|^2 dt = 1. \tag{2.6}$$

The transitions of a data symbol are assumed to coincide with the transition of a chip and the processing gain or the spreading gain is defined as:

$$N_c = \frac{T_b}{T_c} \tag{2.7}$$

where N_c is an integer equal to the number of chips in a data symbol interval.

The two-sided power spectral density (W/Hz) of a data modulated binary phase-shift keyed carrier, $S_d(f)$ and data- and spreading code-modulated carrier, $S_c(f)$ are given by [10]:

$$S_d(f) = \frac{1}{2} P T_b \left\{ \text{sinc}^2[(f - f_0)T_b] + \text{sinc}^2[(f + f_0)T_b] \right\} \tag{2.8}$$

$$S_c(f) = \frac{1}{2} P T_c \left\{ \text{sinc}^2[(f - f_0)T_c] + \text{sinc}^2[(f + f_0)T_c] \right\} \tag{2.9}$$

where f_0 is the carrier frequency. Figure 2.4 illustrates one sided power spectral density both the cases of data-modulated and data- and spreading code modulated carrier. Spectrum for the later case spreads over a longer bandwidth and the peak of the spectrum is reduced by the spreading gain factor.

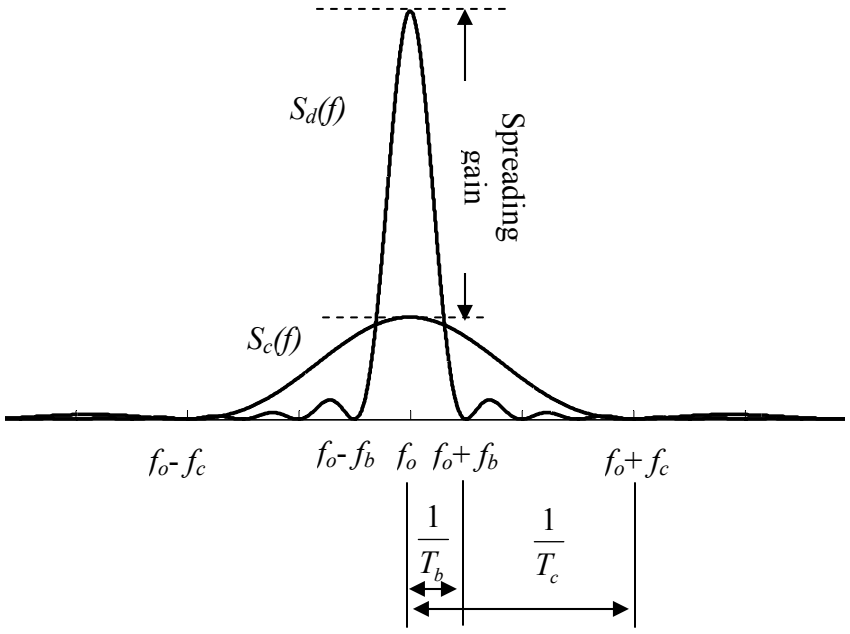

Figure 2.5 Power spectral densities of data-modulated and data- and spreading code modulated carrier signals

2.1.3.1 Transmitter and Receiver Structure in CDMA

Figure 2.6 illustrates the transmitter and the receiver of a basic CDMA system. The total received signal is:

$$r(t) = s(t) + i(t) + n(t) \tag{2.10}$$

where $i(t)$ is the interference and $n(t)$ denotes the zero-mean white Gaussian noise. After code synchronization has been established (i.e. $c_1(t) = c_2(t) = c(t)$) , the input to the demodulator is [11]:

$$r_1(t) = s(t)c(t) + i(t)c(t) + n(t)c(t) \tag{2.11}$$

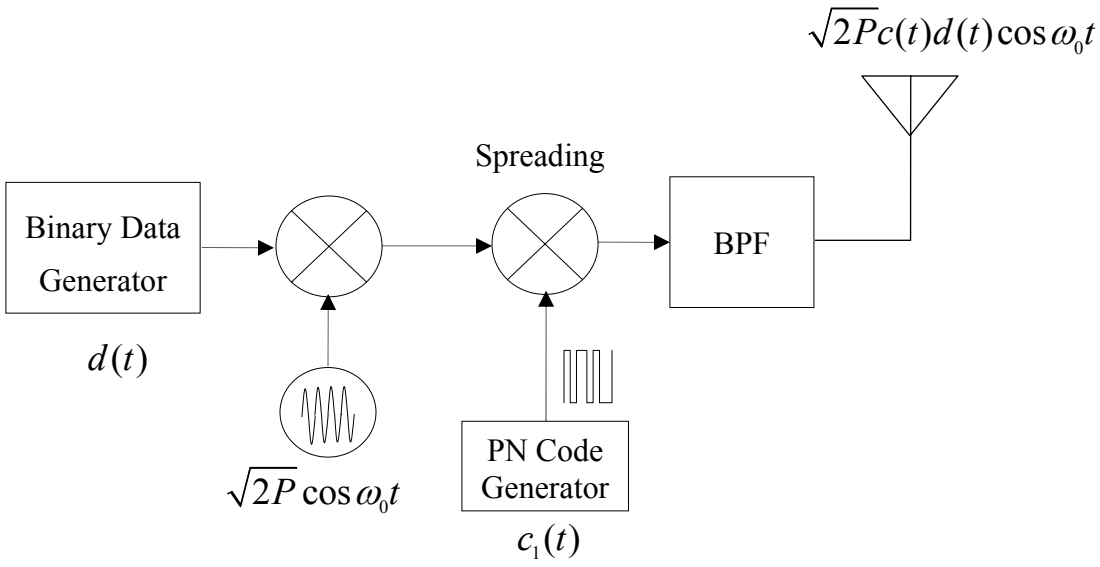

(a)

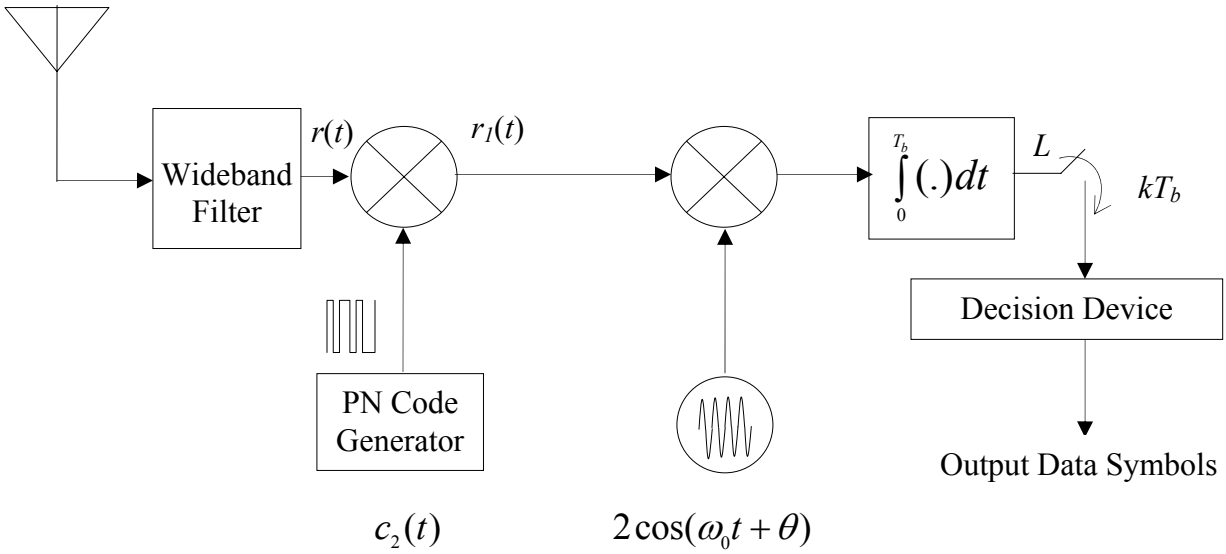

(b)

Figure 2.6 DS-CDMA (a) transmitter and (b) receiver [10]

The factor $c(t)$ in $i(t)c(t)$ ensures that the interference energy is spread over a wide band. The input sample applied to the decision device at the end of the interval T_b is [11]:

$$L = \int_{o}^{T_b} 2r_1(t)\cos[\omega_0 t + \theta]\, dt \tag{2.12}$$

In practice, $T_b >> 1/f_0$, so that integration of the double frequency term is negligible. It has also been assumed that the receiver has acquired both chip and data bit synchronizations. It follows from data bit synchronization, that $d(t)$ is constant over [0, T_b] yielding [11]:

$$L \cong \sqrt{2P}\int_{0}^{T_b} d(t)\sum_{i=0}^{N_c-1}\psi^2(t-iT_b)dt + L_1 + L_2 \tag{2.13}$$

Where

$$L_1 = \int_{0}^{T_b} 2i(t)c(t)\cos[\omega_0 t + \theta]dt \tag{2.14}$$

$$L_2 = \int_{0}^{T_b} 2n(t)c(t)\cos[\omega_0 t + \theta]dt\,. \tag{2.15}$$

where N_c is the number of chips per bit (N_c is equal to the spreading gain). The decision device produces the symbol 1 if $L > 0$ and the symbol -1 if $L < 0$. An error occurs if $L < 0$ when $d(t) = +1$ or if $L > 0$ when $d(t) = -1$.

Since in a CDMA system, adding users only slightly increases the noise, it provides soft capacity: more users can be accommodated at the cost of gracefully reduced Quality-of-Service (QoS). The upper limit for the number of simultaneous users in the system using the same frequency spectrum is determined by the total power of the multi-user interference [12].

In 1995, the first CDMA technology for the second generation wireless communication system, called Interim Standard (IS-95), was commercially launched. CDMA with its proven capacity enhancement over TDMA and FDMA together with other features such as soft capacity (or graceful degradation), multi-path rejection, and the potential use of advanced antenna and receiver structures has been used as the main multiple-access scheme for 3G mobile cellular systems [7].

2.1.3.2 Circuit-Switched CDMA Systems

Circuit-switched CDMA systems are connection oriented. They represent conventional CDMA concepts in which users share the time and frequency resources, but each user is uniquely identified through assigned spreading or signature sequence. This system is characterized by continuous transmissions between the users and the base station.

In theory, users can transmit information using spreading sequences that are orthogonal to each other. In practice, the asynchronous nature of CDMA transmissions (especially in the reverse link) makes the implementation of orthogonal code virtually impossible. As a result of losing orthogonal properties, user transmissions interfere with each other. The performance of a CDMA system is limited by the interference that users create for each other during information transfer. As the interference gets worse, it becomes more difficult for the users to maintain reliable communication. In particular, a strong interference from a portable unit near the base station can destroy the communication link to a more distant portable unit. This effect is known as the near-far

effect [13]. Power control mechanism of the portable devices is employed to eliminate near-far effect. This is further explained in Chapter 5.

2.1.3.3 Packet-Switched CDMA Systems

The circuit-switched CDMA model is convenient for voice communications and even for voice-data systems with long data sessions. However, current third generation (3G) CDMA systems and also the future systems will support more diverse applications. Therefore, systems should have flexible resource sharing. Thus, assigning a dedicated spreading code sequence sequences and keeping a continuous connection even with a lower synchronization rate is a luxury that should be avoided [14].

Packet-switched CDMA is basically a connectionless architecture. In this system, connection is established when the users need to transmit an information packet. Therefore, user recognition and acquisition are needed for every data packet. One of the important features of packet CDMA is that active users are assigned a spreading sequence at the beginning of a call and any one of the system's available spreading sequences can be used to spread the data packet. As a result, the number of potential users is much larger than the number of active users and the number of active users at a given instant of time for a packet CDMA system is comparable to the processing gain of the system [15].

2.1.4 Space-Division Multiple Access

In a space-division multiple access (SDMA) technique (Figure 2.7), the spatial separation of the individual users is exploited to achieve multiple access capability. It uses a smart antenna (i.e. multibeam antenna) technique that employs antenna arrays with

some intelligent signal processing to steer the antenna pattern in the direction of the desired user and places nulls in the direction of the interfering signals. Antenna arrays produce narrow spot beams and, therefore, the frequency can be re-used within the cell provided the spatial separation between the users is sufficient [16]. SDMA systems are suitable for fixed wireless communication systems where the spatial characteristics are relatively stable [17].

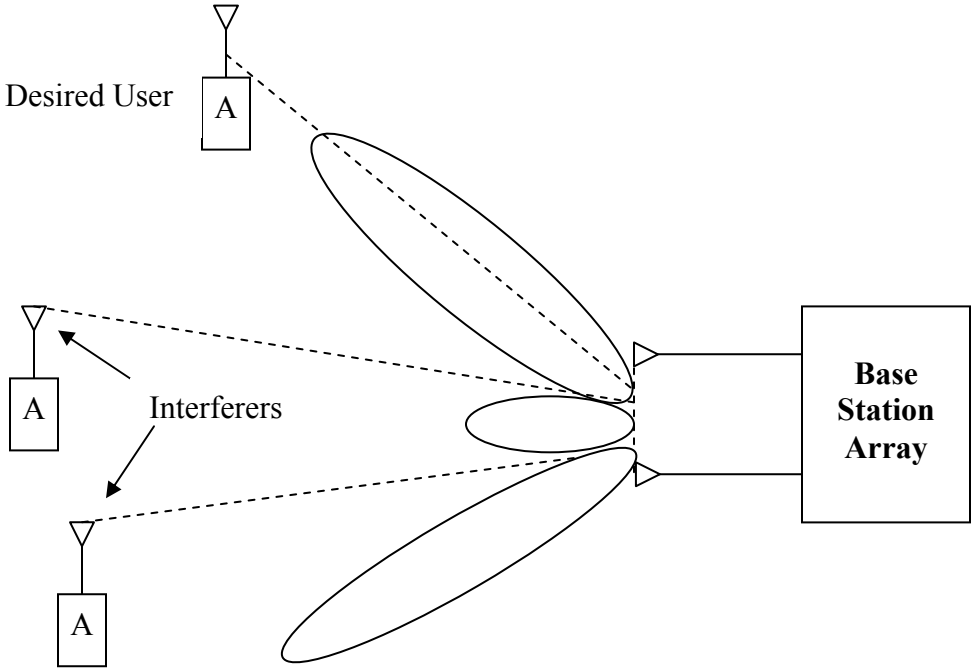

Figure 2.7 SDMA system [16]

2.2 Direct-Sequence Spread Spectrum Spreading Codes

The importance of the code sequence to spread spectrum communication is evident from the fact that type of code, its length, and its chip rate set bounds on the capability of the system [18]. The codes ensure the following two characteristics:

i) The auto-correlation peak must be much greater than the autocorrelation sidelobes and cross-correlation peaks.

ii) The code sequence must be easily generated.

One popular class of codes, suited for DS-CDMA, is maximum length (ML) sequences. ML sequences are the longest pseudo-noise sequences that can be generated by a given shift register or a delay element of a given length. Figure 2.8 shows the structure of the ML linear feedback shift register sequences.

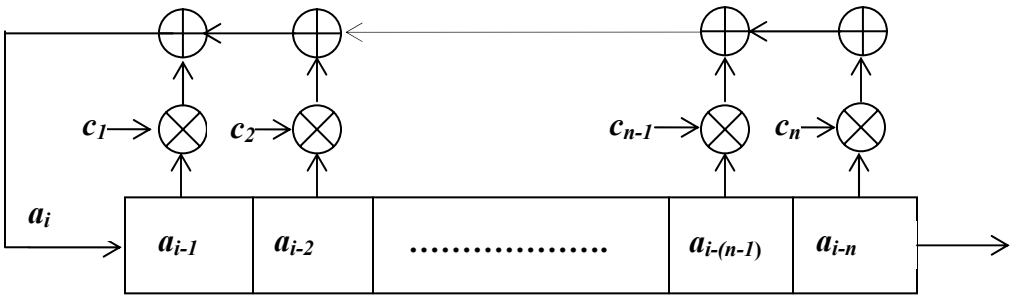

Figure 2.8 ML-Sequence generator structure

The sequence a_i is generated according to the following recursive formula [16]

$$a_i = c_1 a_{i-1} + c_2 a_{i-2} + ... + c_n a_{i-n} = \sum_{k=1}^{n} c_k a_{i-k} \qquad (2.16)$$

where all the terms are binary, and the addition and the multiplication are modulo-2.

ML codes with order n have a period of $N = 2^n$-1. The sequences have the following three important properties in every period of length $N = 2^n$-1:

i) The number of ones and zeros only differs by one.

ii) Half the runs of ones and zeros have a length 1, 1/4 have a length 2, 1/8 length 3, and $1/2^k$ of length k ($k < n$).

iii) Sequence autocorrelation

$$R_c(k) = \sum_{n=1}^{N} a'_n a'_{n+k} \tag{2.17}$$

where $\delta(k)$ is the Kronecker delta function and $a'_n = 1\text{-}2\ a_n$ is the ±1 sequence. When $k = 0$, then Equation 2.19 computes the autocorrelation of the sequence. When $k \neq 0$, then $R_c(k)$ computes crosscorrelation. If the code waveform $p(t)$ is the square wave equivalent of the sequence a'_n with pulse duration T_c, then the autocorrelation value is given by [13]

$$R_c(\tau) \triangleq \begin{cases} N - \dfrac{N+1}{T_c}|\tau|, & |\tau| \le T_c \\ -1, & \text{otherwise} \end{cases} \tag{2.18}$$

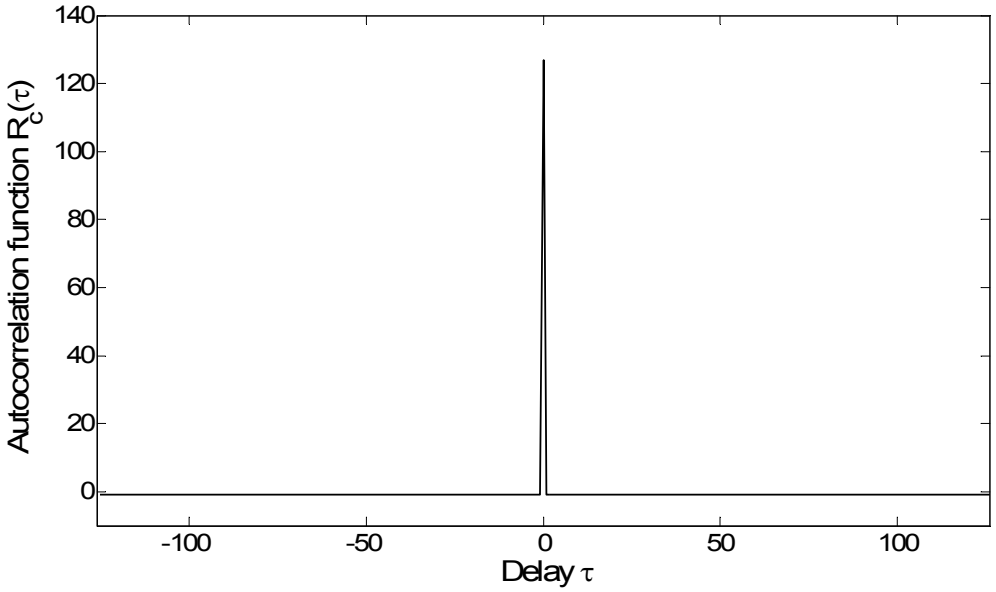

Figure 2.9 Autocorrelation function of a ML sequence of period 127 [16]

ML codes exhibit low crosscorrelation value, -1. Thus ML cross-correlations between two codes are low compared to auto-correlation peak and this feature makes them suitable for DS-CDMA (Figure 2.9). Another advantage of ML codes is their ease of generation, requiring only shift registers and XOR gates. One disadvantage with the

ML codes is that there are very few different ML codes for a given order of codes, thus limiting the number of multiple access users available (Table 2.1).

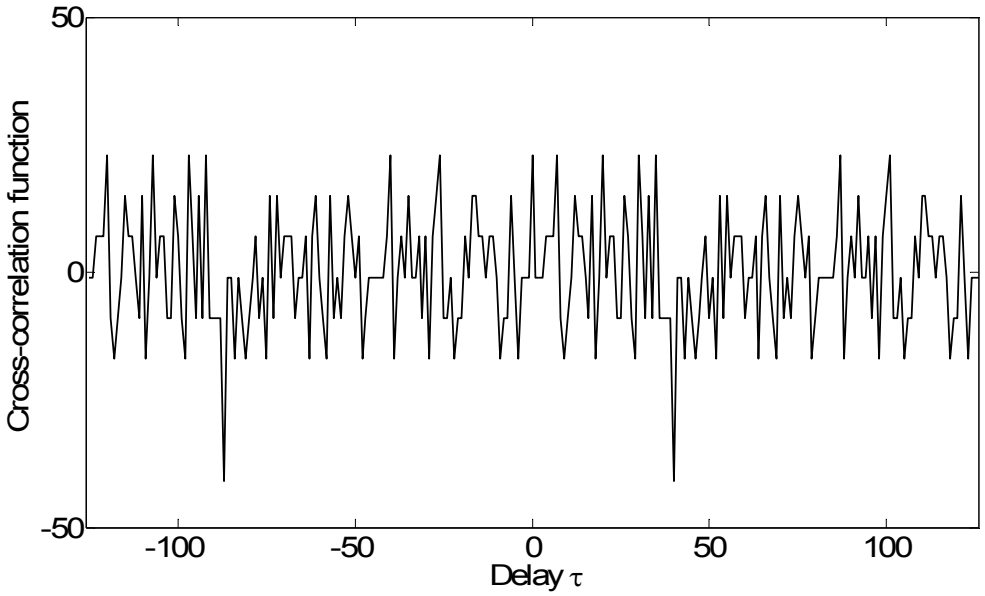

Figure 2.10 Cross-correlation function of a pair of PN sequences period $N = 7$ [16]

Table 2.1 Available number of ML codes for various order of code length

Order, *n*	Period, *N*	Available Codes
2	3	1
3	7	2
4	15	2
5	31	6
6	63	6
7	127	18
8	255	16
9	511	48
10	1023	60

Gold sequences are useful because they supply a large number of codes. The Gold codes are actually XOR combinations of preferred pairs ML codes of the same order. An order n Gold code is developed from two order n ML codes (Figure 2.11). There are 2^n+1 different Gold codes, including the two ML codes, for every preferred pair of ML codes of order n [18].

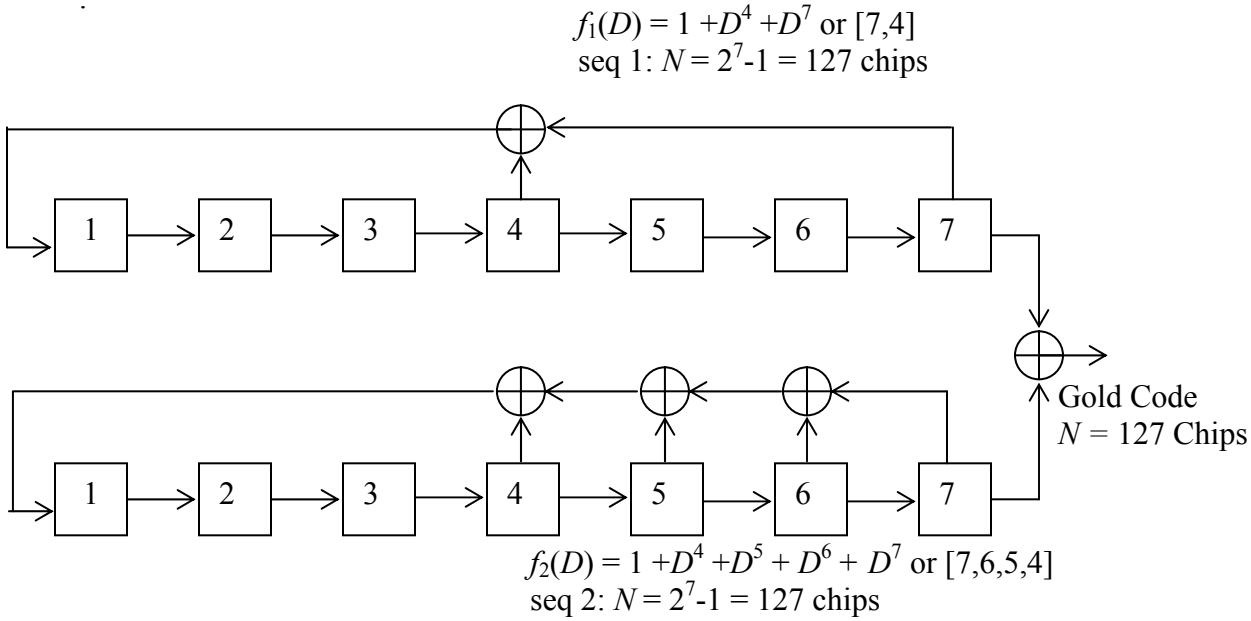

Figure 2.11 Generation of Gold sequence of length 127

Two M-sequences a and a' are called the preferred pair if [18]:

i) $n \neq 0 \pmod 4$; that is, n odd or $n = 2 \pmod 4$.

ii) $a' = a[q]$, where q is odd and either $q=2^k+1$ or $q = 2^{2k}-2^k+1$.

iii) $\gcd(n,k) = \begin{cases} 1 \text{ for } n \text{ odd} \\ 2 \text{ for } n \text{ even} \end{cases}$

The cross-correlation spectrum between a preferred pair is three valued: $-t(n)$, $t(n)-2$, and -1 where (Figure 2.12) [16]

$$t(n) = \begin{cases} 1 + 2^{\frac{n+1}{2}} & \text{for } n \text{ odd} \\ 1 + 2^{\frac{n+2}{2}} & \text{for } n \text{ even} \end{cases} \tag{2.19}$$

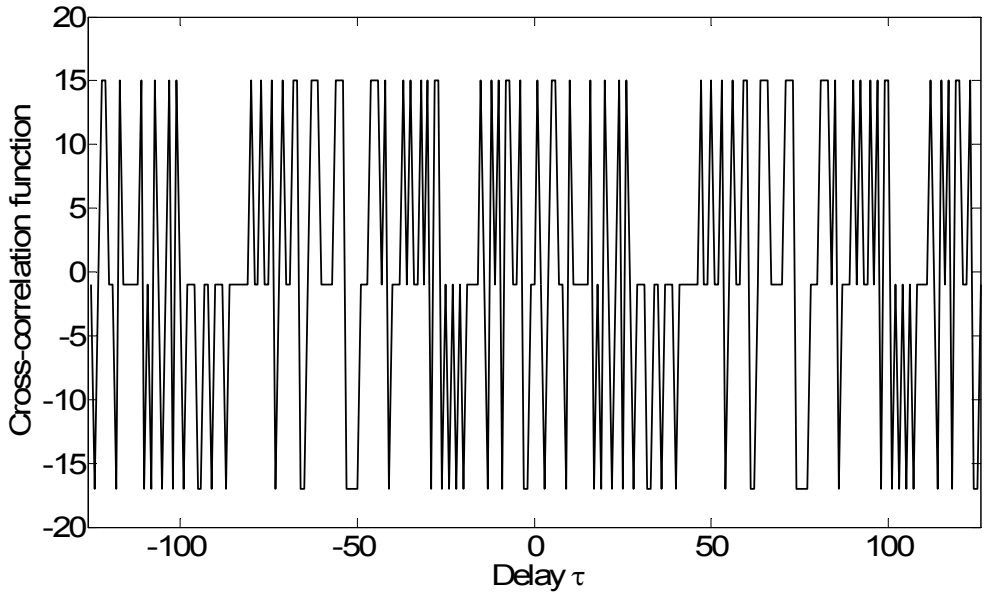

Figure 2.12 Cross-correlation function of a pair of Gold sequence based on the two PN sequences [7, 4] and [7, 6, 5, 4] [16]

2.3 The Role of CDMA in Packet Communications

Several properties of CDMA are exploited in packet communications. These properties are derived from the signal structures used in CDMA systems and from the processing that takes place in the receiver. By the use of CDMA, four desirable characteristics of communication systems are obtained, namely: signal capture effect, multiple access capability, anti-multipath, and narrow-band interference.

When two packets arrive in the receiver at the same time, packets will be considered to have collided. Capture effect refers to the ability of the receiver to

demodulate at least one of the colliding packets (e.g. receiver B in Figure 2.13). If the receiver cannot demodulate more than one packet at a time, then the goal is to provide the capability for the receiver to demodulate one of the overlapping packets. This packet is said to have captured the receiver. Capture is achieved by distinguishing between the packets on the basis of their power levels or arrival times. CDMA techniques with good capture capability significantly improve the throughout performance of a packet communication systems [19].

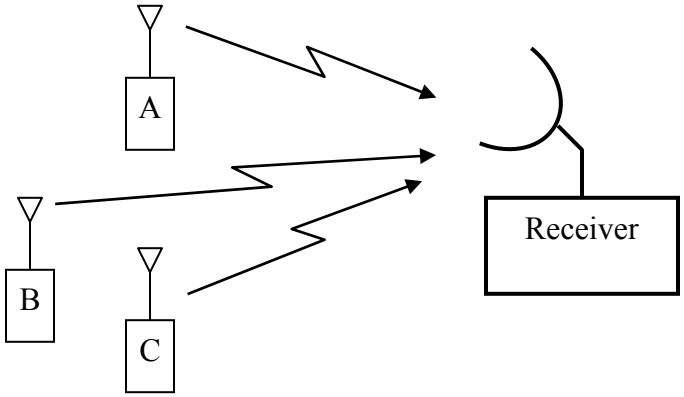

Figure 2.13 Capture effect in packet communication systems

Since CDMA is based on spread-spectrum techniques, the receiver will be able to distinguish between packets received at the same time provided each packet has a unique spreading code sequence and the cross-correlation between these codes is low [19]. This feature is illustrated in Figure 2.14 where the simultaneous transmission of one packet addressed to Receiver 1 and Receiver 2 is illustrated. For Receiver 1, packet from Station A is the desired packet where as packet from Station B is interfering packet.

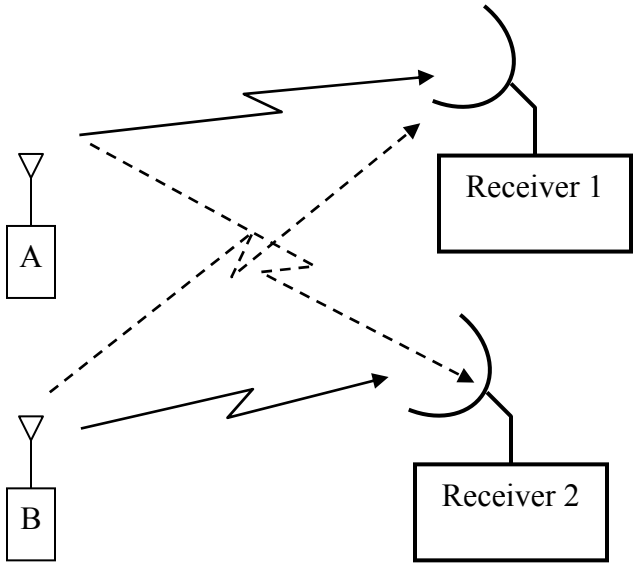

Figure 2.14 Multiple access in packet communication systems

A Rake receiver for CDMA provides improved multipath performance. A RAKE receiver uses several correlators to individually process different received multipath signals [13]. Outputs from different multipaths are combined in–phase to strengthen the received signal. As a result, multi-path signals are constructive in a CDMA system with RAKE receiver rather than being destructive.

Resistance to narrow-band interference is another important desirable characteristic. Hostile jamming or other signals operating in the same frequency band coming from adjacent cells act as an interference. For example, a leaky microwave oven would present narrow band interference. In the case of a narrow band jamming signals within the spread-spectrum bandwidth, the de-spreading action at the receiver spreads the jamming signal. The demodulator input signal will perceive the spread jammer as low power noise as seen in Figure 2.15. Despreading a received signal over a code length of N yields a processing gain of N over the jamming power [8].

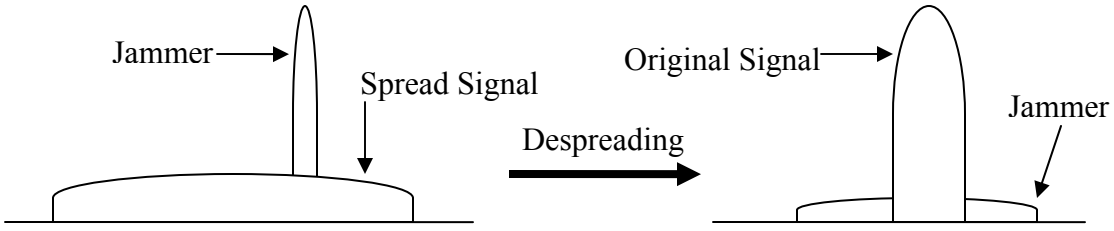

Figure 2.15 Narrow band jamming in CDMA in frequency domain

2.4 Chapter Summary

In this chapter, various multiple-access technologies are described. Transmitter and receiver employed in a CDMA system are illustrated. Both circuit-switched and packet-switched CDMA systems are mentioned. As well, the role of CDMA in packet communications is described.

3. Codephase Synchronization in CDMA Systems

3.1 Introduction

Synchronization plays a very important role in all analog and digital communication systems. It is a pre-requisite for successful transmissions of information between transmitters and receivers. Synchronization process involves estimating one or more parameters from a received signal. In all practical communication system, several levels of synchronization are required: carrier, code, bit, symbol, frame and network [20].

3.2 Codephase Synchronization in CDMA systems

Codephase synchronization is an important aspect in a CDMA system and the performance of codephase synchronization quite often limits the number of interfering co-users in a system [21]. In CDMA systems, PN code is modulated by the data bits before transmission. At the transmitter this PN code must be removed before data can be demodulated. In order for successful demodulation of the data bits, locally generated PN code must be time-synchronized with the received PN code sequence.

Synchronization in a CDMA system is carried out in two steps (Figure 3.1):

i) coarse acquisition,

ii) fine tuning.

In the coarse acquisition process, the locally generated codes are brought into phase with the received code within a fraction of single chip duration. After the codes get roughly aligned, a code tracking operation brings these codes into perfect alignment and maintains synchronism.

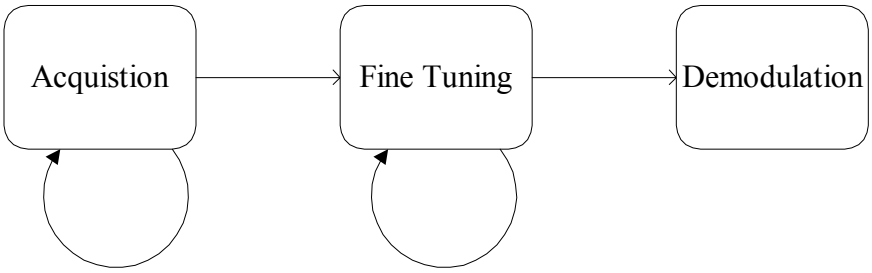

Figure 3.1 Steps of Synchronization in a CDMA system

The formulation of the code acquisition problem can be stated by first defining the transmitted and the received signal of the form

$$s(t) = \sqrt{2P}d(t)c(t)\cos\omega_c t \tag{3.1}$$

$$r(t) = \sqrt{2P}d(t+\delta_b T_b + \delta_c T_c)c(t+\delta_c T_c)\cos[(\omega_c+\omega_d)t+\theta] + n(t) \tag{3.2}$$

where P is the signal power, $c(t)$ is the code sequence or spreading sequence or PN code waveform of period N, $d(t)$ is the data modulation which might or might not be present during the acquisition mode, T_c is the duration of a chip in the spreading code sequence, T_b is the data bit time, ω_c and θ are the carrier frequency and random phase respectively, ω_d is the frequency offset, $n(t)$ is the additive white Gaussian noise with one sided power spectral density N_0 (W/Hz), $\delta_c T_c$ is the received code-phase offset, $\delta_c T_c + \delta_b T_b$ is the received data-bit-phase offset.

The acquisition process finds an estimate $\delta_{est} T_c$ of the unknown time shift $\delta_c Tc$ so that $(\delta_c T_c - \delta_{est} T_c)$ is within the pull-in range of the code tracking loop. Since the spreading

code has a period NT_c, we can assume that $\delta_c \in [0, N)$. Therefore, the signal is said to be acquired if [22]

$$\min\left\{\left|\delta_c - \delta_{est}\right|, N - \left|\delta_c - \delta_{est}\right|\right\} \le \zeta \tag{3.3}$$

where ζ denotes the pull-in range of the code-tracking loop.

3.3 Synchronization in circuit-switched CDMA and packet-switched CDMA systems

Accurate synchronization has to be established regardless of the type of the communication systems. However, circuit-switched and packet-switched communications differ in some aspects. In the packet mode, synchronization must be established at any arbitrary time because the arrival of the data packet is unknown to the receiver. Usually, a training symbols or un-modulated PN codes are at the beginning of the data packets for codephase acquisition purpose. The duration of the training symbols or the preamble is usually short and synchronization should be completed within this duration. This means there is only one chance for synchronizing a received packet. Systems such as IEEE 802.11(a) and HyperLan/2 use a training sequence to achieve synchronization [23]. Effective implementation of packet CDMA becomes difficult on the reverse link (from portable to base) because of the necessity of rapid synchronization of spreading sequences when the transmitter start sending packets after a period of silence [24].

In a circuit-switched CDMA such as the IS-95 standard, there is no stringent requirement on the acquisition time. Timing information is always available in the form of pilot signals. A separate low bit rate physical control channel is provided for the pilot.

This approach creates multiuser interference due to the continuous transmission of the low bit rate channel [25]. For circuit-switched CDMA, synchronization rate is low because once acquisition is done the receivers can start demodulating as continuous transmission of information is maintained.

3.4 Performance Measures in Packet CDMA synchronization

Mean acquisition time (T_{acq}) is widely used as the measure of performance of acquisition schemes. This is defined as the expected time needed to acquire the timing of the spreading waveform or pseudo-random (PN) code. Since communication can only be accomplished after codephase synchronization, T_{acq} should be as short as possible.

The probability of detection (P_d) is the probability that the detector correctly indicates synchronization when the two codes are actually aligned.

The false alarm probability (P_f) is the probability that the detector will falsely indicate synchronization when the two codes are actually nonaligned.

The misacquisition probability (P_m) is the likelihood of the event that the acquisition process cannot acquire the timing of the PN code within a given preamble length. In conventional packet communications, the acquisition must be completed within the preamble of a packet. Otherwise, the packet will be lost. Therefore, this is the key acquisition performance criterion for packet CDMA systems. P_d and P_m are related by the following equation:

$$P_m = 1 - P_d \tag{3.4}$$

Both P_d and P_f have a major impact on acquisition performance. Higher values of P_f increase the mean acquisition time. In the case of misdetection, received packet will

be lost and the lost packet needs to be retransmitted. It is desirable to minimize both the false alarm and the miss probabilities [26].

The preamble is placed at the beginning of a packet for acquisition purpose. It has no contribution once the acquisition is achieved. So, the preamble length should be as short as possible in order to use the communication channel efficiently. On the other hand, it should be long enough to provide high probability of acquisition. For this reason, length of the preamble is another important performance measure [27].

In essence, the objectives of the coarse acquisition for both packet-switched and circuit-switched are as follows:

i) Probability of correct codephase detection is maximized.

ii) Mean acquisition time required for acquisition is minimized.

3.5 Basic approaches and techniques for CDMA codephase synchronization

A codephase refers to each relative position of the PN code. The codephase position in which both the received and the locally generated sequences are in phase is called aligned codephase and the out-of-phase positions are called nonaligned codephases. The uncertainty region for PN codephases is composed of a finite number of codephases which need to be searched for synchronization.

The receiver uses a procedure to determine the position of the locally generated code so that code alignment with the received code is achieved. The testing procedure basically involves correlation between the received and the locally generated codes over a finite duration of time [28].

3.5.1 Detector Structures

The detector plays the fundamental role of detecting the aligned and non-aligned code phases. The received signal $r(t)$ containing the spreading code is correlated with the locally generated version of the same code $c(t)$ in search for the correct codephase. Detector performs the following correlation operation [20]:

$$\int_0^{\tau_d} r(t)c(t-\tau)dt \tag{3.5}$$

where the finite period of time over which correlation is computed is called integration time or dwell time (τ_d).

The correlation between received and local codes can be performed sequentially (active) or concurrently (passive).

In an active correlator (Figure 3.2 (a)), the received signal is multiplied with the locally generated replica of the spreading sequence, and the result is integrated over some observation interval [29]. The multiplication and the integration are performed step-by-step for each codephase. Chip matched filter (CMF) has been shown in the Figure 3.2.

A transversal matched filer (TMF) is utilized in the passive method. The impulse response of the MF is a time reversed and delayed version of the spreading sequence used in the received signal. The MF waits until the code in the received signal obtains the correct codephase, which leads to the name passive [30]. Figure 3.2(b) shows a block diagram of noncoherent correlators employing passive correlating units.

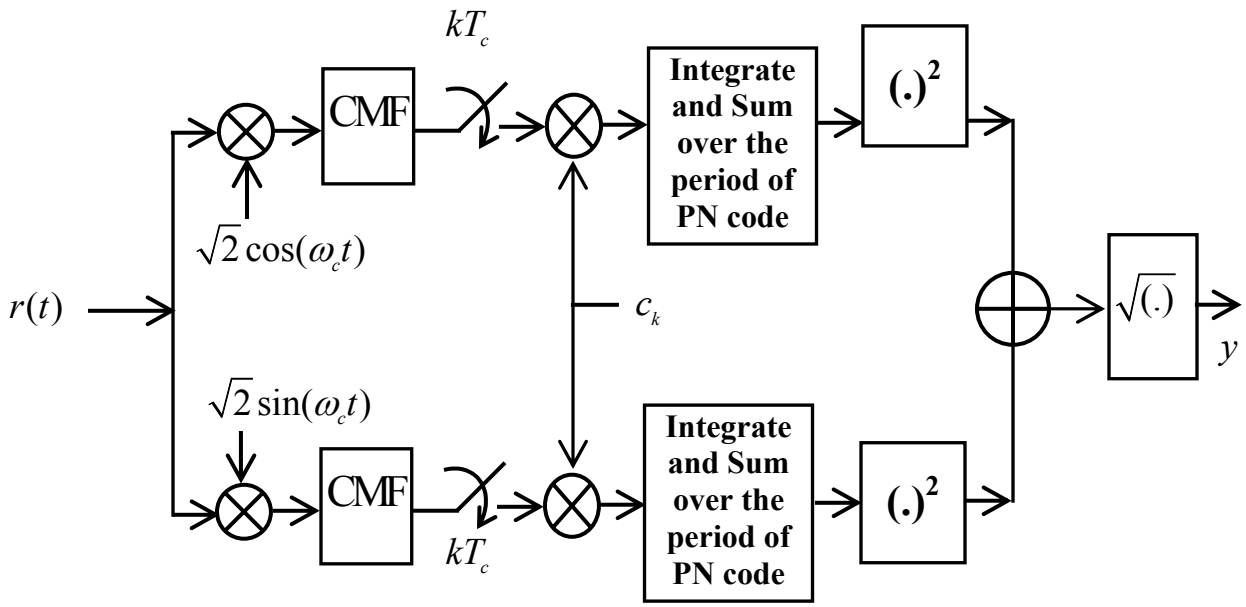

(a)

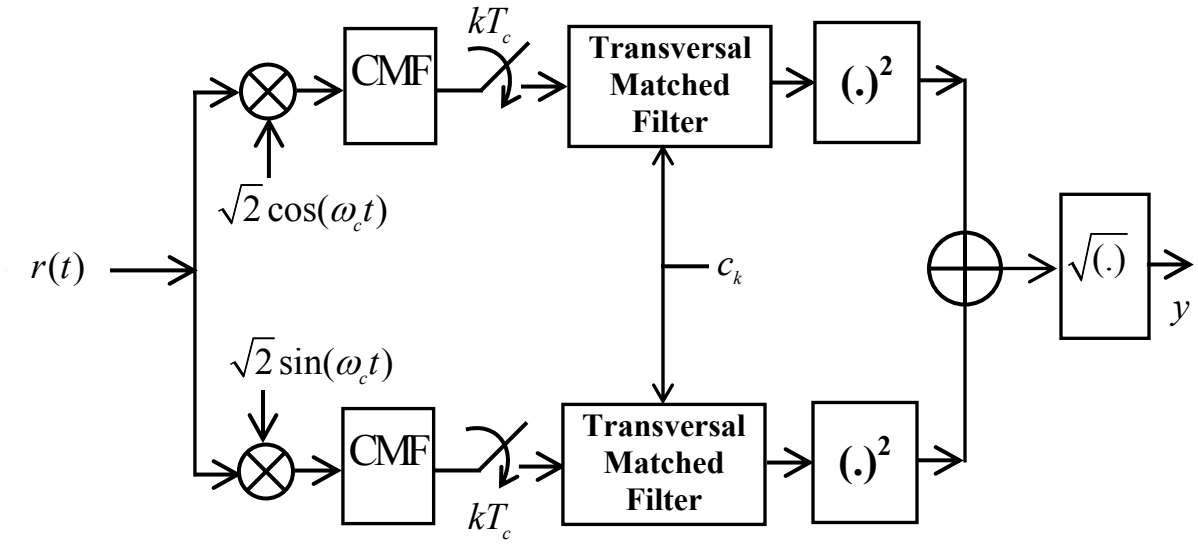

(b)

Figure 3.2 Non-coherent I-Q correlators : (a) active and (b) passive

There exist some practical differences between these two kinds of correlation units. Active correlation of M spreading code chips requires MT_c seconds whereas the same operation with a passive correlation unit requires T_c seconds. So, passive correlator speeds up the acquisition process by a factor of M [30]. But it comes with a cost of complexity. The active correlation is considered as minimum complexity approach where a single and simple correlation unit is employed.

3.5.2 Search Strategies

Two criteria are used in determining codephase synchronization. These are:

i) threshold crossing

ii) maximum likelihood

In the threshold crossing criterion, a test variable obtained from the detector for each codephase is compared to a preselected threshold (V_{Th}) value. If the test variable for a codephase position exceeds the threshold value then it is assumed that codephase acquisition has been achieved. Threshold value is kept at a fixed value in case of a stable channel whereas adaptive threshold scheme is employed for a dynamic channel [20].

Both P_f and P_d depend on the selected threshold value (Figure 3.3). From Figure 3.3 it is evident that if the threshold is set to a high value, P_f will get smaller along with P_d. On the other hand, low value of threshold makes P_f high along with P_d. Average acquisition time depends on the value of signal-to-noise ration (SNR), P_f, and P_d. Therefore, optimum value of threshold is selected to minimize the mean acquisition time [31].

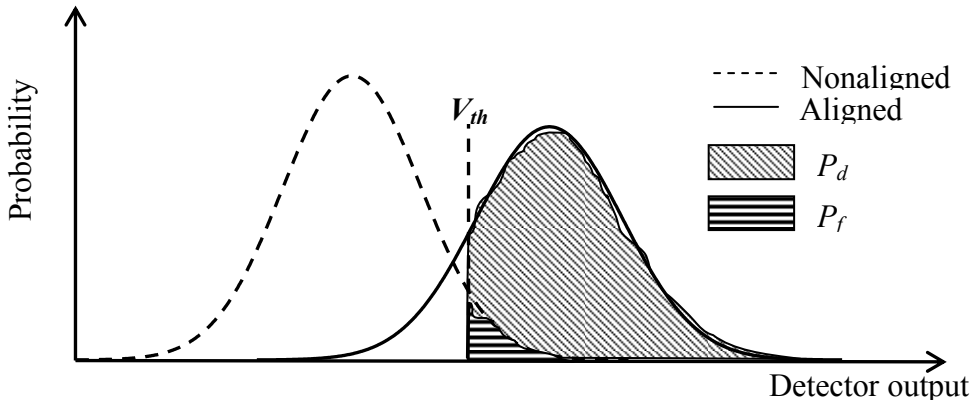

Figure 3.3 Effect of threshold value on P_f and P_d

In a maximum likelihood criterion, test variables for all codephases are compared and codephase associated with maximum value of the test variable is chosen as the aligned codephase. It is known as MAX criterion. Test variables can be obtained either in serial or parallel ways. MAX criterion performs faster acquisition than the threshold crossing method, but it requires more hardware for storing the test variables [30].

Both threshold crossing and MAX criteria can used to form a hybrid criterion. In this case, the entire uncertainty region of codephases is divided into a number of sectors and inside a sector, a codephase is selected according to the MAX criterion. Then, the test variables are compared with a threshold value is search for an aligned codephase [32]. The test variables can be collected in series or parallel or a combination of these two.

Serial search is the most common approach to codephase acquisition. This method uses a single active correlator. The uncertainty region is quantized into a finite number of codephases. Codephase of the local PN code generator is shifted progressively in fixed steps

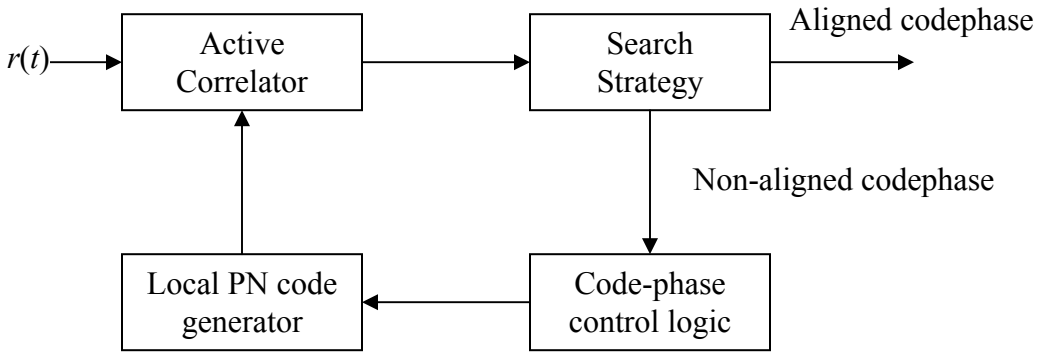

Figure 3.4 Serial search

of length μT_c, where μ =1, or 1/2, or 1/4 , in a serial fashion from an arbitrary initial codephase position [29].

In the absence of *a priori* information about the most likely codephase position, straight-line serial-search code acquisition is employed. In this case, the probability density function (pdf) of the aligned codephase is assumed to be uniformly distributed within the uncertainty region. Straight line serial search acquires the codephase successfully, but it takes long time when if the code period is large.

When the receiver has some *a priori* information about the position of the correct codephase in the uncertainty region, the search procedure can be optimized in accordance with the distribution. A priori information is obtained with the aid of timing references, a short preamble code, or may be calculated from the information obtained from the past successful acquisition [31].

Sometimes, serial search is employed with multiple active correlators in a hybrid search method in order to reduce acquisition time. In this strategy (Figure 3.5), the total uncertainty region of codephases is divided into a number of groups. One group of

codephases is tested at a time in parallel. The codephase with the highest correlation value of the cells is tested against a predefined threshold value. If the highest correlation value is above the threshold, the search will go into verification mode, else if the highest correlation value is not above the threshold, the correct codephase is declared as not being present and the next group of parallel codephases is searched [32].

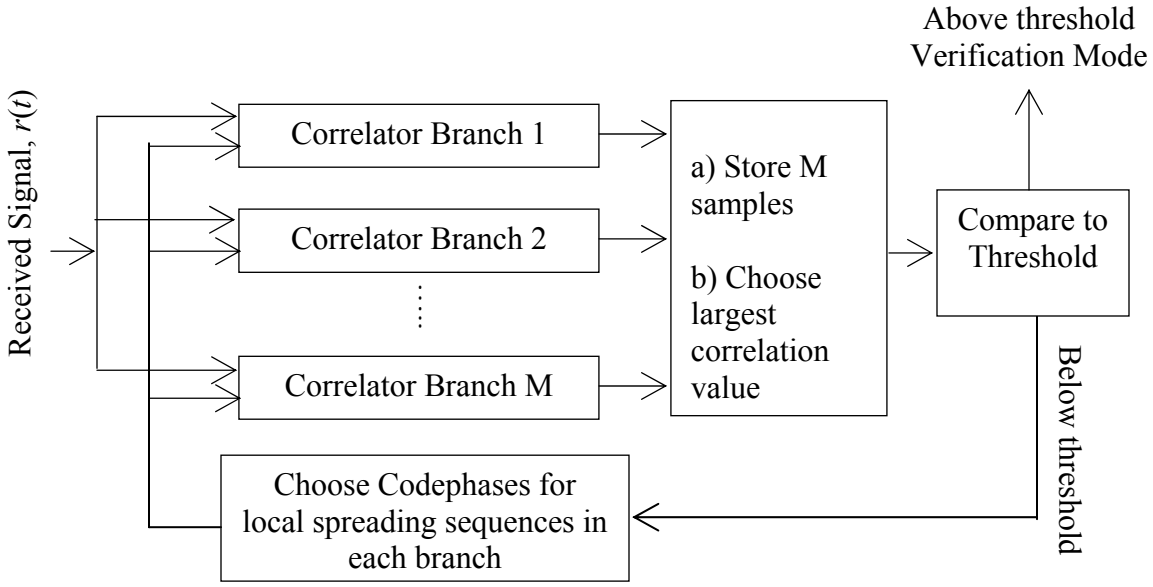

Figure 3.5 Receiver structure of the hybrid acquisition system

Parallel search is the limited case of hybrid search. It uses a large number of correlating elements. In the extreme case, the receiver uses q correlating elements to search the q codephases composing the uncertainty region simultaneously. In terms of performance, parallel code acquisition schemes offer shorter acquisition time at the expense of complexity when compared to simple serial-search technique [33] [34]. Increasing the hardware complexity usually means an increase in the cost of the receiver. Figure 3.6 shows the structure of a parallel coarse acquisition circuitry.

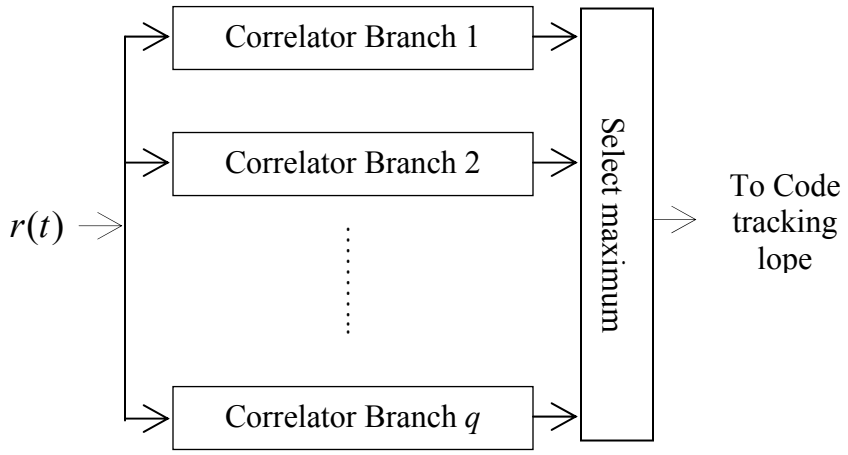

Figure 3.6 Receiver structure of the parallel acquisition system

3.5.2.1 Synchronization using Matched Filters

Matched-filter acquisition is useful when fast acquisition is needed. The filter is matched to one period of the spreading sequence or a fraction of a period, which is usually transmitted without data modulation during acquisition. The output of the matched filter is either led to a threshold detector or the maximum value during a given observation interval is selected, from which decision is made about acquisition. One of the major applications of matched-filter acquisition is for burst or packet communications, which are characterized by short and infrequent communications [35].

In a continuous time matched filter, the input continuously slides past the stationary stored PN waveform until two are in synchronism. At some point matched filter output value exceeds the threshold value and then, the local PN generator will be enabled [35].

In the digital implementation of the matched filter, the content of the shift register which holds the signal samples digitized to one bit and the holding register containing

fixed segment of the code permanently used for the comparison are correlated by comparing them stage by stage, generating a "+1" if the two stages match and a "-1" if they don't match, and summing the resulting set of "1's" and "-1's". It is also possible to digitize the signal samples to 2, 3 or more bit resolution [36].

For an input signal $r(t)$ of duration T_0 seconds, the impulse response $h(t)$ of the matched filter is given by the reverse of $r(t)$ in its T_0 seconds time slots, i.e.,

$$h(t) = \begin{cases} r(T_0 - t); & 0 \le t \le T_0 \\ 0; & \text{otherwise} \end{cases} \tag{3.6}$$

where $r(t)$ corresponds to an M-chip segment of a PN waveform, i.e., $T_0 = MT_c$. Then,

$$r(t) = \sum_{n=1}^{M} c_n p[t - (n-1)T_c] \tag{3.7}$$

where $c_n \in \{-1, +1\}$ and $p(t)$ is the basic chip pulse shape. For a baseband matched filter [35]:

$$p(t) = \begin{cases} 1; & 0 \le t \le T_c \\ 0; & \text{otherwise} \end{cases} \tag{3.8}$$

whereas for a band-pass matched filter [36] ,

$$p(t) = \begin{cases} \sqrt{2}\cos\omega_0 t; & 0 \le t \le T_c \\ 0; & \text{otherwise} \end{cases} \tag{3.9}$$

Matched filter acquisition offers rapid acquisition. Since the correlator output occurs and threshold testing is done at N times the chip rate, the search rate for matched filter $R_M = (N/T_c)(1/N) = 1/T_c$ chip position per second which is a factor NM faster than that of the serial search technique. This improvement is due to the fact that only a new fractional $(1/N)$ chip of received signal is used for each correlation test since prior NM-1 received signal samples are already stored the shift register [37].

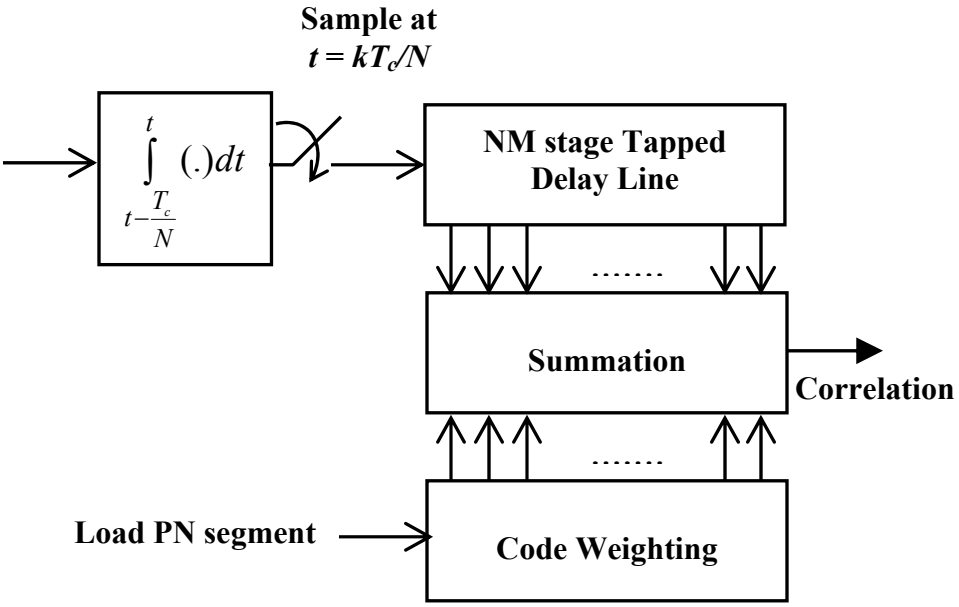

(a)

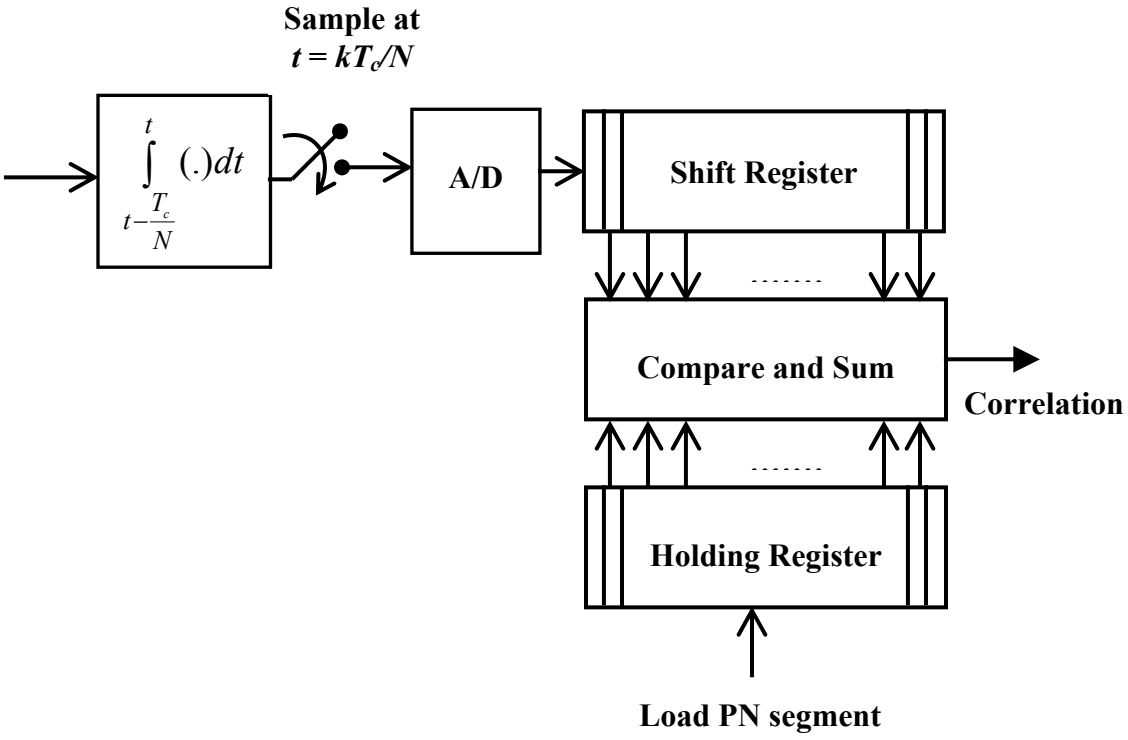

(b)

Figure 3.7 Matched Filter Correlators: (a) Analog (b) Digital [36]

3.6 Synchronization under special conditions

3.6.1 Effects of Frequency Offset and Doppler shift

An important number of practical communication scenarios (i.e. satellite communications, cellular networks, military communication systems, GPS positioning, etc) are characterized by a considerable degree of mobility. When a transmitter and a receiver are moving relative to one another, the received carrier frequency and the received code-frequency will not be the same as at the transmitter. These are defined as carrier Doppler and code Doppler respectively.

The following equation of received signal takes the Doppler effects into account [38]:

$$r(t) = \sqrt{2S}\, d(t) c\left(\frac{t}{1-\zeta'} + \zeta T_c \right) \cos\left[(\omega_c + \omega_d) t + \theta \right] + n(t) \qquad (3.10)$$

where the parameter ζ' is the received code-frequency offset (expanded or compressed PN pulse) and ω_d is the carrier-frequency offset.

Carrier frequency offset or carrier Doppler causes large mean acquisition time and decreases probability of acquisition. When Doppler shift is small, code frequency offset is negligible. Code Doppler becomes significant only under severe Doppler condition. It affects the correlation process due to the code-chip slipping during the dwell time. Mean acquisition time increases due to the code Doppler effect [38] [39].

3.6.2 Effect of Data Modulation

It is usual to consider that data modulation is not present during the initial synchronization process. In other words, a PN-code-only preamble is used for initial acquisition purpose. This approach works for the systems where data is transmitted only after initial synchronization procedure has been concluded. But, there are some cases when it is necessary to perform the synchronization with data modulated PN codes.

In CDMA systems, when data modulates the PN sequence, we obtain the products of the data signal and PN signal. The two signals are expressed as

$$d(t) = \sum_{k=-\infty}^{\infty} d_k P_{T_b}(t - kT_b) \tag{3.11}$$

$$c(t) = \sum_{k=-\infty}^{\infty} c_k P_{T_c}(t - kT_c) \tag{3.12}$$

where d_k is the kth bit of the data sequence, c_k is the kth chip of the spreading sequence, T_b is the data bit duration, T_c is the chip duration, and $P_T(t)$ is the unit magnitude rectangular pulse with duration T, i.e. $P_T(t) = 1$ for $0 \le t < T$ and 0 elsewhere. Without data modulation and noise, the output of the correlator during a time interval of τ_d is given by:

$$\int_0^{\tau_d} c(t - \Delta_i T_c) c(t - \Delta_j T_c) dt \tag{3.13}$$

where Δ_i and Δ_j are the phases of the received and local PN sequences. For the aligned codephases Δ_i, the output of the correlator is τ_d. However, if data modulation is present, the output is given by

$$\int_0^{\tau_d} d(t - \Delta_i T_c) c(t - \Delta_i T_c) c(t - \Delta_j T_c) dt \tag{3.14}$$

The magnitude reduces to below τ_d if the data polarity changes during the integration interval. If the polarity changes at the middle of the integration interval, then the output magnitude becomes zero. Therefore, acquisition systems, which are designed with the assumption of PN codes with no data modulation, perform poorly under data modulation conditions. In general, data modulation considerably degrades P_d [40].

3.7 Chapter Summary

In this chapter, the concept of PN codephase acquisition in CDMA systems is presented. Various methods of acquisition are mentioned along with their advantages and disadvantages. Detector structures, search strategies and most importantly, the matched filter acquisition method are described. At last, the effect of carrier frequency offset and data modulation are presented.

4. Packet CDMA Acquisition using SMF

4.1 Conventional Packet CDMA Acquisition Method

The PN code synchronizer is an essential element of any CDMA communication receiver. As discussed in Chapter 3, data demodulation starts after PN code phase alignment is achieved. In a conventional packet CDMA communication, a preamble is inserted at the beginning of the packet for PN code phase acquisition purpose. The acquisition circuit works on the preamble. Once the acquisition is achieved, data demodulation begins. If the code phase timing information is not available by the end of the preamble length, the packet is lost and retransmission of the lost packet is required. Figure 4.1 shows the block diagram of a basic PN code acquisition for packet CDMA.

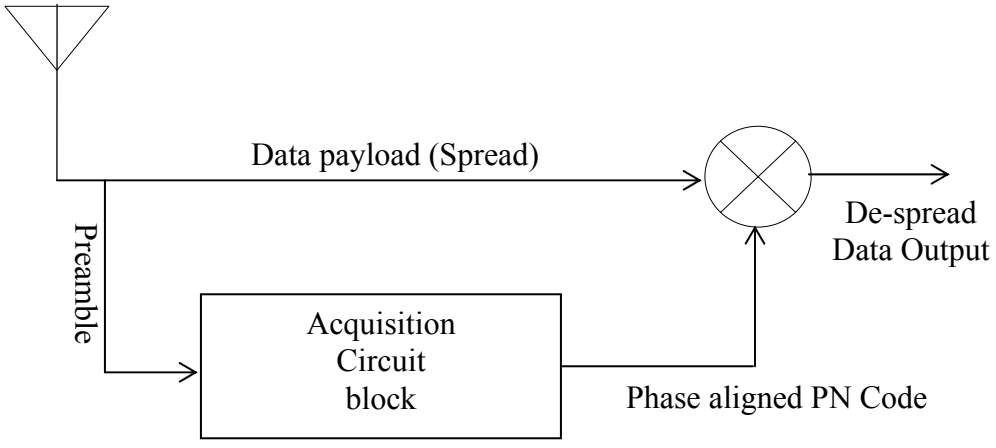

Figure 4.1 Conventional packet CDMA acquisition method

4.2 Packet CDMA Acquisition Method without Preamble

Two code phase acquisition methods for packet CDMA have been proposed in this thesis work. In the first method, an approximate delay of the amount of 10% of the packet length is incurred on the received packet. This delay is provided for the acquisition circuit block to achieve aligned code phase and the acquisition is expected to achieve within this delay. As a result, when the beginning of the packet arrives at the receiver, aligned code phase information is available and data is ready to be decoded. Figure 4.2 shows this simple acquisition method. As mentioned, this has the disadvantage of delay in processing the acquisition method.

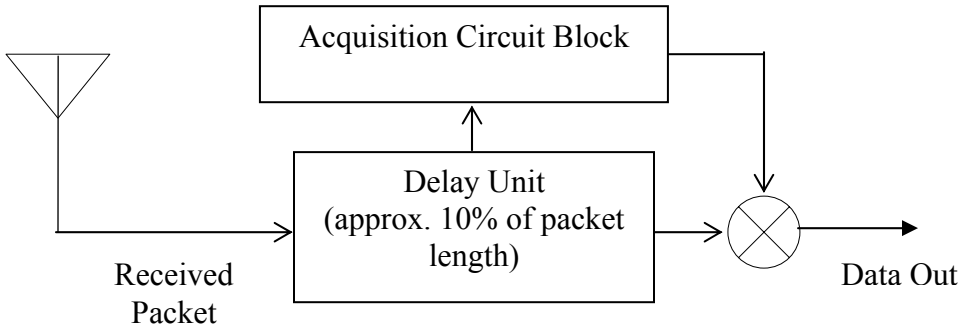

Figure 4.2 Packet CDMA acquisition without preamble

In a different model (Figure 4.3), an initial part of the received packet is stored in the spread data buffer. The required length of the stored spread data buffer increases with the number of simultaneous interfering packets and carrier frequency offset at the receiver. The acquisition block uses this initial part of the received data packet to determine the aligned PN codephase. Storage of this initial part of the received data packets is necessary so that this part can get de-spread after the aligned code phase is determined.

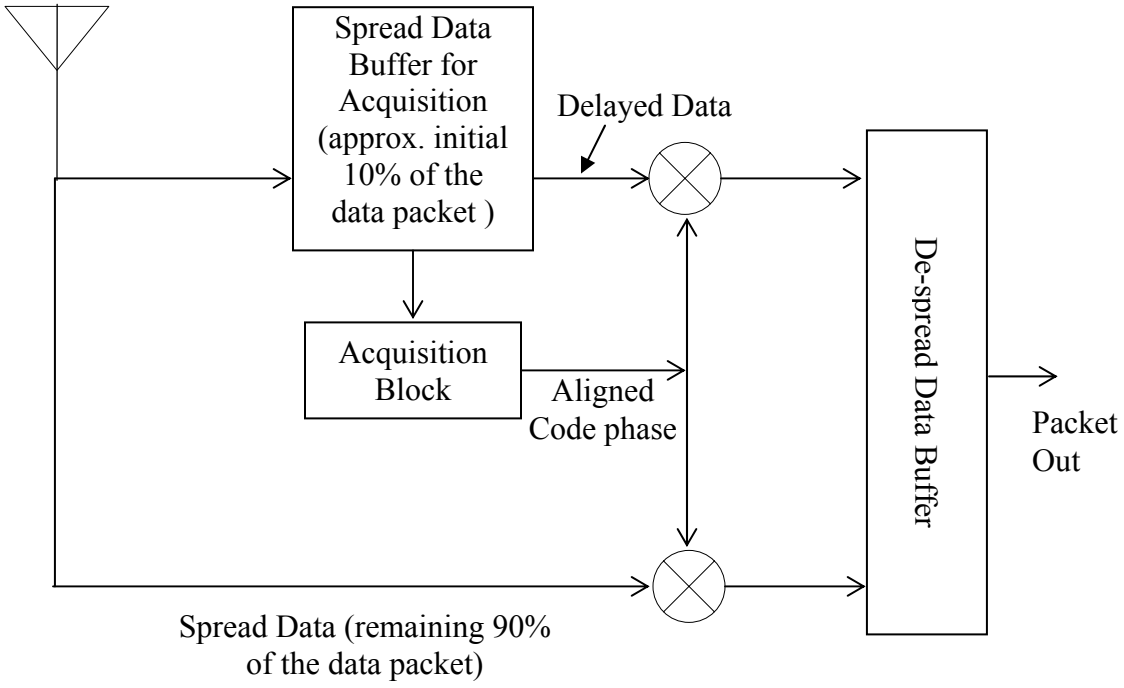

Figure 4.3 Modified Packet CDMA acquisition without preamble

4.3 Acquisition Block

Matched filter acquisition is employed in this thesis work. At first, a conventional Transversal Matched Filter (TMF) is explained along with its acquisition performance with data modulated PN signal and carrier frequency mismatch. Then, SMF is introduced and its performance with data modulated PN signal and carrier frequency mismatch are shown.

4.3.1 Transversal Matched Filter

A passive matched filter (MF) can perform fast acquisition in high noise environments [35]. The matched filter (MF) shown in Figure 4.4 consists of analog shift

registers. Because the data transverses the structure with time, this is known as transversal matched filter (TMF). Analog samples of the received chip signal are stored in the shift registers and these are shifted through the register when new samples are available. For each consecutive sample shift, each element of the stored sample sequence is multiplied by the corresponding element of the ±1 code sequence and the results from these multiplications are then summed to form the detector output. The detector output is proportional to the correlation value between the received signal and the local code sequence. If all of the samples match the PN code coefficients, a maximum correlation value is obtained [41].

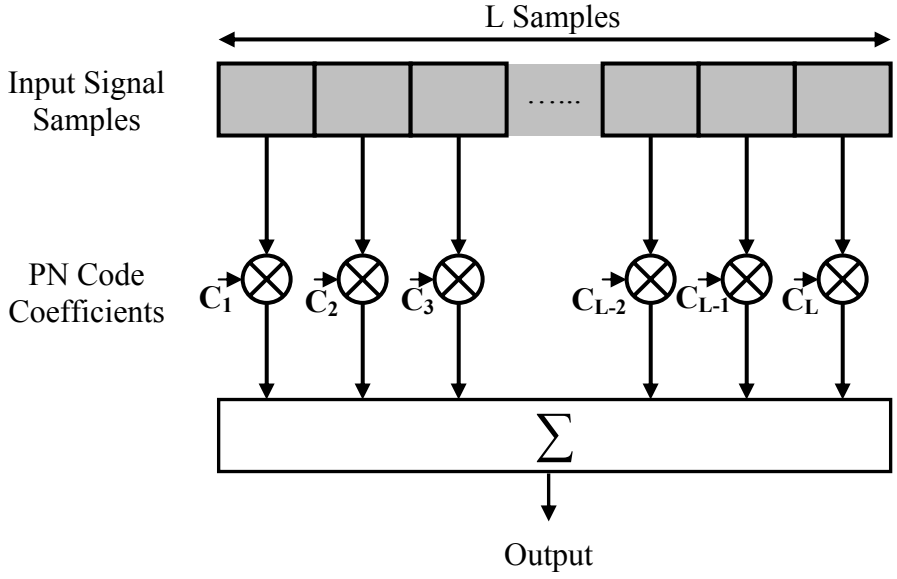

Figure 4.4 Transversal matched filter structure

The TMF operates in baseband and, therefore, it is necessary to use a pre-acquisition circuit block which brings the incoming signal down to baseband and then samples of the downconverted signal. These samples are shifted through into the TMF. In

the pre-acquisition block, the incoming signal is multiplied with a demodulating sinusoid and then the system integrates the result for single chip duration in order to gather energy. The output of the integrator is then dumped into the shift register of the TMF. The chip timing on the signal code is unknown, so the integration process will not necessarily start at the beginning of a chip and the code phase alignment detected by the TMF will not necessarily correspond to an exact alignment between the spreading code and the stored PN code coefficients in the TMF [41]. If the integration doesn't start at the chip boundaries, then the autocorrelation peak will not be sampled at its peak.

If only one TMF is used for acquisition purpose, then the correlation value is dependent on the phase of the incoming signal. If the local oscillator utilized to bring down the received signal to baseband has a sinusoid that is 180^0 out of phase with the transmitted carrier sinusoid, then all the received samples will mismatch with the reference samples for aligned codephase condition. If half of the samples match, and half mismatch, the output is zero, even when the code phases are actually aligned.

In a CDMA system, code de-spreading occurs before carrier synchronization due to the fact that received signal has very low signal-to-interference ratio. So, carrier phase information is not available during PN code acquisition process. Therefore, TMF is required to operate non-coherently.

Two TMFs are used in an in-phase and quadrature (I-Q) structure as shown in Figure 4.5. If one of the demodulators experiences a 90^o phase shift, the other will have a phase shift of 0^o and full correlation value will be found at the detector output. The result from each TMF is squared so that the two outputs can be added in a polarity insensitive fashion without cancelling one another. So, when the results from two matched filter are

added, the I-Q structure is insensitive to the carrier phase offset and is capable of performing non-coherent acquisition. In this structure, θ may be a function of time, $\theta(t)$, and thus this structure will work with small frequency offset.

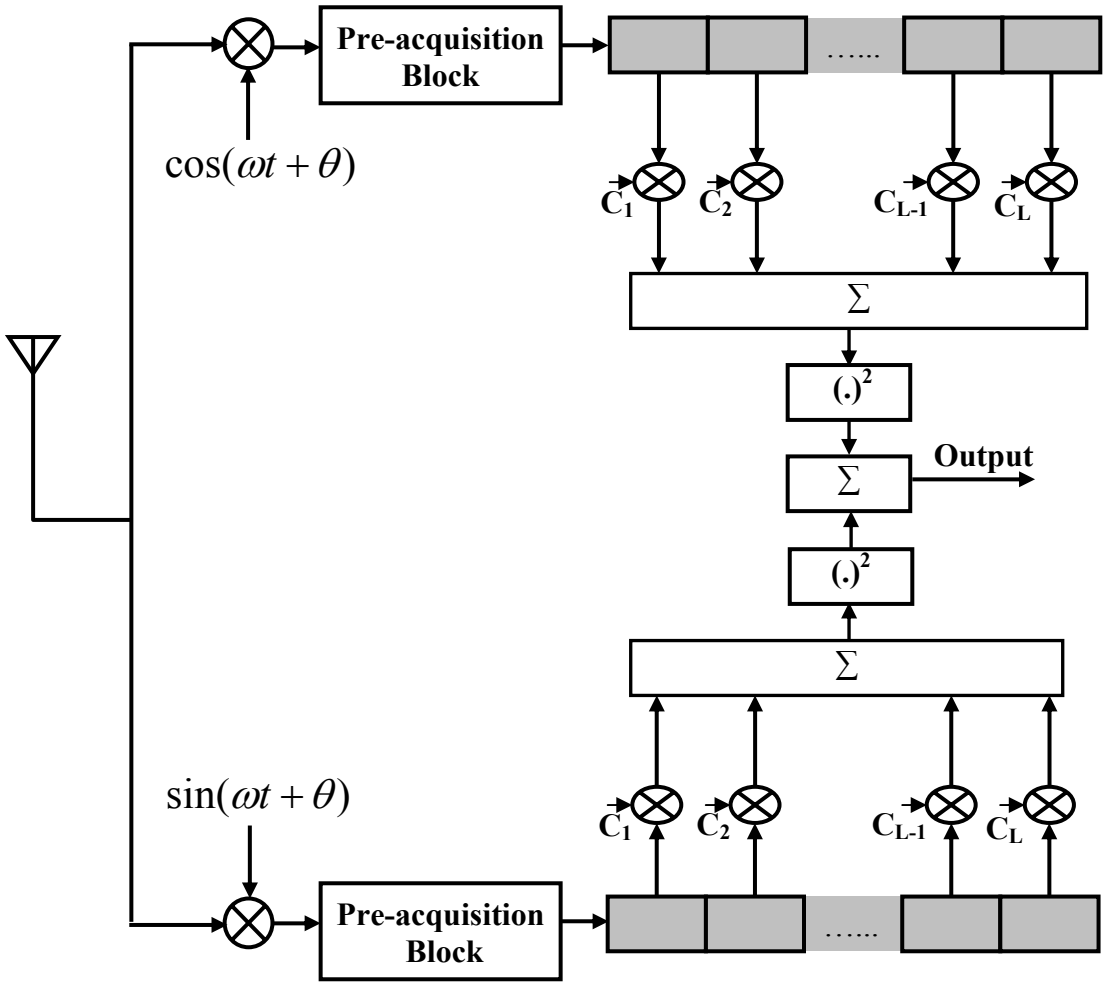

Figure 4.5 I-Q TMF structure

The I-Q TMF structure will handle static carrier phase offset and slowly changing phase offset. However, the presence of significant carrier frequency offset or data bit

transitions will impair the performance of the TMF. The frequency offset occurs due to poorly matched transmitter/receiver local oscillators, or from the Doppler shift.

4.3.1.1 Effect of Carrier Frequency Offset in TMF

Carrier frequency offset causes phase rotation of the baseband signal and amplitude modulation of the sampled chip sequence (Figure 4.6). At times, this modulation inverts the received chip sequence due to the 180 phase rotation of the transmitted and local oscillator.

If the transmitted signal carrier angular frequency and the locally generated receiver carrier angular frequency are ω_0 and ω_r respectively then the received signal can be expressed as

$$\begin{aligned} r(t) &= \sqrt{2P}d(t)c(t)\cos(\omega_0 t)\cos(\omega_r t) \\ &= \sqrt{2P}d(t)c(t)\frac{1}{2}[\cos(\omega_0 t - \omega_r t) + \cos(\omega_0 t + \omega_r t)] \end{aligned} \tag{4.1}$$

where P is the average power, $d(t)$ is a binary baseband data signal and $c(t)$ is a baseband spectral-spreading signal, ω_0 is the carrier frequency. The double frequency term is eliminated by the receiver filter and the first term results in a rotation of the received signal before de-spreading.

At low carrier frequency offset or Doppler rate, one I-Q branch output has low amplitude while the other has high output. The sum of the two branches is constant in amplitude. At higher carrier frequency offset or Doppler rate, the period of the phase rotation approaches the length of the TMF and some chips are inverted while the others are not inverted. The output sum of each TMF is then reduced in amplitude and I-Q sum is more susceptible to noise.

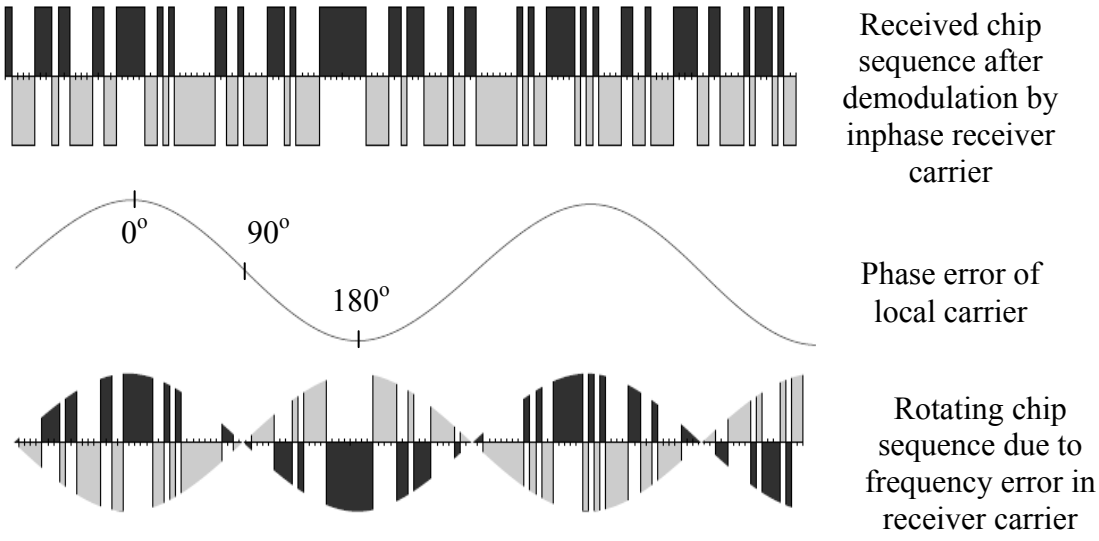

Figure 4.6 Effect of carrier frequency mismatch in TMF. From [42].

In Figure 4.6, effect of carrier frequency mismatch has been illustrated. During the positive phase error of the receiver carrier, both the positive and the negative PN chips add positively. But, during the negative portion of the phase error, both positive and negative PN chips get inverted and they add up negatively with the reference PN chips.

4.3.2 Segmented Matched Filter

The segmented matched filter (SMF) offers both fast acquisition and tolerance to carrier frequency offsets [41]. In the TMF, better tolerance of frequency offset is maintained by reducing the filter length. But this has the deleterious effect of reduced noise averaging. So, a compromise is required between the noise performance and the Doppler tolerance [43].

The SMF divides the TMF into segments which are processed independently before combining their outputs. The SMF structure is shown in Figure 4.7, where the filter with length *L* is broken into segments of length *M*. So, the filter consists of several 'short' TMFs that are cascaded. The averaging is improved by combining results from successive short 'TMF's after the result being squared. Segment sum is squared before being added together. Since the addition is insensitive of polarity, any inversion caused by the carrier frequency offset between segments will have no impact [41][42].

4.3.2.1 Carrier Frequency Offset in SMF

In order to illustrate the effect of carrier frequency offset on the TMF and SMF, the aligned codephase condition is considered (Figure 4.8). During the first half of the Doppler modulation period illustrated, the polarity of the signal will be sampled correctly, but for the second half-period, the polarity of the samples will be inverted. When the original PN sequence is compared with this, all of the samples in the second portion generate mismatches. As they are summed, these mismatches will cancel the matching portion. As a result, with the TMF, it is not possible to detect an aligned codephase condition with Doppler frequency offset (carrier frequency mismatch).

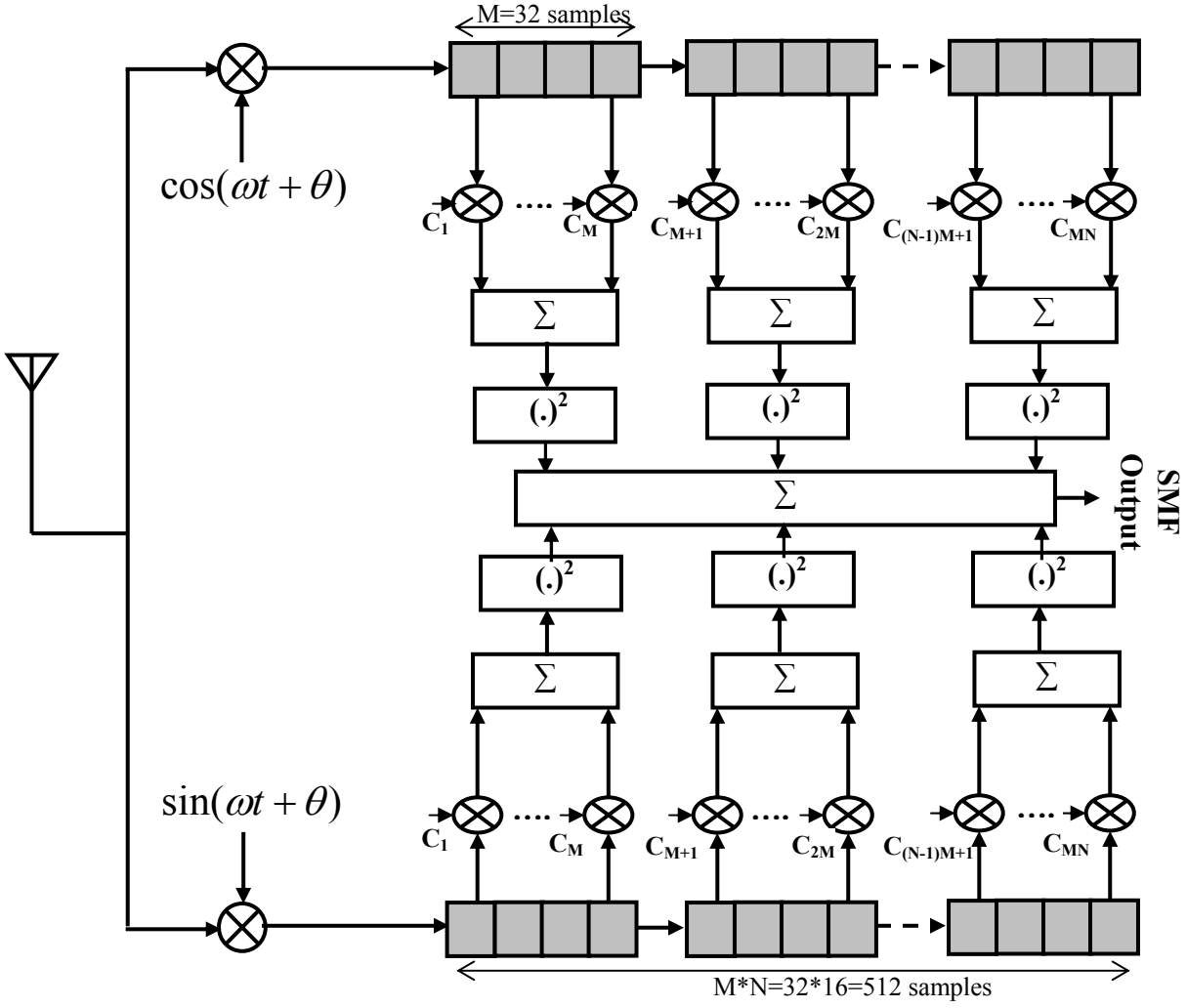

Figure 4.7 I-Q SMF Structure

Transmitted positive polarity

Polarity change

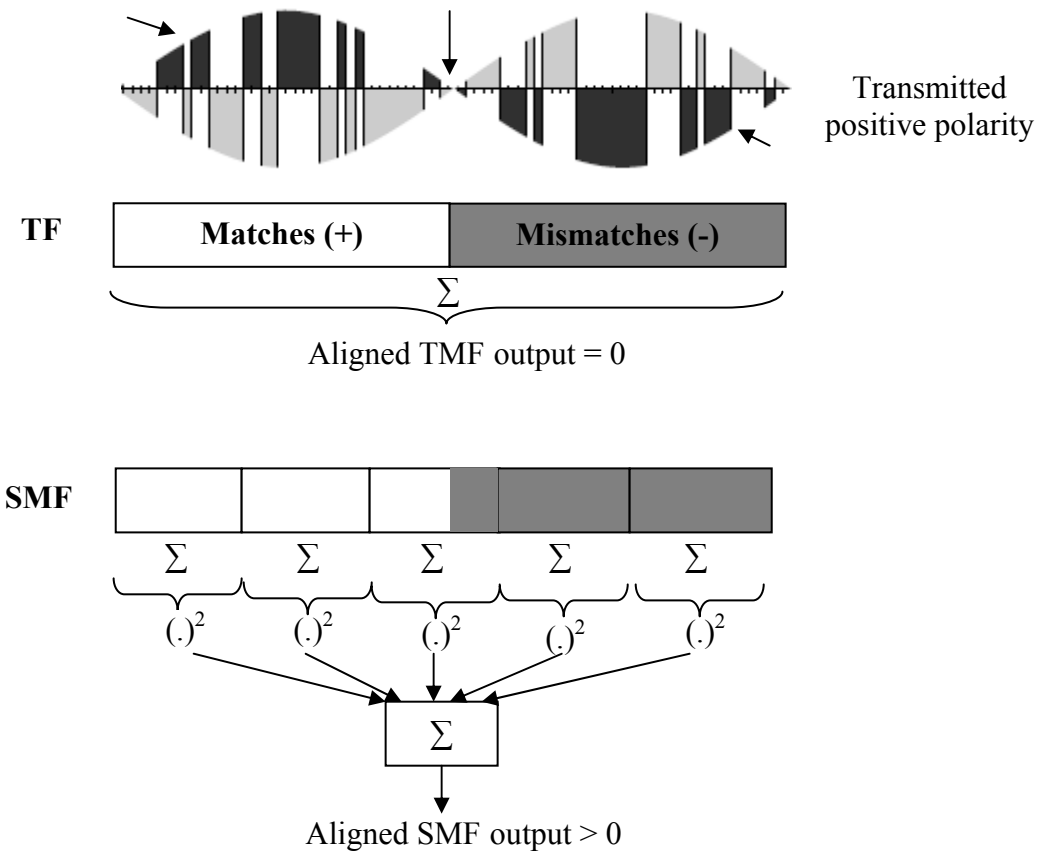

Figure 4.8 Effect of carrier frequency offset on TMF and SMF. From [42].

Each segment in the SMF is designed to have equal responses both to the number of matches and mismatches (Appendix A). Segments with a transition along its length have low correlation value. If a segment has a transition in the middle of its length, then the segment output will be zero. When the carrier frequency offset is not high so that many segments do not experience phase reversal, a meaningful measure of alignment is achieved.

4.3.2.2 Acquisition with Data-modulated PN code using SMF

Figure 4.9 illustrates the effect of data modulation on the performance of TMF and SMF. Data modulation causes polarity transitions similar to those caused by carrier frequency offset. This means that SMF can perform acquisition while data is being sent and thus not require a training sequence or preamble to perform acquisition prior to the transmission of data.

Due to the logic 0 data, the PN sequence gets inverted. With the conventional matched filter, the inverted section cancels out correlation results from the aligned section. So, the correlation value is zero. However, with SMF, segment output is squared before combining them together so that correlation results from inverted sequence portion add to the correlation sum. As, a result, nonzero correlation value is obtained with SMF.

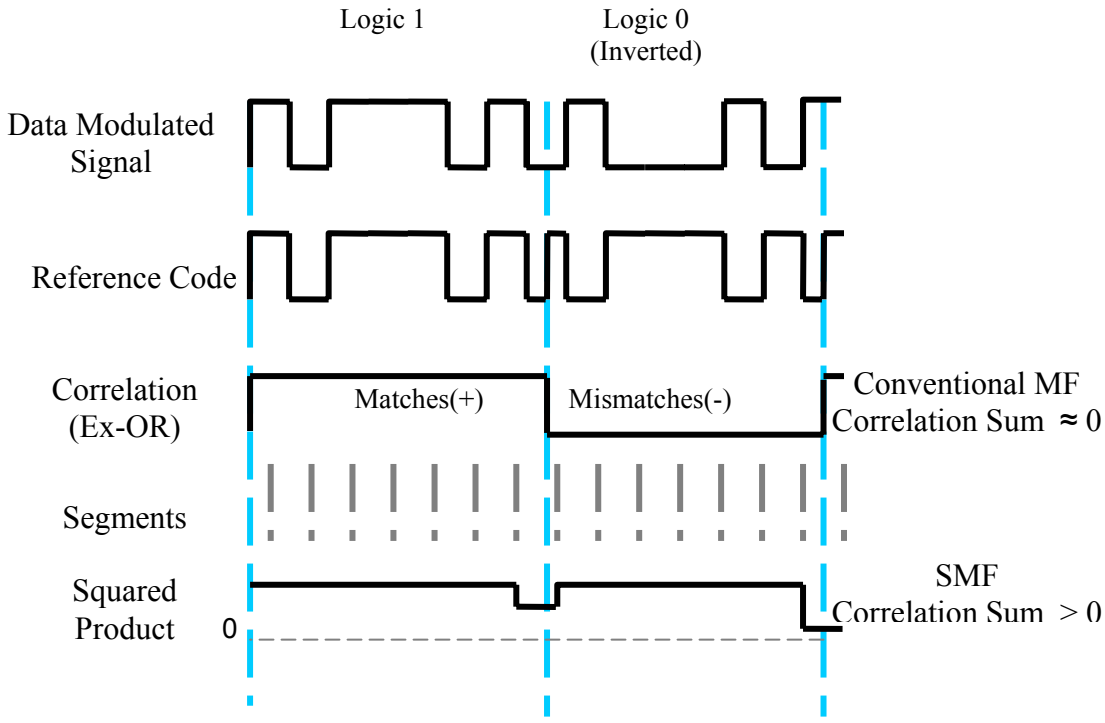

Figure 4.9 Effect of Data Modulation on TMF and SMF

4.4 SMF Structure

In the digital version of a matched filter, the signal is quantized into binary form and passed along a digital shift register. The digital shift register may have several bits per sample. The reference code sequence is loaded in a separate register. Exclusive-NOR gates perform sample by sample comparison between the two sequences.

The received signal consists of the desired PN sequences plus co-user interference which is modeled as additive white Gaussian noise (AWGN). This signal is quantized in two levels. Multilevel quantization provides better performance but the performance improvement of 4 level quantization over 2 levels is equivalent to only an increase in SMF length by 20% [42]. Increasing the filter length is always preferable to using multilevel quantizer in terms of hardware cost. Besides, two-level-quantization (hard limiting) does not require level optimization [41].

In the preacquisition block (Figure. 4.10), the received signal is first downconverted to baseband and sampled. Then, the sampled signal is passed on to a ‘chip-matched filter’. For a rectangular chip waveform, integrate and dump operation gathers the maximum signal energy in each chip [13]. But, the block cannot be chip-synchronized until acquisition is performed. Therefore, the acquisition process must be independent of the chip transition time.

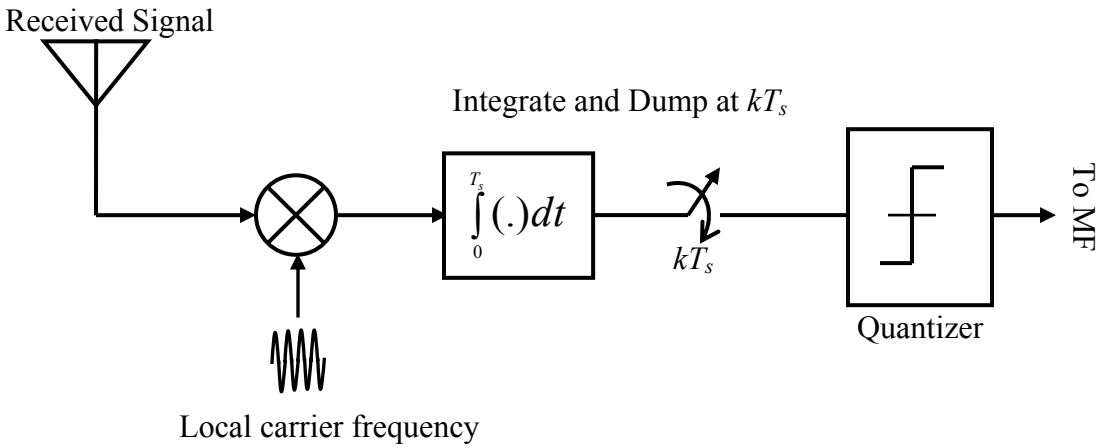

Figure 4.10 Preacquisition Block

The maximum chip energy is obtained when the received signal is sampled once per chip, and the sampling timing is aligned with the received chip timing. In this case, the PN sequence autocorrelation is sampled at its peak value. When the sampling timing is moved out of alignment by a chip fraction, τ_D, then integrate and dump process occurs across chip transitions. The autocorrelation function will be sampled off the peak. With single sampling per chip (Figure 4.11), the detected peak correlation can have a timing error of $\pm T_c/2$ after coarse acquisition is achieved. The timing error can be reduced by increasing the sampling rate.

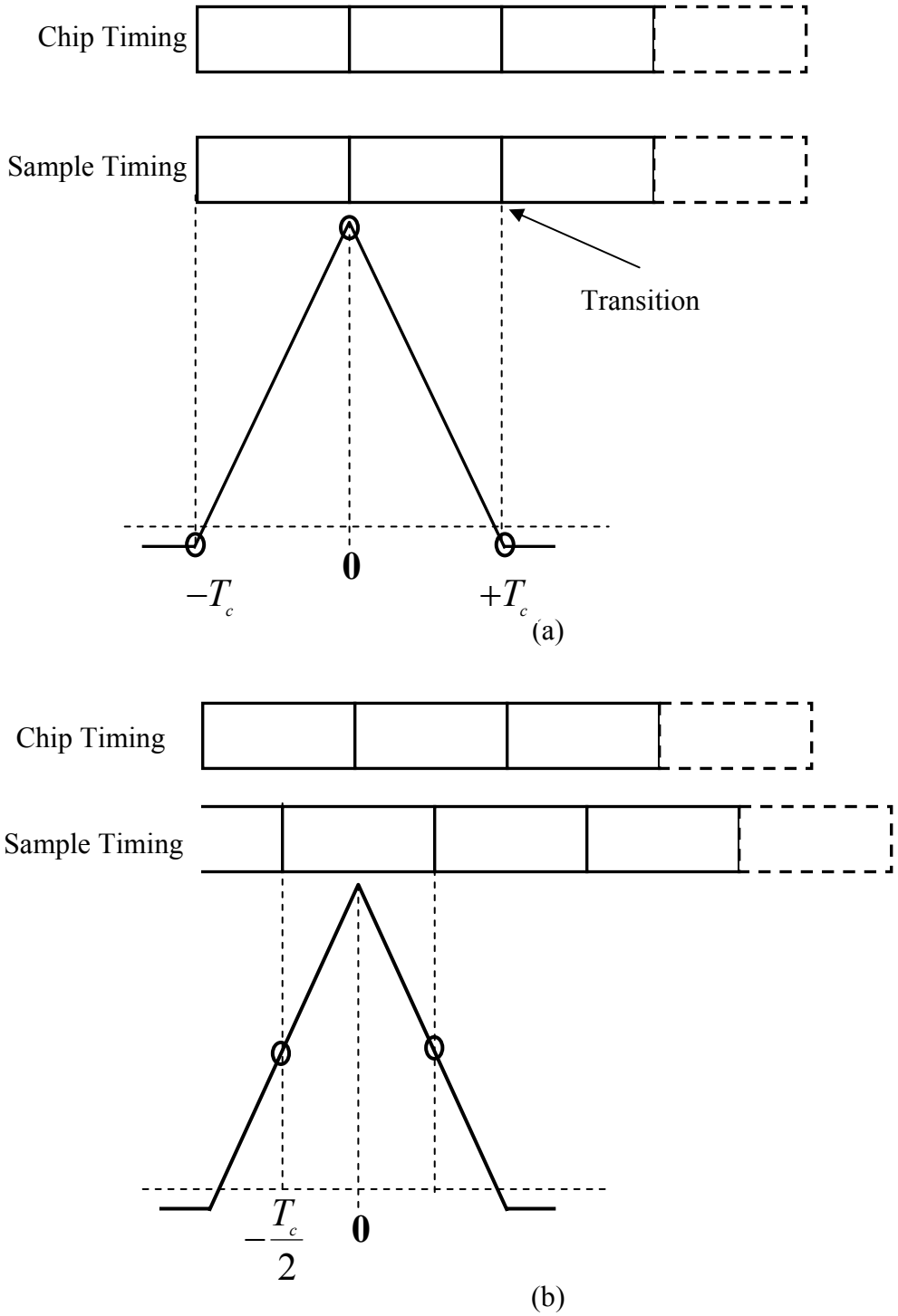

Figure 4.11 Chip sample timing using 1 sample per chip. (a) best case, and (b) worst case. From [42].

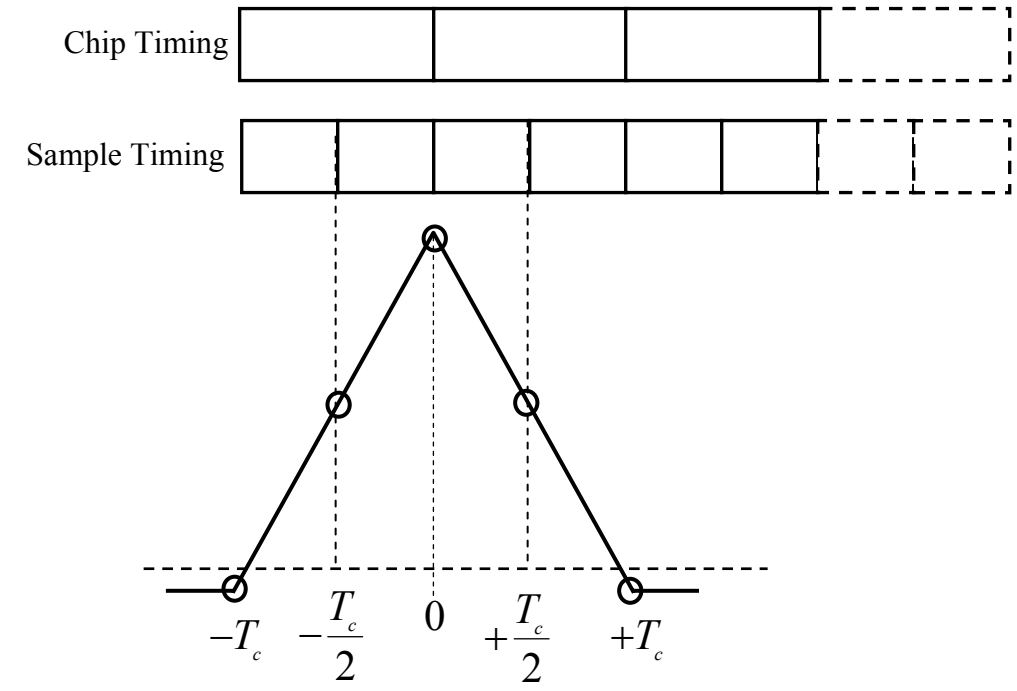

(a)

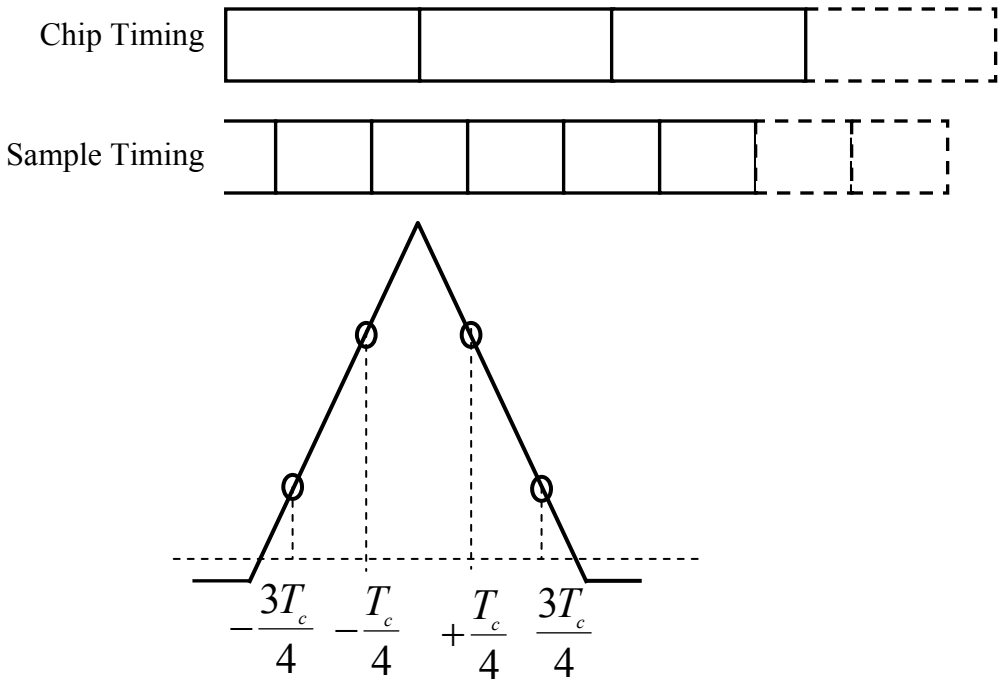

(b)

Figure 4.12 Chip sample timing using 2 samples per chip. (a) best case, and (b) worst case. From [42].

Figure 4.13 shows an alternative scheme. In this case, the received signal is sampled twice per chip but only every second sample is processed in the filter. So, the sample stream consists of two interleaved streams. One stream will encounter chip transitions and the other has samples taken during each chip [42].

For the best case (Figure 4.14a), each stream will yield the same results. For all other cases, one of the streams will provide undisturbed correlation and the second stream will have samples that includes a chip transition. Since the correct stream is unknown, the timing error will remain as $\pm T_c/2$. The advantage of this technique is that the filter will always sample the correlation near the peak regardless of the chip timing. The interleaved processing technique is easily implemented by doubling the length of the matched filter register, but only every second flip-flop is processed. With each sample clock, the filter shifts one stream into the set of connected flip-flops for processing, and the other enters the unconnected flip-flops and awaits the next clock.

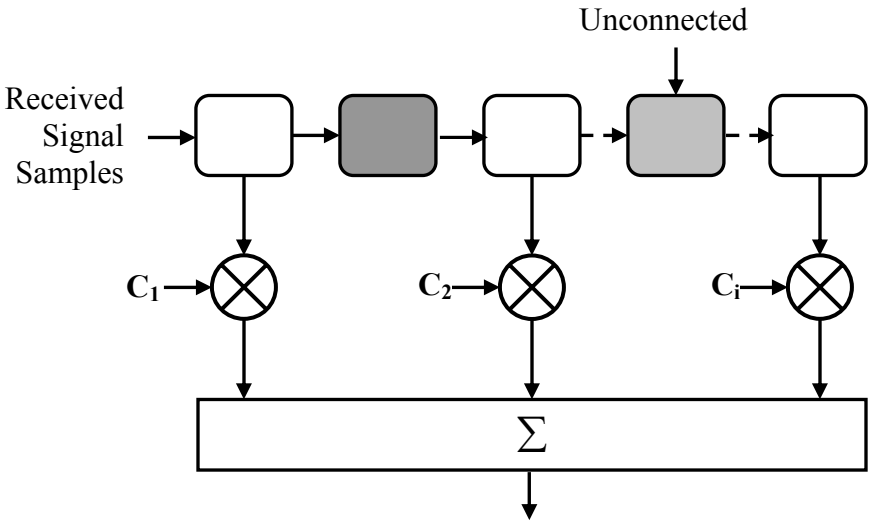

Figure 4.13 Interleaved shift register

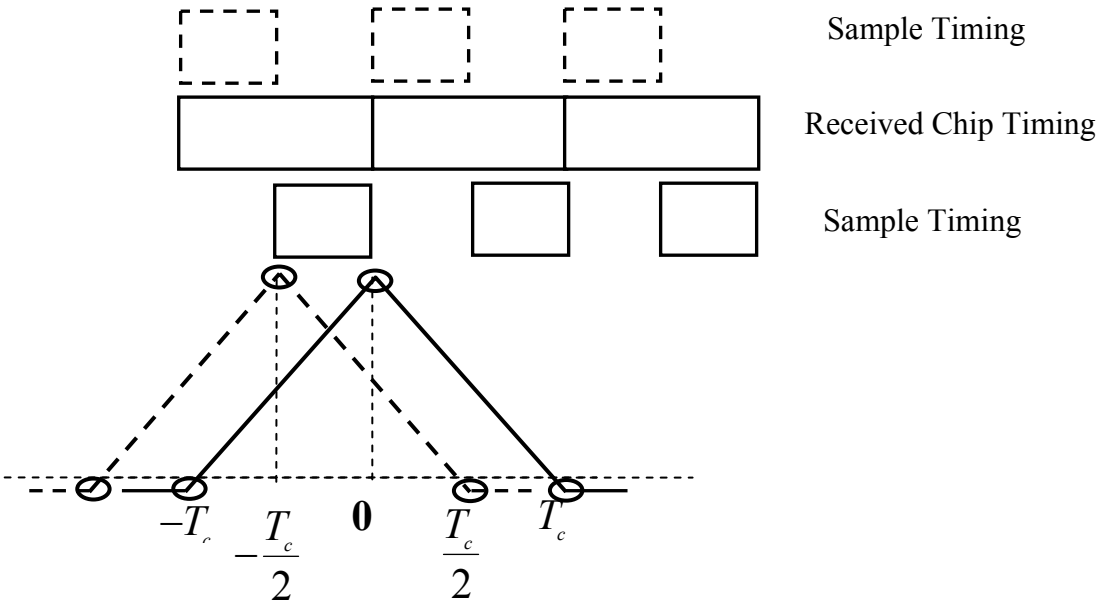

(a)

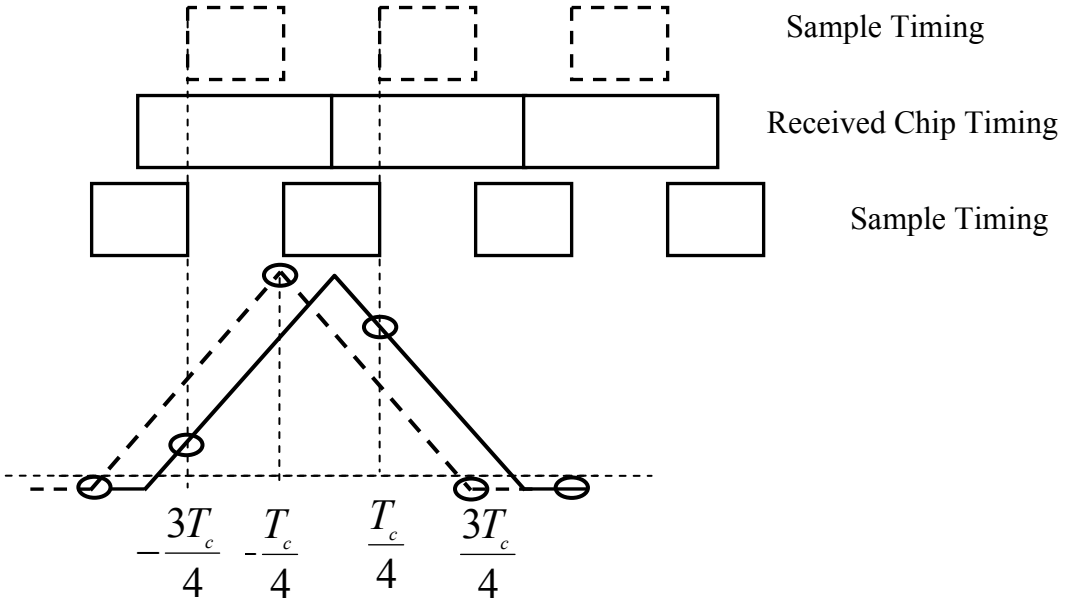

(b)

Figure 4.14 Chip sample timing using 2 samples per chip. (a) best case, and (b) worst case. From [42].

4.5 Chapter Summary

In this chapter, some acquisition schemes are shown using segmented matched filter which enables PN codephase acquisition without preambles. The structure of a transversal matched filter and performance of this filter in the presence of data modulation and carrier frequency offset were described. Then, the structure of a segmented matched filter was shown and its ability to provide code acquisition in the presence of data-modulated PN codes and carrier frequency offsets were described.

5. System Model and Simulation Results

5.1 Introduction

Direct-sequence spread-spectrum multiple-access (DS/SSMA) has proven to be highly successful in circuit-switched cellular networks due to increased system capacity, reliability in hostile environments, and more secure communications compared to TDMA, and FDMA. Lately, packet-switched DS/SSMA has attracted much attention for military communications and for random access data burst in Wideband CDMA [44].

Packet acquisition has been a topic of active research. Usually, it is assumed that the packet acquisition methods use only the preamble. A period of preamble consisting of the PN sequence without data modulation is used at the beginning of each packet. The acquisition process is less reliable if data modulation is present.

This chapter analyzes a segmented matched filter (SMF) acquisition system where the receiver stores the initial part of the packet and data modulation begins at the start of each packet. Based on the stored packet, the SMF can accumulate the results of several spreading sequence code cycles and then select the correct code phase based on the best match selection criterion.

Parameters of interest are the number of simultaneous users, allowable carrier frequency offset, the probability of correct codephase detection, acquisition time and the packet throughput.

This chapter is organized as follows. In Section 5.2, the signal and system model is given. Section 5.3 describes the modeling of the effects of active co-users interference. In Section 5.4, analytical equations are derived for both non-aligned and aligned

codephases. Effect of carrier frequency offset on the acquisition process is discussed in Section 5.5. In Section 5.6, simulation methodology is described and a series of MATLAB simulation results for various cases of data modulation and carrier frequency shifts are shown. Acquisition by threshold crossing and maximum likelihood selection are described along with the simulation results in Sections 5.7 and 5.8, respectively. The dependence of the acquisition process on the performance of packet throughput is examined in Section 5.9. Section 5.10 concludes this chapter.

5.2 Signal and System Model

In this section, the signal and the system model is described. We consider a packet system where each packet consists of L_D data bits that are spread-spectrum modulated with N_c chips per data bit. It is important to note that the length of the spreading code is longer than N_c. Data bit rate increases when N_c decreases for a fixed length of code sequence. In other words, the period of the spreading sequence code is longer than the data bit duration. The packet structure is shown in Figure 5.1.

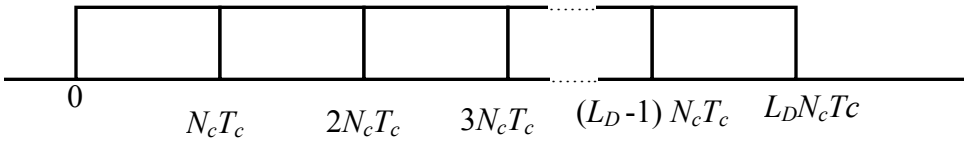

Figure 5.1 Packet structure

We assume that there are K active users in a given transmission and all user signals use the same packet structure of Figure 5.1. At the receiver, the overall signal has

three components: the desired signal, other interfering signals or active users' noise, and the thermal noise. The received signal is given by

$$r(t) = r_0(t) + \sum_{k=1}^{K} r_k(t) + n(t), \tag{5.1}$$

where $r_0(t)$ is the desired signal, $r_k(t)$ is the k^{th} co-user signal and $n(t)$ is the white noise process with power spectral density $N_0/2$ (W/Hz). The desired signal is expressed as

$$r_0(t) = \sqrt{2P_0}\, d_0(t) c_0(t + \beta T_c) \cos(2\pi f_0 t + \theta(t)), \tag{5.2}$$

where $d_0(t)$ is the transmitted data sequence with $d(t) \in \{+1,-1\}$, $c_0(t)$ is the binary spreading code of length L_C chips, T_c is the chip duration, β is the relative delay of the spreading code in the range $0 \leq \beta \leq L$, P_0 is the signal power of the desired user, $f_0(t)$ is the receiver carrier frequency, $\theta(t)$ is the phase of the received signal carrier with respect to the local oscillator. The sequences $d_k(t)$ and $c_k(t)$ are independent and identically distributed, taking values +1 and -1 with equal probability. We will further assume that all received signals have equal power, i.e., $P_k=P, \ \forall\, k$. In practical systems, power control is employed at a central station to instruct the active users on whether to increase or decrease their power level [45]. The knowledge of the desired user's spreading waveform is also available at the receiver.

It is assumed that the number of simultaneous transmissions remains fixed throughout an observation period of the desired packet. Therefore, a CDMA packet system can be considered as an asynchronous CDMA system [46]. The channel is assumed to be non-fading and it is modeled as a single transmission path with carrier frequency offset. Since multiple-access interference is the dominant source of impairment, we ignore the thermal noise.

Figure 5.2 shows the packet CDMA system model.

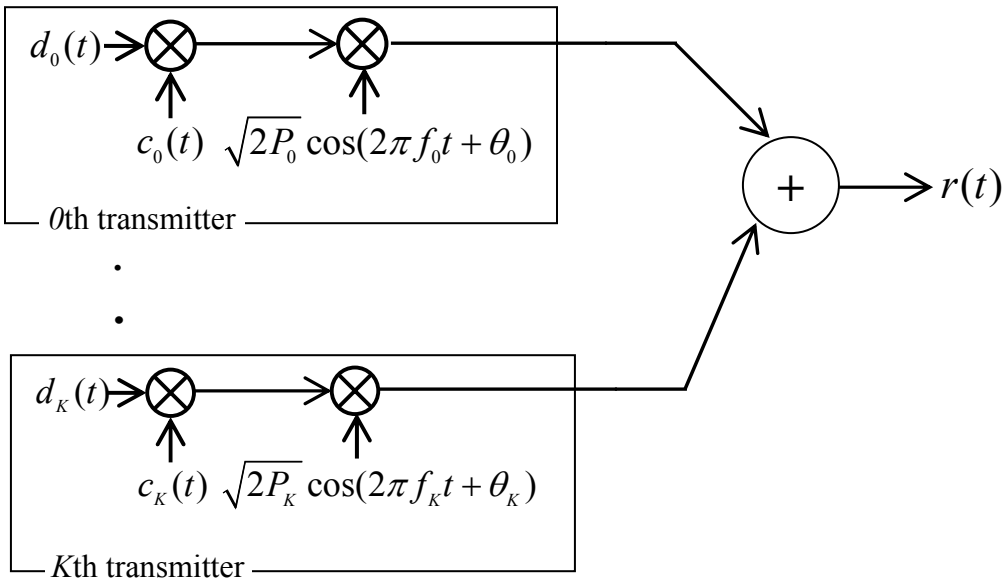

Figure 5.2 Packet CDMA System Model

5.3 Active Co-users' Interfering Signal Modeling

The active co-user sequences are modeled as random binary sequences with equal received power and the received active user noise is the sum of these sequences. Some of the input signal chips will become corrupted by the active user interference; the more active users in the system, the more signal chips will be corrupted. The ensemble sum of n binary values is a binomially distributed random variable, with probability that $x = k$ given by [47]

$$P(x=k) = \binom{n}{k} p^k q^{n-k}, \tag{5.3}$$

where the probability of 1 or 0 are p and q, respectively. The mean (μ) and variance (σ^2) of the above distribution are given by

$$\begin{aligned} \mu &= np \\ \sigma^2 &= npq \end{aligned} \tag{5.4}$$

Random active co-user spreading sequences use bipolar form and take the values of +1 and -1 with equal probabilities $p = q = 0.5$. The mean (μ_c) and variance (σ_c^2) of the active interfering user signal distribution are given by [Appendix B]

$$\begin{aligned} \mu_c &= 0, \\ {\sigma_c}^2 &= n. \end{aligned} \tag{5.5}$$

where the subscript c indicates co-users. In case of large numbers of active users (n), the discrete distribution can be approximated using a Gaussian distribution [47]. Then, the probability density function (pdf) is given by (Figure 5.3)

$$p(x) = \frac{1}{\sigma_c \sqrt{2\pi}} e^{-\frac{(x-\mu_c)^2}{2\sigma_c^2}} \tag{5.6}$$

where μ_c and σ_c are the mean and standard deviation of the active interfering co-users' noise.

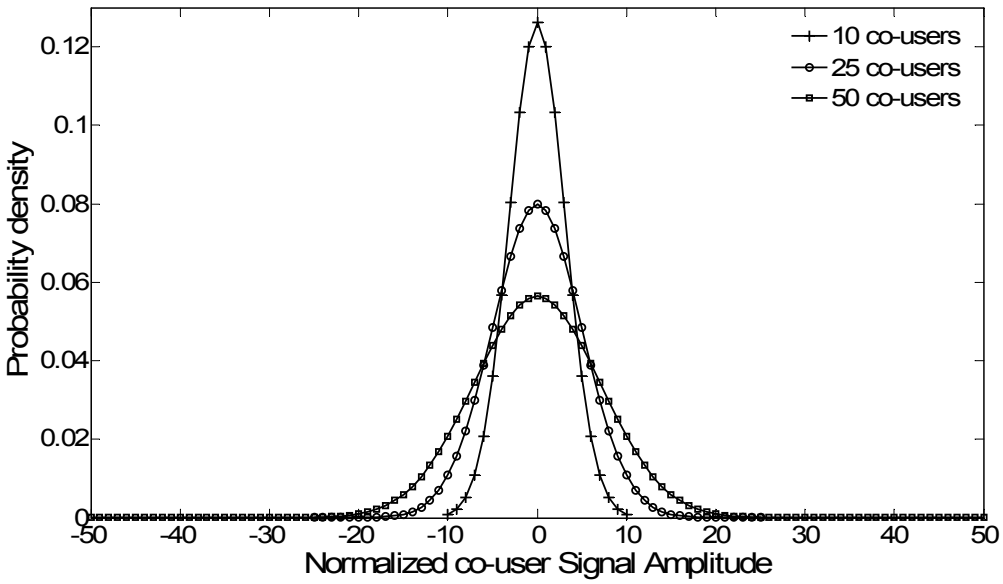

Figure 5.3 Co-users' Interfering signal probability density function. From [42].

If a +1 chip is received from the desired user, the pdf in Figure 5.3 is shifted to the right by one unit. The probability of received chip error (P_{ce}) is then calculated by determining the area of the received signal pdf to the left of zero. In the presence of more active users, the variance increases and the received signal pdf becomes more spread out.

Active users' signals have random phases; therefore, their contributions are equal in the in-phase (I) and quadrature (Q) channels. Average amplitude is reduced by $1/\sqrt{2}$ in each channel, and their combined power is reduced by 1/2 when the effect of the reception of the desired user signal is considered. Initially, it is assumed that a coherent receiver is employed. Chip error rate in the in-phase channel is then given by

$$P_{ce} = Q\left(\frac{1}{\sqrt{\frac{\text{number of active interfering users}}{2}}}\right). \tag{5.7}$$

where, $Q(\alpha) = \frac{1}{\sqrt{2\pi}} \int_{\alpha}^{\infty} e^{-\frac{x^2}{2}} dx$. Chip error probabilities are illustrated in Figure 5.4.

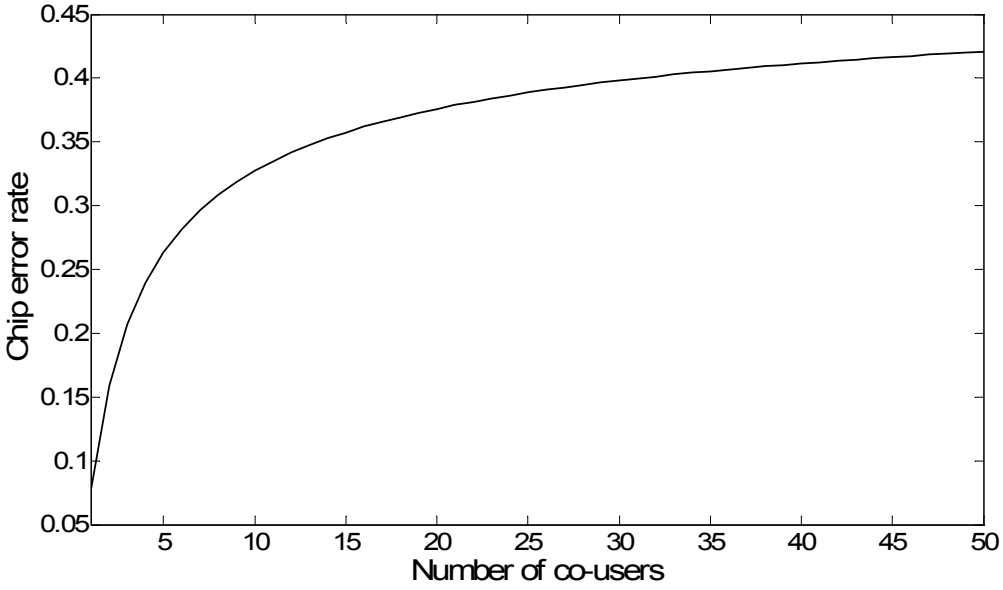

Figure 5.4 Chip error rate

5.4 Probability Densities for Aligned and Non-aligned Codephases

Two codephase conditions are considered here: i) aligned, and ii) non-aligned. In an aligned codephase condition with no chip error, the entire chip samples in the SMF match the stored reference PN code sequence. Therefore, SMF generates its full scale value for an aligned code phase. The presence of interfering co-users' signals causes errors in the chip samples and a subsequent reduction in the SMF output.

In the case of a non-aligned codephase condition, little correlation exists between the desired user signal and the reference PN code sequence. At the matched filter, the desired user signal appears like that of co-users [42].

In order to calculate the probability of detection (P_d), distributions are calculated for both aligned and non-aligned codephases with co-user noise. The non-aligned case is modeled as a random sequence with P_{ce} = 0.5 and, for aligned codephase case, P_{ce} depends on the number of co-users.

In each segment of the SMF, the number of errors e follows a binomial distribution:

$$P(E=e)=\binom{m}{e}P_{ce}^{e}(1-P_{ce})^{m-e} \tag{5.8}$$

where m equals the segment length (i.e., m = 32). Similarly, the number of correct bits c follows the same distribution with p = 1- P_{ce}.

$$P(C=c)=\binom{m}{c}(1-P_{ce})^{c}P_{ce}^{m-c} \tag{5.9}$$

where c and e are related by the following equation,

$$c+e=32. \tag{5.10}$$

Figure 5.5 shows the pdfs of correct bits in a segment for both of the code phases with 25 active co-users. The mean of the distribution in the non-aligned case is 16 and the mean for the case of aligned codephase condition depends on the chip error rate which is a function of number of active co-users as defined in the Equation 5.7. The discrete probability distribution is approximated by a continuous Gaussian distribution.

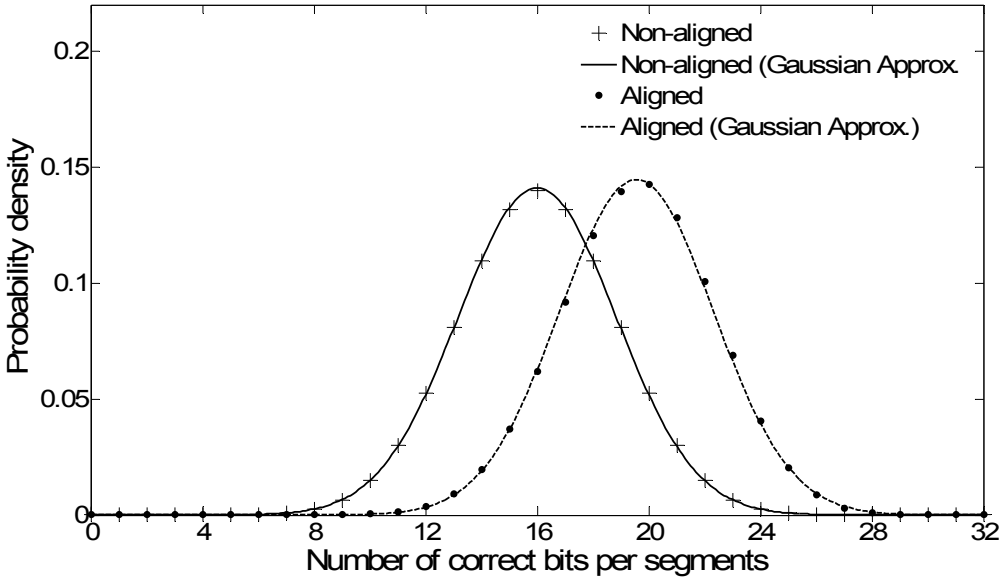

Figure 5.5 Number of Correct Bits in a Segment with 25 co-users. From [42].

Each segment in the SMF provides an output, *s*, which is the difference between the number of matches and the number of mismatches.

$$s = c - e = 2(c - 16). \tag{5.11}$$

In the case of an aligned codephase condition with no chip errors (no active co-users' interfering signal), all of the bits match exactly and the segment sum is 32. Each error causes a match (+1) to change to a mismatch (-1) which reduces the sum by 2. Maximum chip error rate (max P_{ce} = 0.5) occurs for non-aligned case. Since the average

number of matches and mismatches are equal to16, the mean of s is zero. The distribution for the segment sum is given by

$$\begin{aligned} \mu_s &= 2(\mu_c - 16), \\ \sigma_s^2 &= 4\sigma_c^2. \end{aligned} \tag{5.12}$$

where μ_s, σ_s are the mean and the variance of the segment sum. Figure 5.6 shows the pdfs of the segment sum for both the cases.

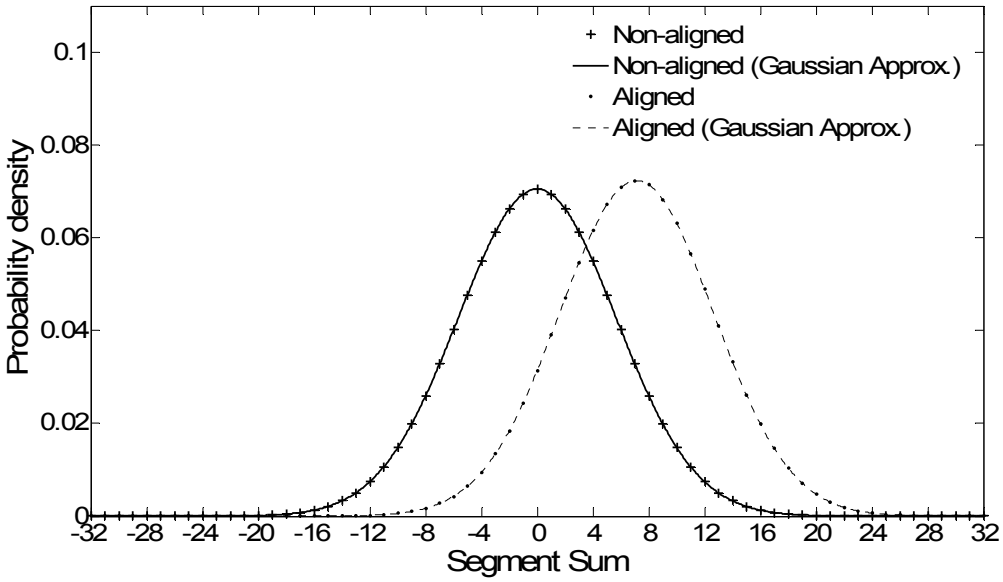

F**igure 5.6** pdfs of the segment sum with 25 co-users. From [42].

Each segment output in the SMF is squared and, the resultant new random variable is denoted as χ.

$$\chi = s^2. \tag{5.13}$$

If the distribution of s is assumed to be Gaussian, then χ will have a chi-square distribution [47]. The distribution is given by in terms of mean (μ_s) and variance (σ_s^2) of segment sum

$$p_{\chi}(x) = \frac{1}{\sqrt{2\pi\sigma_s^2 x}} e^{-\frac{x+\mu_s^2}{2\sigma_s^2}} \cosh\left(\frac{\mu_s\sqrt{x}}{\sigma_s^2}\right), \tag{5.14}$$

Equations for the mean (μ_χ) and the variance (σ_χ) of χ are given by [42]

$$\begin{aligned} \mu_\chi &= \sigma_s^2 + \mu_s^2, \\ \sigma_\chi^2 &= 2\sigma_s^2(\sigma_s^2 + 2\mu_s^2). \end{aligned} \tag{5.15}$$

Figure 5.7 shows the resulting chi-square distribution for the two example cases. It is evident from Figure 5.7 that the non-aligned case has a lower probability of having a large squared sum.

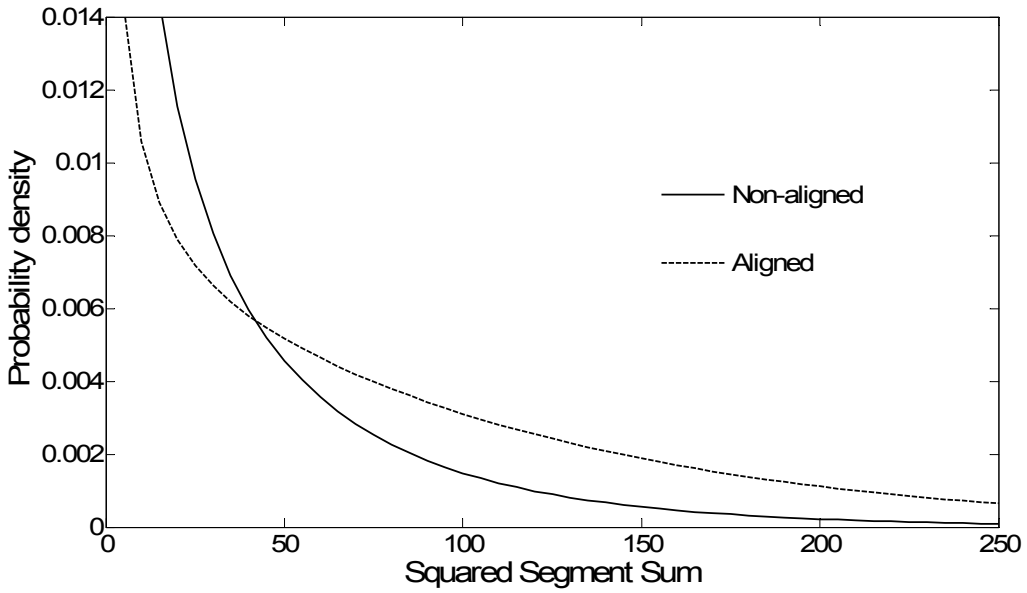

Figure 5.7 pdfs of segment squared random variable with 25 co-users. From [42].

If the Gaussian approximation is used for the segment sum, and assuming that errors in different segments are statistically independent and identically distributed, then summing over n segments will result in chi-square pdf with n degrees of freedom [48].

For a large value of *n*, the central limit theorem states that the resulting pdf can be approximated by a Gaussian distribution with mean (μ_{SMF}) and variance (σ^2_{SMF}) as illustrated in Figure 5.8 [49]

$$\begin{aligned} \mu_{SMF} &= n\mu_{\chi}, \\ \sigma^2_{SMF} &= n\sigma^2_{\chi}. \end{aligned} \tag{5.16}$$

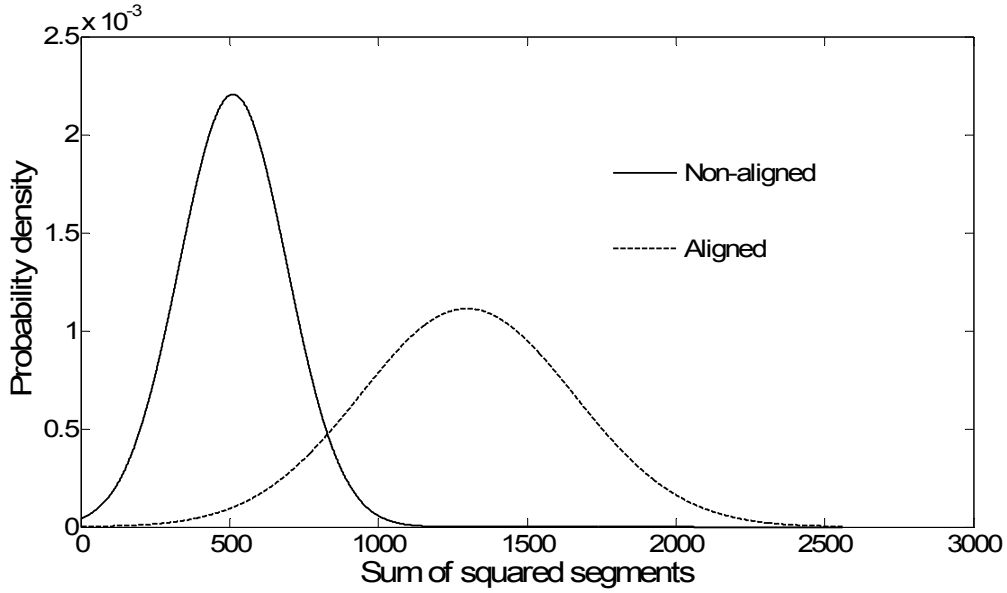

Figure 5.8 Gaussian approximation of 16 segments summation with 25 co-users and coherent detection. From [42].

Due to the low signal-to-noise ratio in the channel of a typical CDMA system, codephase acquisition must be performed non-coherently. In-phase and quadrature (I-Q) arrangement of SMFs are employed at the code acquisition block at the receiver. Equations for the mean ($\mu_{IQ,\,SMF}$) and the variance ($\sigma^2_{IQ,\,SMF}$) of the IQ-SMF test variable (*u*) are given by

$$\begin{aligned} \mu_{IQ,\,SMF} &= \mu_{I,\,SMF} + \mu_{Q,\,SMF}, \\ \sigma^2_{IQ,\,SMF} &= \sigma^2_{I,\,SMF} + \sigma^2_{Q,\,SMF}. \end{aligned} \tag{5.17}$$

where $\mu_{I,\,SMF}$ and $\mu_{Q,\,SMF}$ are the mean of μ_{SMF} in the in-phase and quadrature phase SMFs respectively and $\sigma^2_{I,\,SMF}$ and $\sigma^2_{Q,\,SMF}$ are the variance of σ^2_{SMF} in the in-phase and quadrature phase SMF respectively.

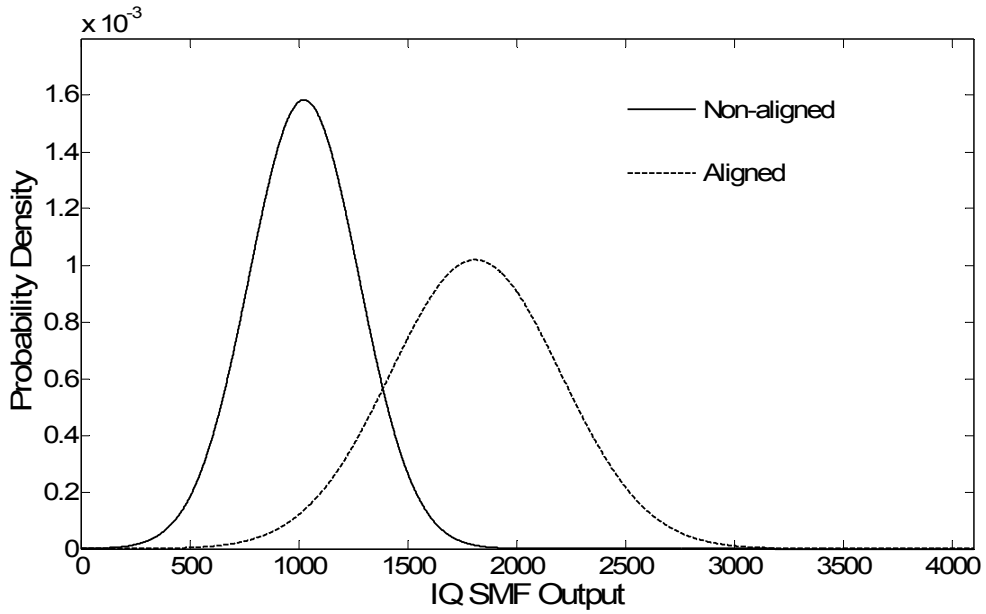

Figure 5.9 I-Q SMF output distribution with 25 co-users and non-coherent detection. From [42].

5.5 Frequency Offset

In case of frequency offset due to the motion or frequency offset at the receiver, the baseband signal spectrum is offset from 0 Hz. Carrier frequency shift causes a reduction in SMF output for the aligned codephase and shifts the aligned pdf towards the non-aligned pdf. A degradation factor (DF_d) of the matched filter output due to the carrier frequency offset is given by [43]:

$$DF_d = \left| \frac{\sin(M 2\pi f_d / 2 f_c)}{M \sin(2\pi f_d / 2 f_c)} \right|^2 = \left| \frac{\sin(M \pi f_d T_c)}{M \sin(\pi f_d T_c)} \right|^2 \tag{5.18}$$

where M is the segment length, f_d is the carrier frequency offset, f_c is the chip rate and T_c is single chip duration.

In [42], simulations were carried out to analyze the effect of carrier frequency offset on the chip error rate. Chip error rate is then given by

$$P_{ce} = Q\left(\frac{\sqrt{DF_d}}{\sqrt{\frac{\text{number of active interfering users}}{2}}} \right). \tag{5.19}$$

Figure 5.10 illustrates the degradation factors at various carrier frequency shifts. Figure 5.11 illustrates aligned and non-aligned pdfs with 25 co-users' interfering signals at 0 kHz, 10 kHz, and 15 kHz of carrier frequency offset respectively [42].

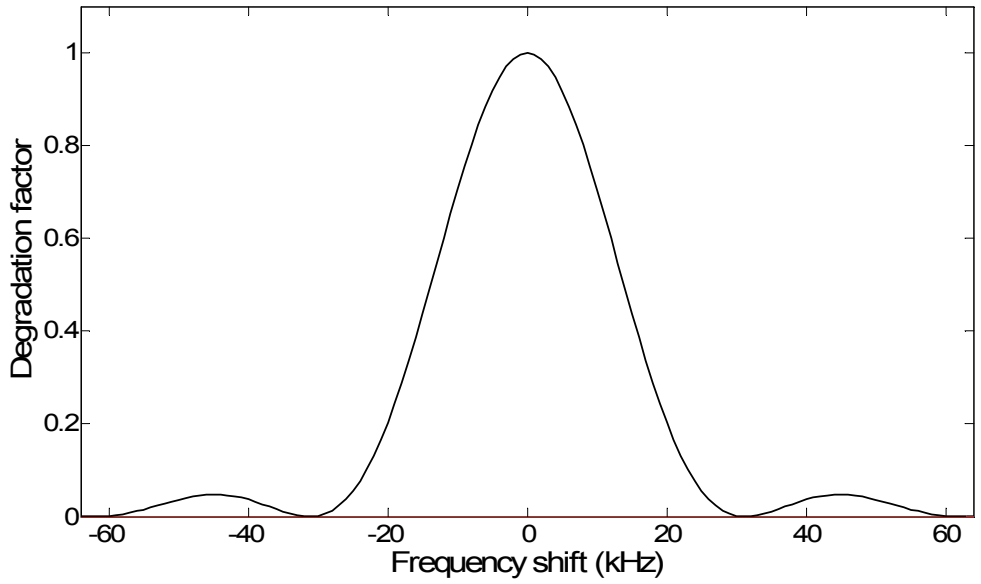

Figure 5.10 Degradation factor vs. carrier frequency offset

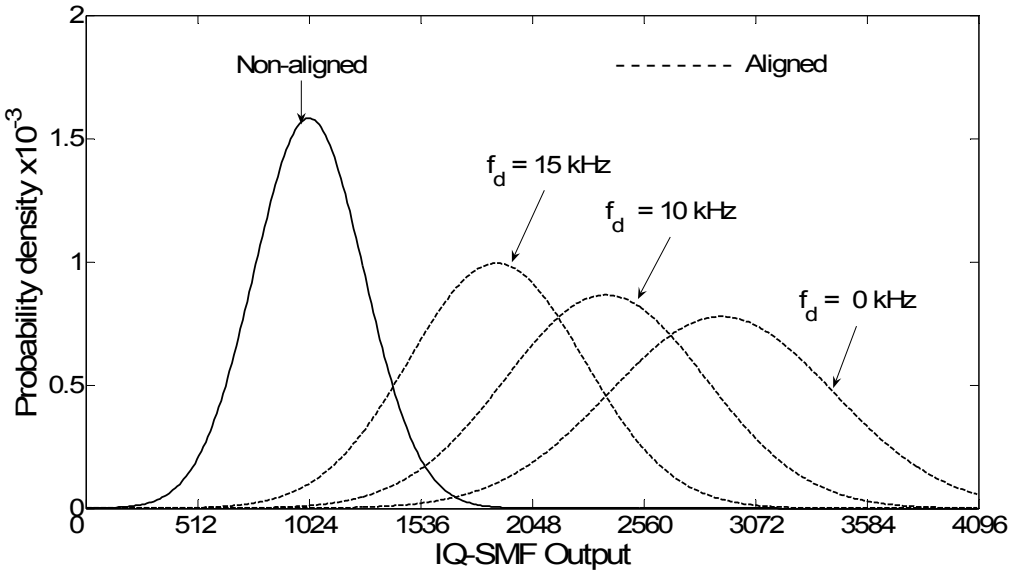

Figure 5.11 Aligned and non-aligned pdfs at various f_d. From [42].

5.6 Simulation

Simulations results are compared with the analytical results found from Equation 5.16. In the simulation, a period of PN code sequence is repeated for 10^6 times and chip errors were introduced in the sequences. Random data bits were generated and each data bit is multiplied with a sequence of 64 chips in the generated PN code sequence in order to modulate the PN codes with the random data bits. Then for every code cycle, errors were introduced at the random chip positions of the sequence. In doing so, we are able to simulate the detection errors which happen in the practical pre-acquisition block at the receiver. The induced errors in the chip sequence depend on the number of interfering users and the value of the carrier frequency offset at the receiver.

Figure 5.12 and Figure 5.13 illustrate the pdfs obtained from simulation and analytical equations. Simulations with 25 interfering co-users have been carried out for no data modulation and for random data modulation at 0 kHz and 10 kHz carrier

frequency offsets in each case. The number of simultaneous users can't possibly be greater than the value of the spreading gain (i.e. 64) and the performance starts to degrade when the number of simultaneous users exceeds about half that number. Consequently, the simulations were performed with 25 simultaneous users.

Simulation results obtained for PN codes with no data modulation closely match with the simulation data obtained in [42 (page 113, 114)]. New simulations were carried out for PN codes with random data modulation. As described in Chapter 4 that SMF is able to perform codephase acquisition with data-modulated PN codes. Similar probability distributions for aligned and nonaligned codephases have been obtained for both 0 kHz and 10 kHz carrier frequency offsets.

Table 5.1 Simulation Parameters

Number of trails	10^6
PN code sequence length	512 chips
Data bits	All 1's and random
Spreading Gain, N_C	64
Number of simultaneous users	25
Carrier frequency Offset	0 kHz and 10 kHz
SMF length	512 chips
Number of segments	16
Each segment length	32 chips

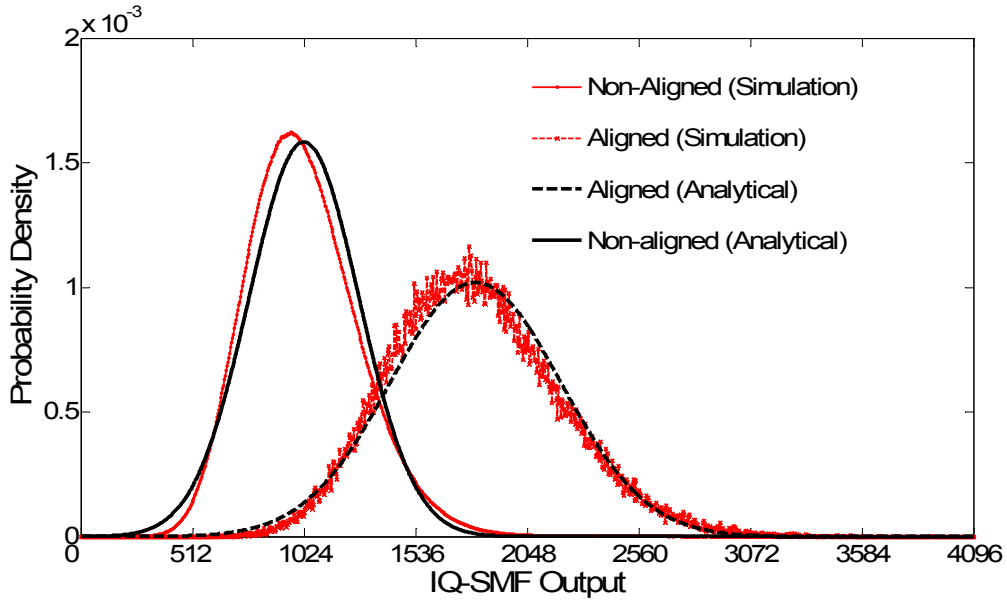

(a)

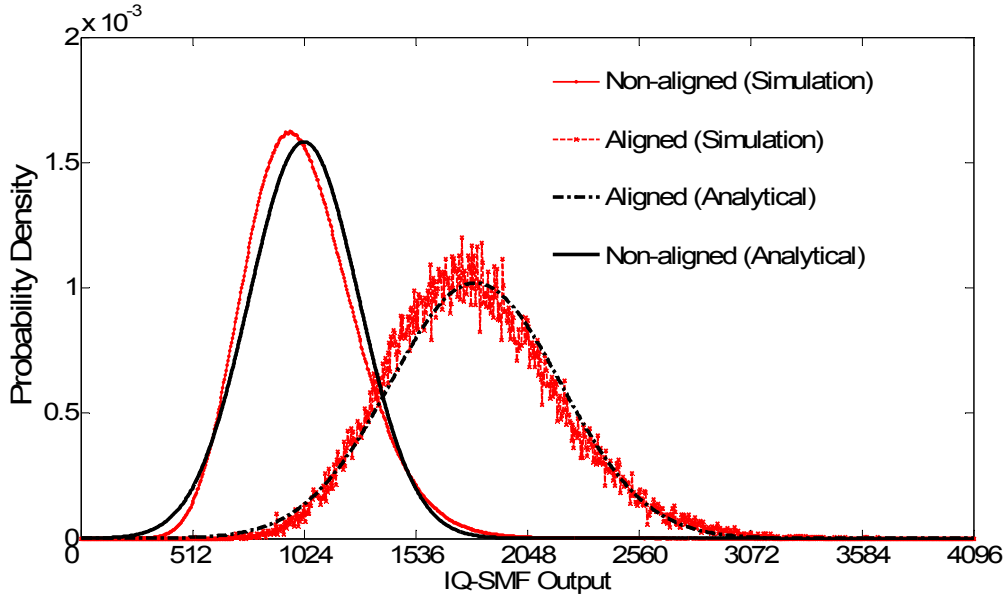

(b)

Figure 5.12 Aligned and non-aligned pdfs (a) no data modulation. Adapted from [42]. (b) random data modulation at f_d = 0 kHz

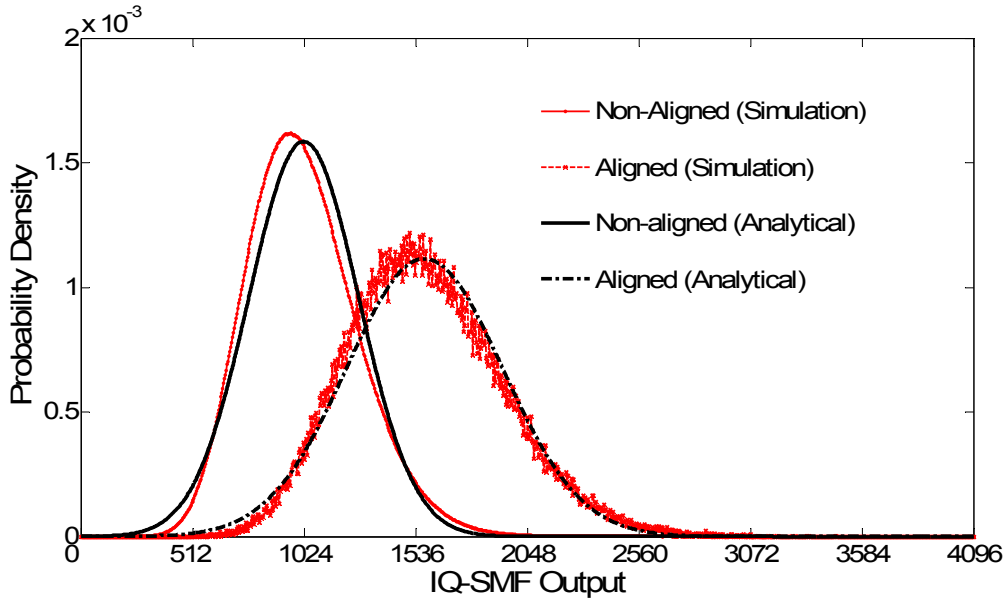

(a)

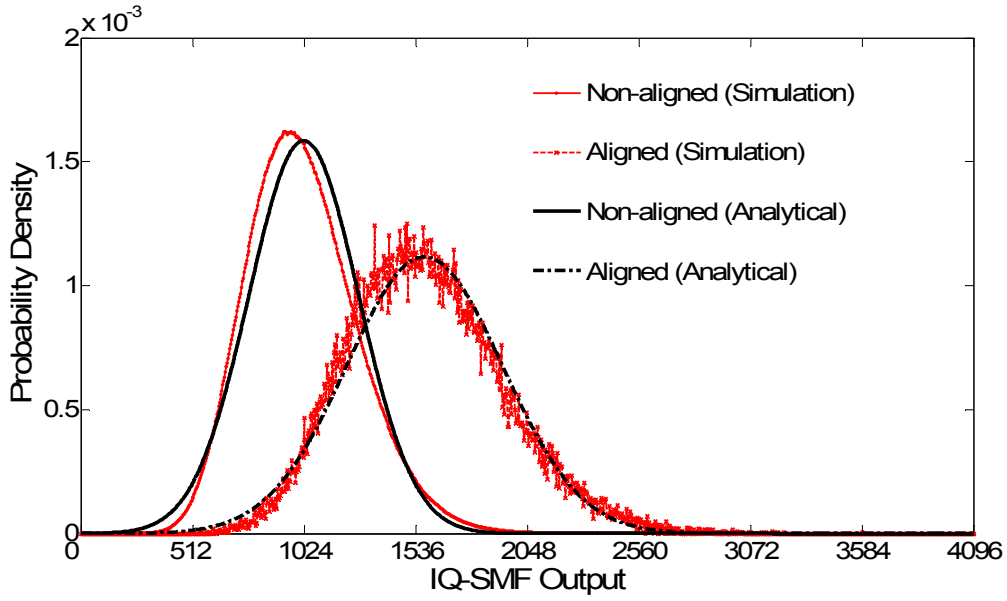

(b)

Figure 5.13 Aligned and non-aligned pdfs (a) no data modulation. Adapted from [42]. (b) random data modulation at at f_d = 10 kHz

5.7 Acquisition by Threshold Crossing Criterion

In the threshold crossing (TC) criterion, the I-Q SMF test variable (u) is compared to a threshold ξ and, if the threshold is crossed, the hypothesis of having acquired synchronism is made. Formally, it is defined in [50].

Choose codephase(j) if $u(j) \geq \xi$, else go to next codephase

With a threshold in place, two detection probabilities are determined as shown in Figure 3.3. The area under the non-aligned pdf above the threshold is the probability that a non-aligned codephase will be mistakenly selected as aligned codephase. This condition is known as a false alarm (P_f). The area under the aligned pdf below the threshold is the probability that the receiver will miss detection of the correct codephase (P_m).

5.7.1 Mean Acquisition Time

In order to estimate the mean time to acquisition, the following equation is used [43]:

$$T_{acq} = \left(\frac{1}{P_d^2} - \frac{1}{2}\right) q T_1 + P_f \left(q-1\right)\left(\frac{1}{P_d^2} - \frac{1}{2}\right) T_3 + \frac{1}{P_d} T_2 \tag{5.20}$$

where P_d is the probability of correct detection, q is the number of samples per code cycle, T_1 is the sample period, T_2 is the code cycle period. T_3 is calculated by the following equation [43]:

$$T_3 = \left(\frac{1}{1-P_F}\right) T_2 \tag{5.21}$$

In the above equation, term 1 is the time spent in searching for the aligned codephase before a correct decision is made. Term 2 is the time spent in all false alarm states. Term 3 is the time spent to verify a correct decision.

5.7.2 Simulation Results

The probability of detection (P_d) and the probability of false alarm (P_f) vs. I-Q SMF threshold value are illustrated in Figure 5.14 with 25 co-users at 0 kHz and 10 kHz of carrier frequency offsets respectively. Best results are obtained with high ratio of P_d to P_f.

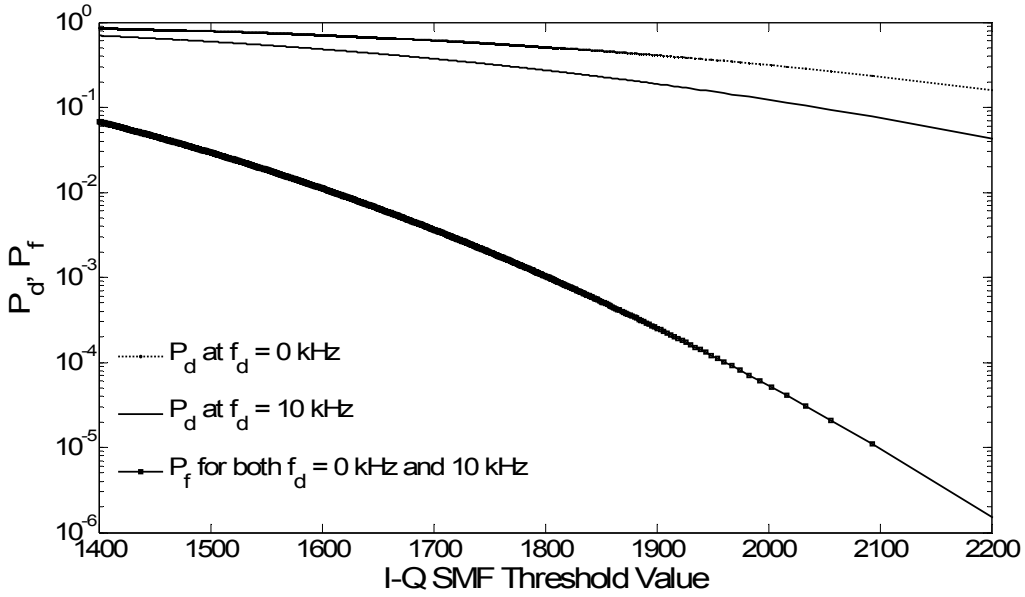

Figure 5.14 P_d and P_f vs. I-Q SMF threshold value at 0 kHz and 10 kHz carrier frequency offsets respectively

Figure 5.15 and Figure 5.16 shows the probability of detection vs. number of co-users and the probability of false alarm vs. number of co-users for various threshold values at 0 kHz and 10 kHz carrier frequency offsets respectively. Mean acquisition time for various threshold values with 25 co-users are shown in Figure 5.17.

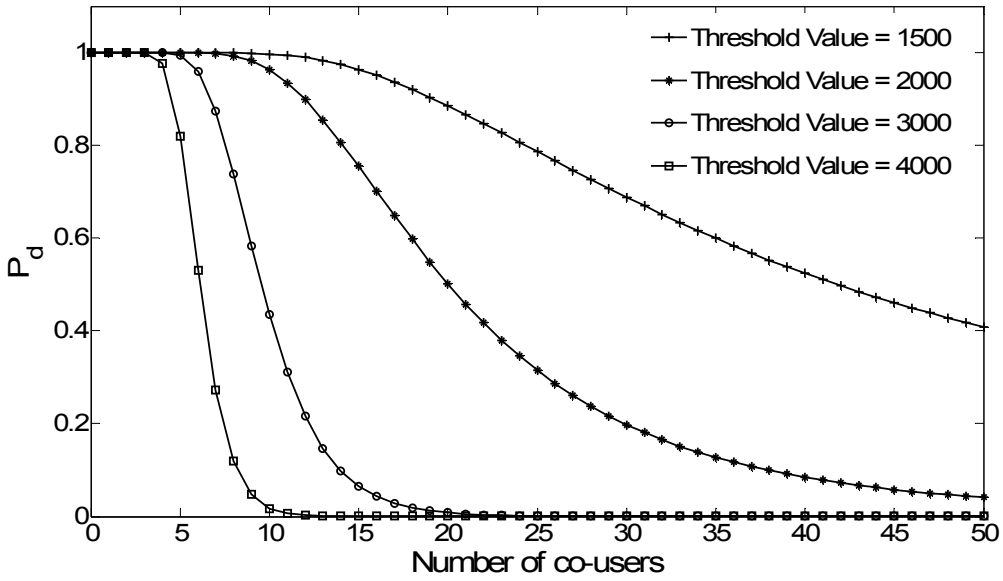

(a)

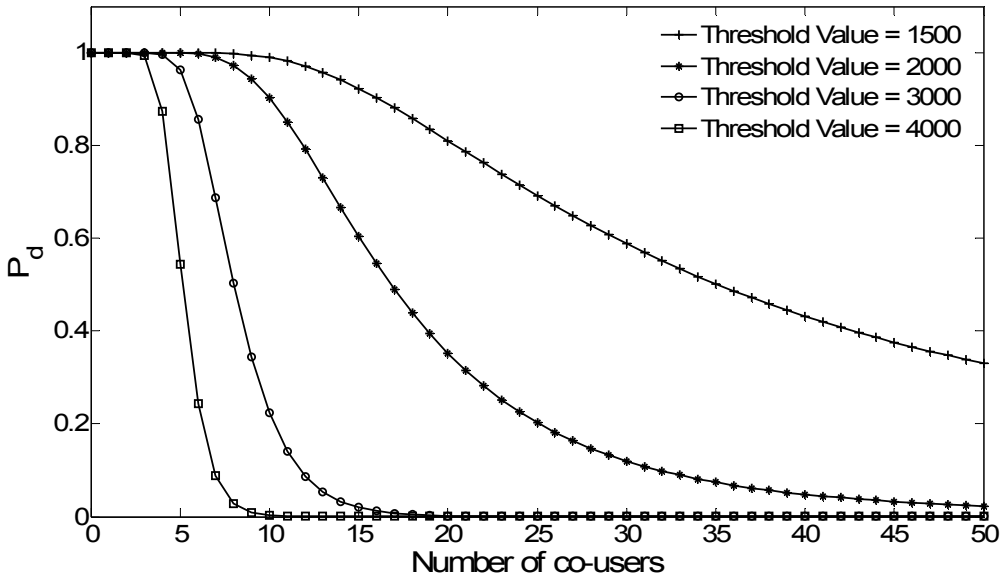

(b)

Figure 5.15 Probability of detection at various levels of co-users (a) f_d = 0 kHz and (b) f_d = 10 kHz

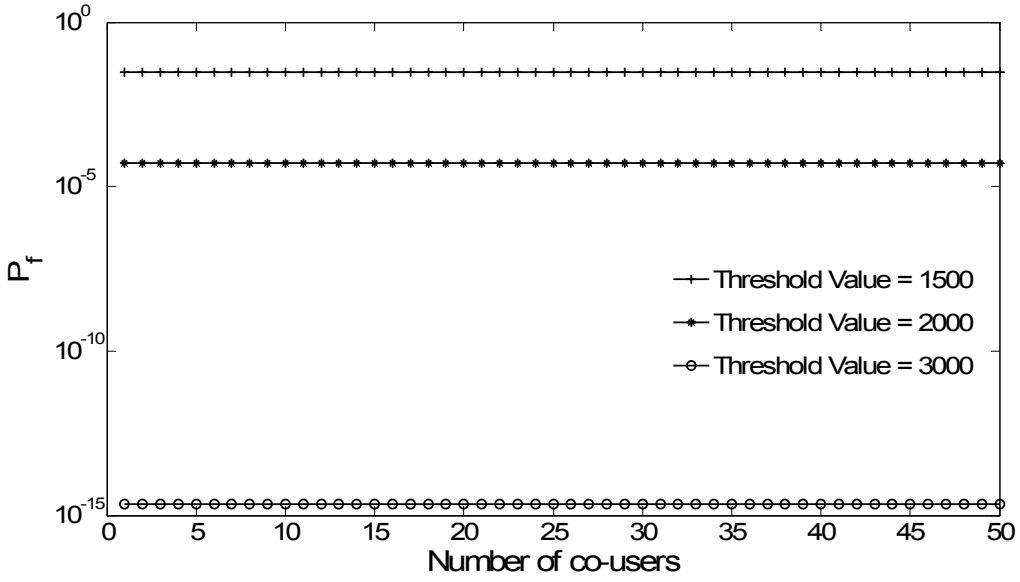

(a)

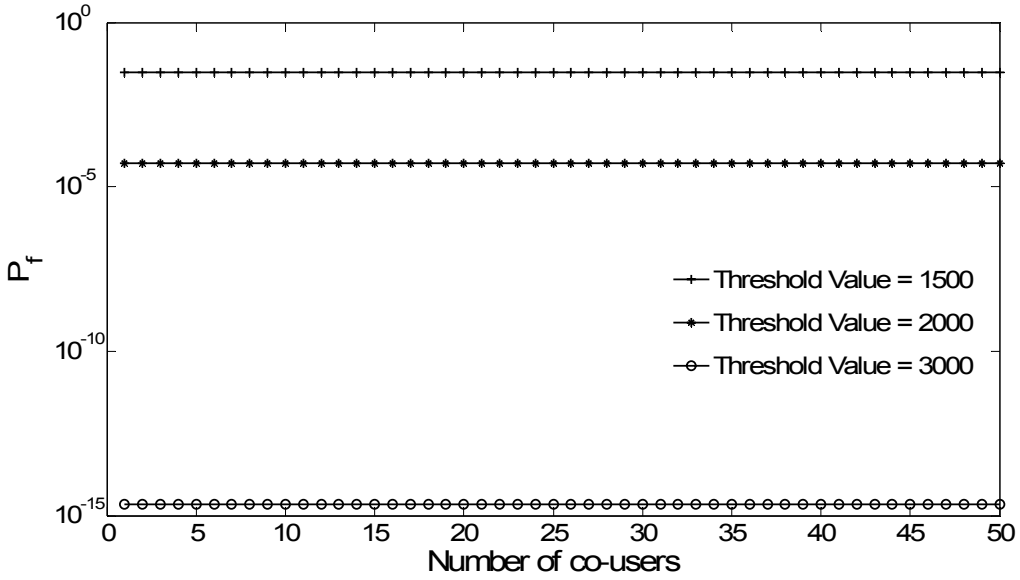

(b)

Figure 5.16 Probability of false alarm at various levels of co-users (a) f_d = 0 kHz and (b) f_d = 10 kHz

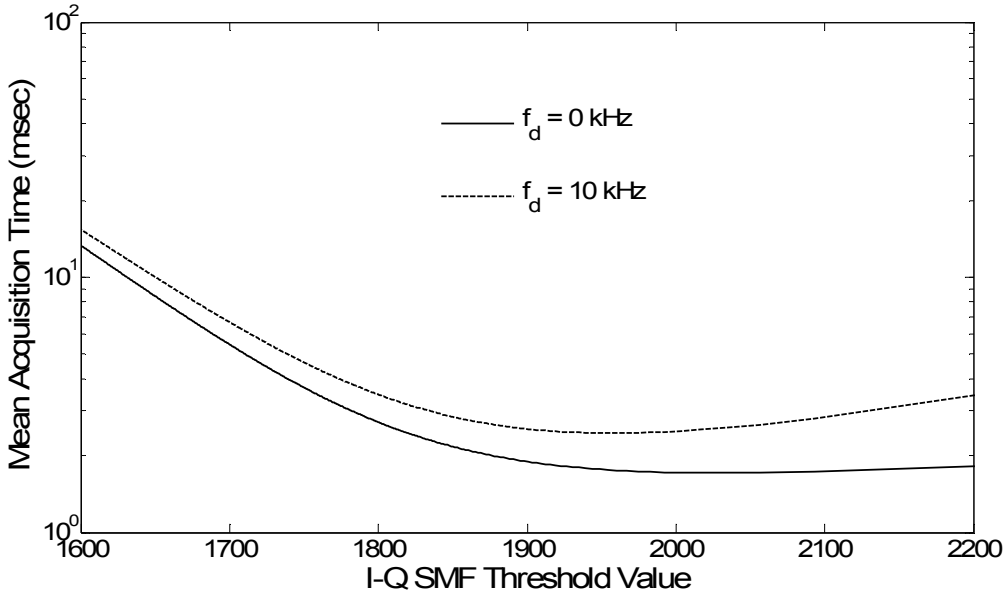

(a)

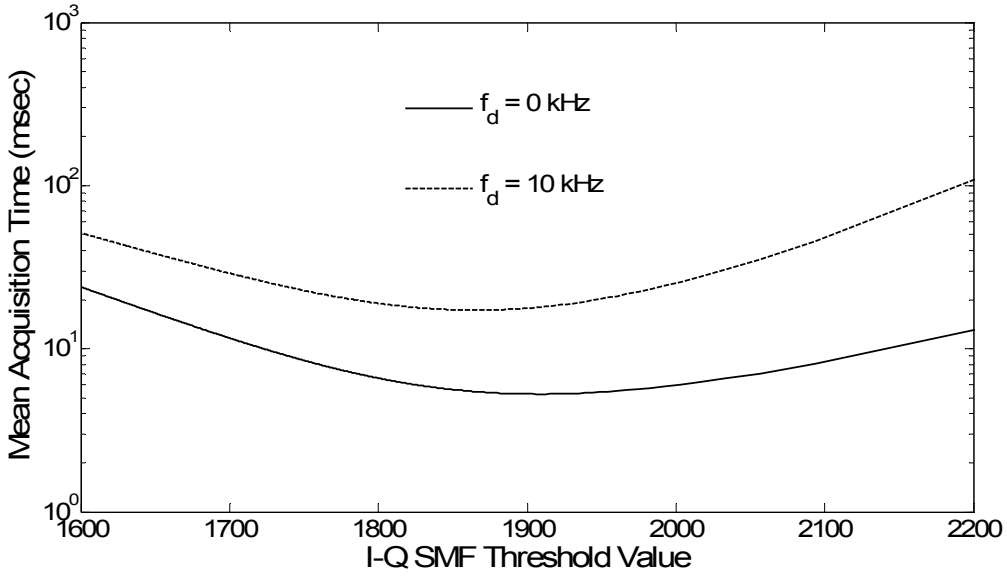

(b)

Figure 5.17 Mean acquisition time as a function of I-Q SMF Threshold values with (a) 10 (b) 25 co-users respectively.

For the calculation of P_d and mean acquisition time, the following parameters have been considered: chip rate = 1 MHz, single code cycle duration = 1 msec, packet length = 64 code cycles = 64 msec. I-Q threshold value must be selected very carefully because as shown in Figure 5.17, mean acquisition time is excessively high for low and high values of threshold. For some cases, mean acquisition time is even greater than the entire packet duration. This happens due to the fact that low false alarm probability for certain threshold values leads to high acquisition time.

5.8 Acquisition by Maximum Likelihood and Accumulation Criterion

A very accurate estimation of the received code phase can be obtained by comparing the test variables from all codephases in the uncertainty region and selecting the maximum. Maximum likelihood criterion performs faster acquisition than the threshold crossing method, but it requires more hardware [42]. In the simplest implementation of this criterion, the maximum output samples from the SMF are measured during one complete cycle of the code sequence. It is assumed that the maximum sample is occurred for the aligned codephase. In order for correct codephase to be selected, the aligned sample must exceed the maximum of all of the non-aligned samples over the entire code cycle [42].

The probability of detection is defined as below

$$P_d = P(O_A - \max(O_{NA}) > 0), \tag{5.22}$$

where O_A and O_{NA} are the output samples from the SMF for the aligned and non-aligned conditions respectively.

The pdf for maximum non-aligned case is determined in order to calculate P_d. Since different non-aligned samples within each code cycle are virtually uncorrelated, the cumulative distribution function for maximum non-aligned sample is given by [47]

$$F_{\max(O_{NA})}(x) = F_{O_{NA}}^{L-1}(x), \tag{5.23}$$

where L is the length of the code sequence and $L-1$ is the number of non-aligned samples per cycle.

Figure 5.18 shows the pdfs for aligned, non-aligned and max non-aligned cases and Figure 5.19 shows the area corresponding to P_d and P_f.

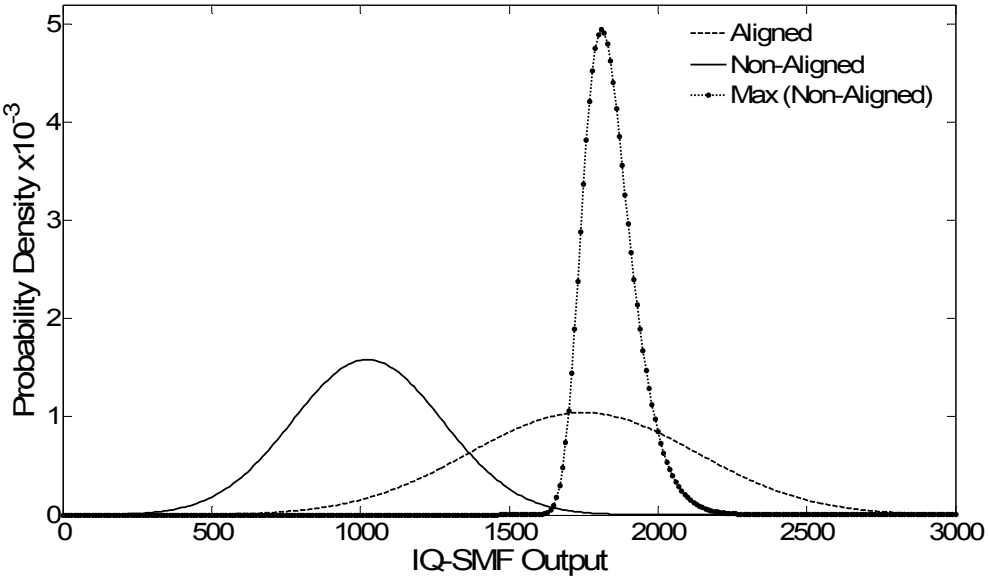

Figure 5.18 pdfs of aligned, non-aligned and maximum non-aligned samples in a code cycle with 25 co-users and f_d = 0 kHz. Adapted from [42].

In order to improve P_d, the SMF output samples at each codephase are accumulated over several code cycles. It is assumed that code Doppler is negligible [40]. For accumulation up to J code cycles, the means of the two pdfs become J times greater,

but the standard deviation σ only increases by a factor of $\sqrt{J}$. This ensures higher probability of detection [51]. P_d at various values of accumulated code cycles is illustrated in Figure 5.19. P_d vs. number of co-users for various values of accumulated code cycles are shown in Figure 5.20.

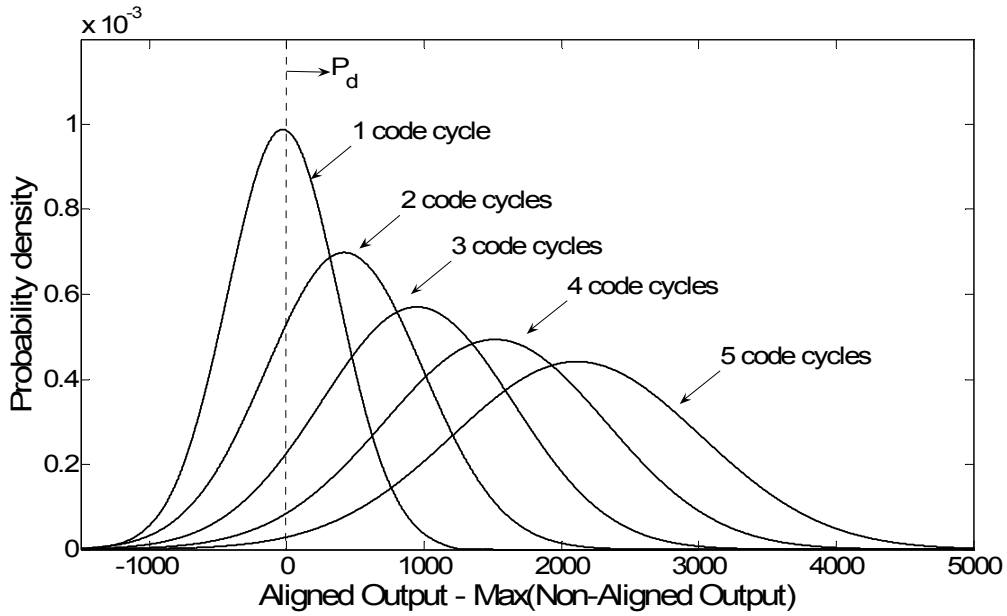

Figure 5.19 P_d as a function of number of accumulated code cycles at f_d = 0 kHz.

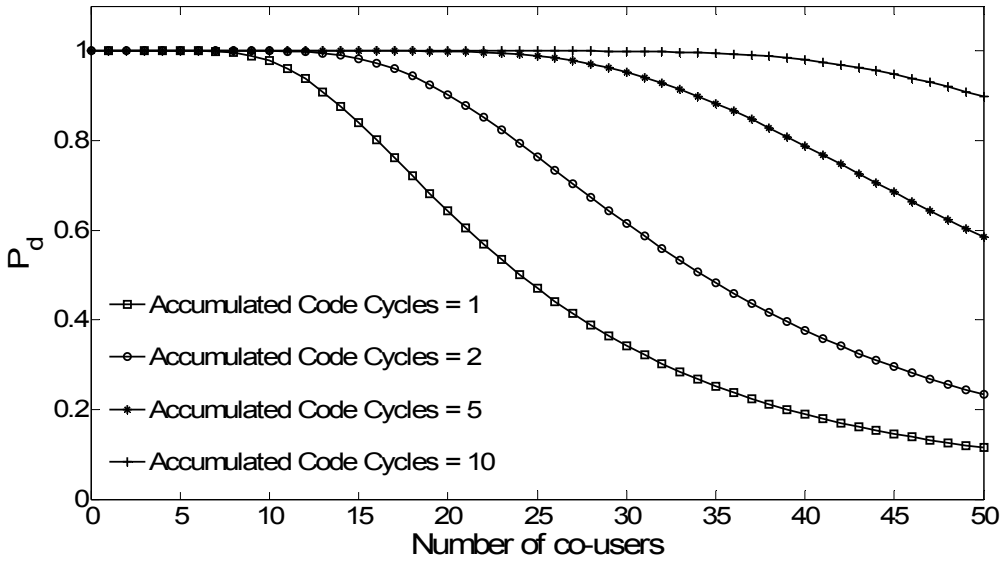

(a)

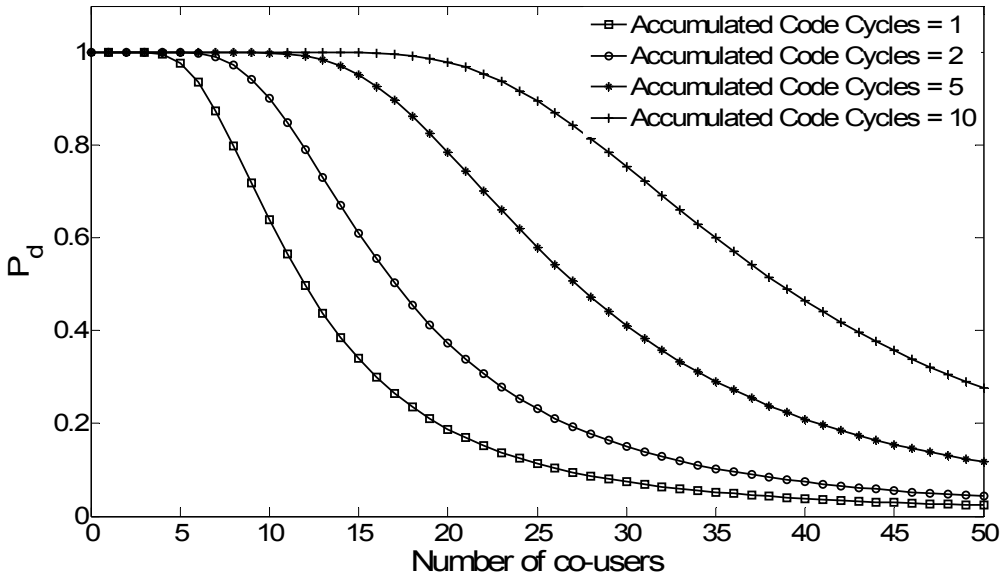

(b)

Figure 5.20 P_d vs. number of co-users at (a) f_d = 0 kHz, and (b) f_d = 10 kHz.

5.8.1 Mean Acquisition Time

The acquisition time for maximum likelihood and accumulation criterion depends on the number of accumulated code cycles for an aligned codephase to be detected. Calculation of the average acquisition time requires the evaluation of the detection probability as a function of the number of accumulated code cycles [51].

Figure 5.21 and Figure 5.22 show the cumulative distribution function (cdf) and pdfs of P_d as a function of the number accumulated code cycles at 0 kHz and 10 kHz of carrier frequency offsets respectively. From the above distribution, the mean is calculated. Estimated means are 1.89 and 3.03 code cycles for 0 kHz and 10 kHz carrier frequency offsets, respectively. Each code cycle is of 1 msec duration. Therefore, the mean acquisition times for these cases are 1.89 msec and 3.03 msec respectively. Mean acquisition time vs number of co-users is shown in Figure 5.23.

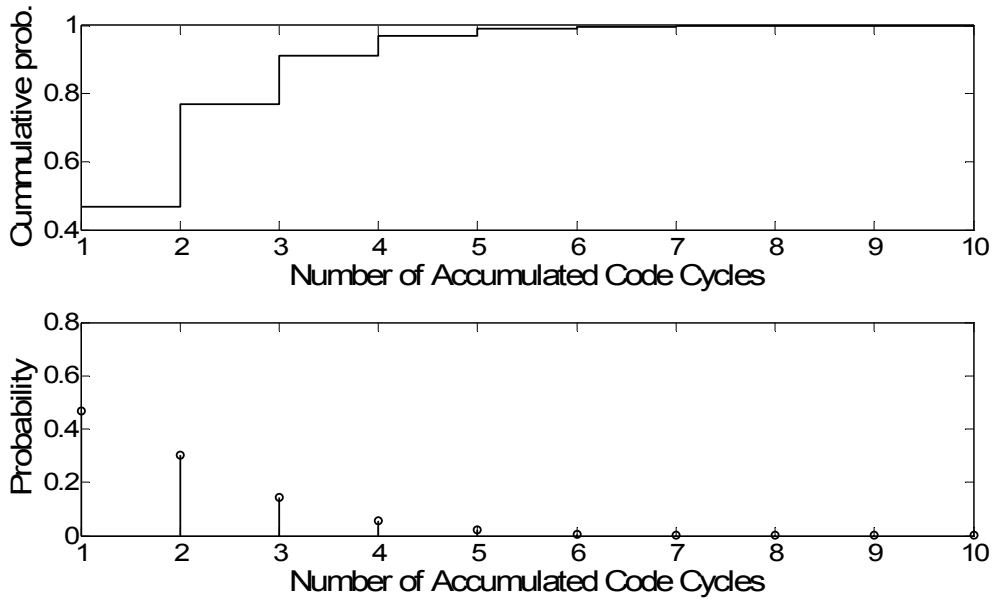

Figure 5.21 P_d vs. number of accumulated code cycles for 25 co-users at f_d = 0 kHz.

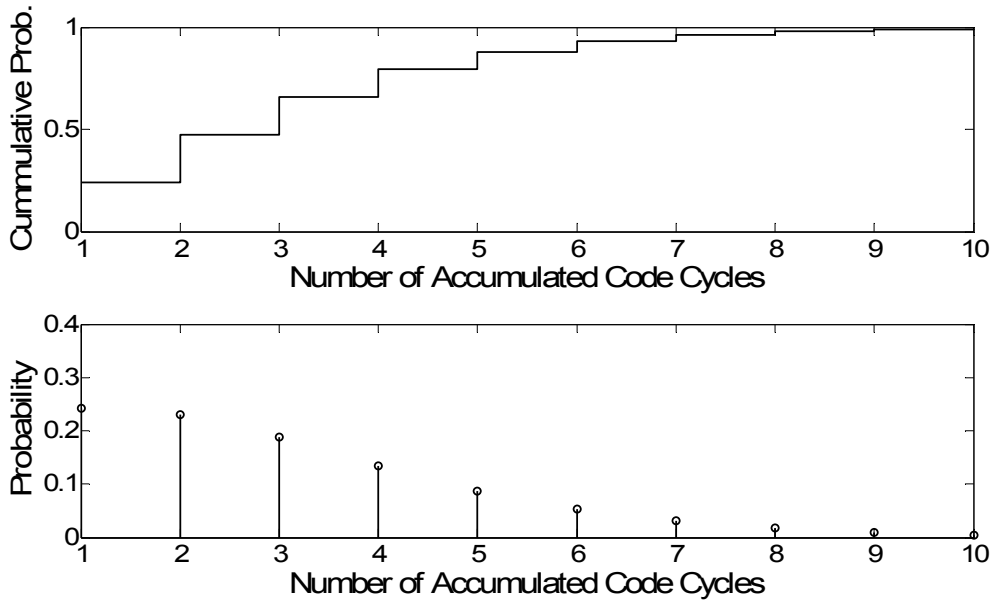

Figure 5.22 P_d vs. number of accumulated code cycles for 25 co-users at f_d = 10 kHz.

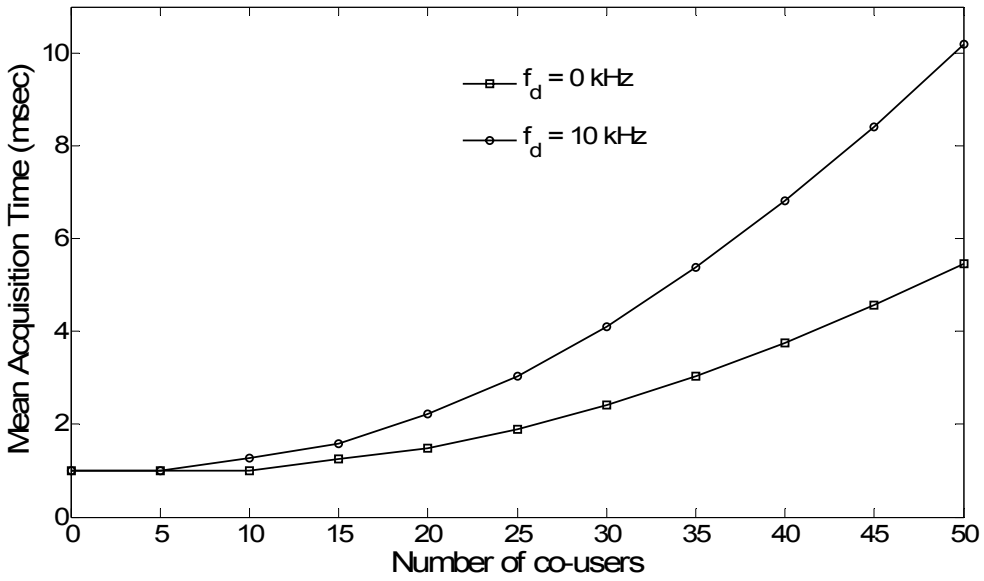

Figure 5.23 Mean acquisition time as a function on number of co-users.

From Figure 5.17(b) and Figure 5.23, mean acquisition times are found to be 6 msec (6 code cycles) and 1.9 code cycles for threshold crossing and maximum likelihood detection criteria respectively. Since the initial portion of the packet is stored in the memory for acquisition purpose, it is desired to reduce the mean acquisition time. For a 1000 data bit packet length, the whole packet consists of approximately 64 code cycles since 1 code cycle is of 1024 chips length and each data contains 64 chips (i.e. spreading gain, N_c = 64). Figure 5.23 shows the mean acquisition time in terms of code cycles within a packet structure.

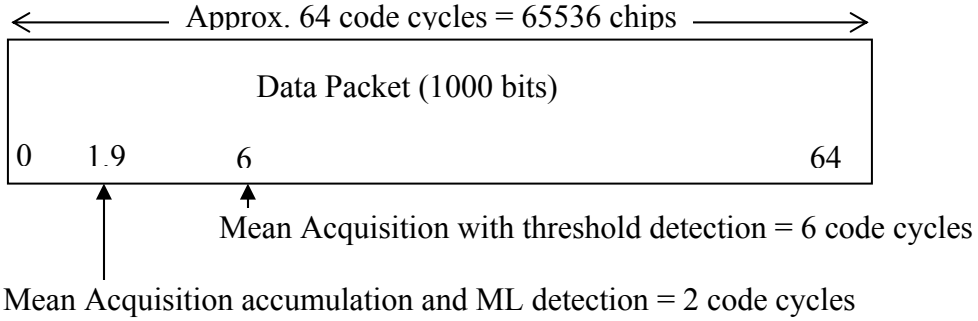

Figure 5.24 Mean acquisition time for 25 co-users at 0 kHz carrier frequency offset.

Although the illustration shows a 1000 bit (125 byte) packet, many packets from a portable telephone will be shorter. Packets carrying ATM cells require only 424 bits (53 bytes). Many transmissions will be simple mouse clicks or Yes/No keystrokes that require less than 64 bits (8 bytes) - 4 code cycles. In this case, there is great advantage in eliminating the preamble and there is also need to employ the fastest possible acquisition method.

5.9 Packet Throughput

Throughput is defined at the number of packets correctly decoded at the receiver. In a traditional packet system, error control coding is incorporated in the packet so that error-free data is decoded at the receiver. Collision-free packets are received correctly at the node as successful packets. Error detection at the receiver allows the collision-corrupted packets to be detected and rejected at the receiver. As a result, the communication channel turns out to be useless when two or more transmitters send packets simultaneously. Lost packets can not be recovered in this case regardless of the amount of error correction capability. If the errors in the data bits of the packets are distributed uniformly among all desired packets received over a period of time, the error control code is able to recover most of the packets transmitted [52]. Inclusion of error control increases in the data packet length L_D and reduces the actual data throughput. If M message bits are to be encoded into a packet of length L_D with a block error control code capable of correcting t errors then $L_D - M$ represents the redundancy in the data packet due to the inclusion of error correction capability.

If a packet of length L_D is transmitted with average probability of data bit success $Q_e = 1\text{-}P_e$, and if the packet includes block error control code with error correction capability of t or fewer errors, then the probability of packet success is given in [52]:

$$P_C(k_p) = g(1 - P_e(k_p); L_D, t) \tag{5.24}$$

where k_p is number of acquired packets, $P_e(k_p)$ is the probability of a data bit error and t is the error correcting capability of the block code used in the packet. $P_C(k_p)$ vs. k_p is plotted in Figure 5.27.

$P_e(k_p)$ is calculated by the widely-used standard Gaussian approximation [53]. This approximation assumes equal received power for all interfering signals, random co-users' spreading sequences, data bit errors due to only multiple-access interference (MAI) and negligible thermal noise. $P_e(k_p)$ and $g(x; L_D, t)$ are given by the following equations [53] (Figure 5.25 and Figure 5.26):

$$P_e(k_p) = Q\left(\sqrt{\frac{3N_c}{k_p - 1}}\right). \tag{5.25}$$

$$g(x; L_D, t) = \sum_{i=0}^{t} \binom{L_D}{i} (1-x)^i \, x^{L_D - i}. \tag{5.26}$$

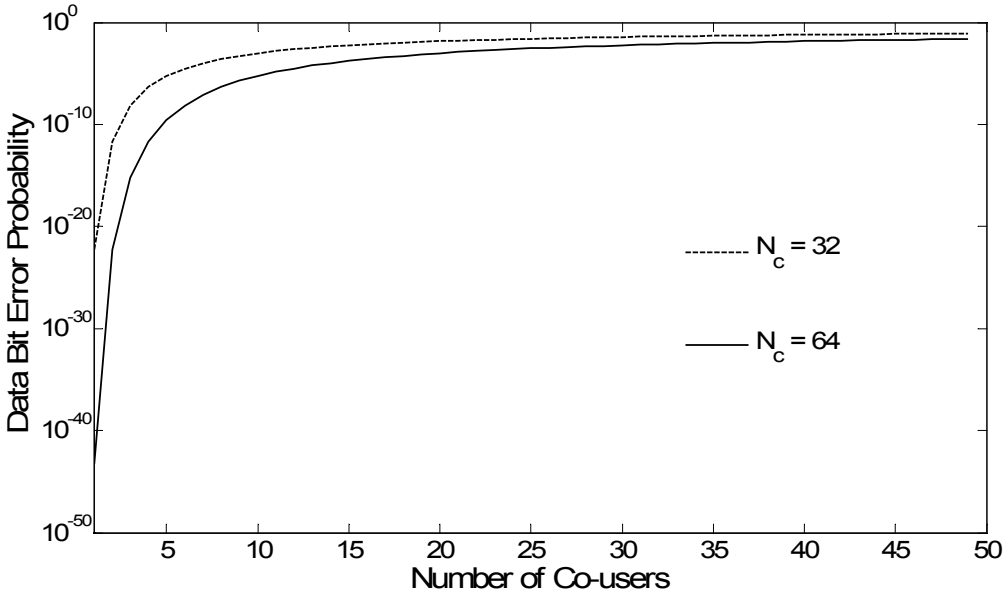

Figure 5.25 Probability of data bit error versus the number of co-users.

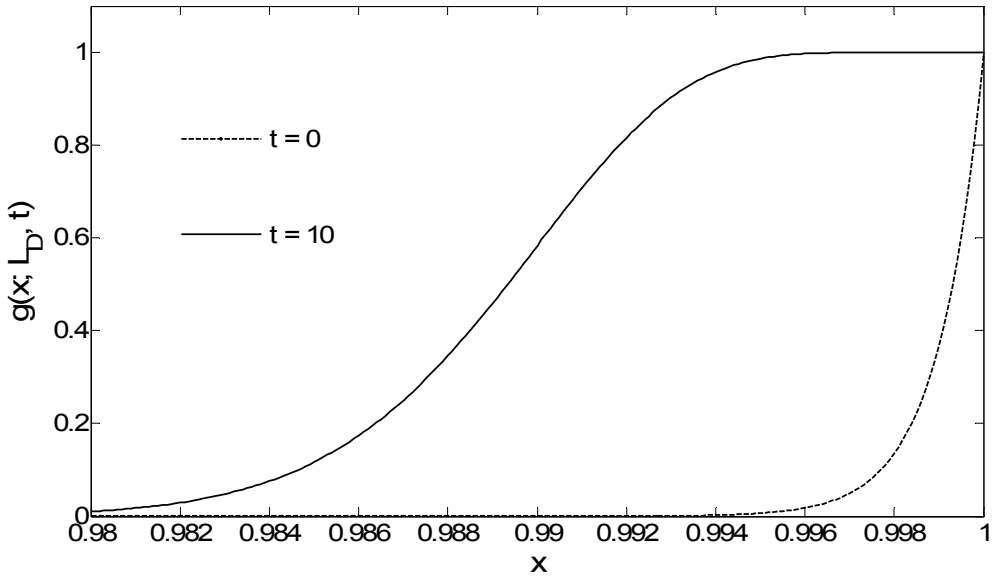

Figure 5.26 Packet success probability $g(x; L_{D,} t)$ with spreading gain $N_c = 64$.

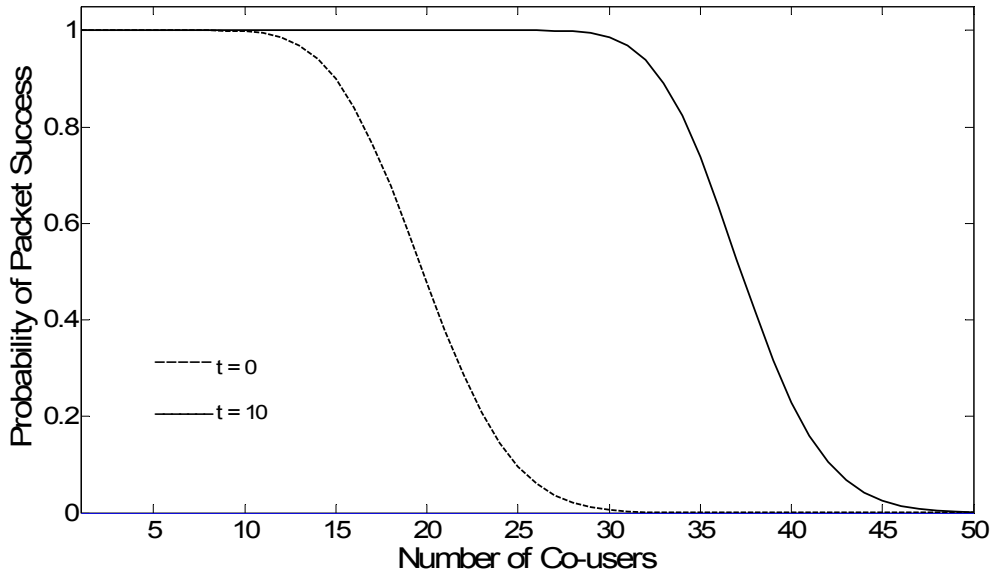

Figure 5.27 Probability of packet success versus the number of co-users.

Since packet CDMA systems exploit the multi-user access capability of CDMA systems, packets are not vulnerable to overlap-related degradation. Still, packet CDMA systems have data bit errors caused by the multiple-access interference. In order for a successful packet reception, two conditions need to be fulfilled - (i) successful PN code acquisition and (ii) no data errors in the packets. It is assumed that, once a packet is successfully acquired; there is no loss in the code tracking operation that follows the coarse acquisition process.

For k_p packets in a given transmission, the probability of the number of successful packets $S = s$, conditioned on the event that A packets out of k_p are acquired is given in [54]:

$$\Pr(S = s \mid k_p, A) = \binom{A}{s} P_C^s\left(k_p\right) P_E^{A-s}\left(k_p\right), \tag{5.27}$$

where $P_C(k_p)$ and $P_E(k_p)$ are the probabilities of packet success and failure, respectively. $P_C(k_p)$ and $P_E(k_p)$ are related by the following equation:

$$P_C(k_p) = 1 - P_E(k_p) \tag{5.28}$$

The throughput is defined as the expected value of S. It is given in [55]:

$$\beta = \mathrm{E}[\mathrm{S}] = \mathrm{E}_K[k_P P_C(k_p) P_d(k_p)] \tag{5.29}$$

where $\mathrm{E}_X[.]$ represents the expectation with respect to the random variable X.

The throughput of packet CDMA under the assumption of perfect acquisition is given in [55]:

$$\beta = \mathrm{E}_K[k_p P_C(k_p)] \tag{5.30}$$

Therefore, packet success probability is reduced by a factor probability of correct codephase detection, $P_d(k_p)$.

For a fixed capacity of a system (i.e, there are at most C users in the systems) , we will assume that the arrival of packets is binomial distributed. For a system wih K active users transmitting K_p simultaneous packets, throughput is given in [56]:

$$\beta = C \sum_{k_p=1}^{C} \binom{C-1}{k_p-1} P_d(k_p) P_C(k_p) \left(\frac{G}{C}\right)^{k_p} \left(1-\frac{G}{C}\right)^{C-k_p} \tag{5.31}$$

where C is the capacity of the network and G is the offered traffic. For a high utilization application such as video or voice, we assume active users that might tranmit pakets 40% of the time. Figure 5.28, Figure 5.29, and Figure 5.30 assume 50 users with packets loading ranging around 20 simultaneous packets.

For sporadic transmissions such as e-mail traffic, a large number of active users are required to generate the same packet loads on the system. In the case of an infinite-user system, the binomial distribution of the arrival of packets converges to the Poisson distribution [47]. The throughput under this arrival model is given in [52]:

$$\beta = Ge^{-G} P_d(1) P_C(1) + Ge^{-G} \sum_{k_p=1}^{\infty} \frac{G^{k_p}}{k_p!} P_d(k_p+1) P_C(k_p+1) \tag{5.32}$$

Figure 5.30 and Figure 5.31 for 0 kHz and 10 kHz carrier frequency offsets assume an infinite number of users generating a load that ranges around 20 simultaneous packets.

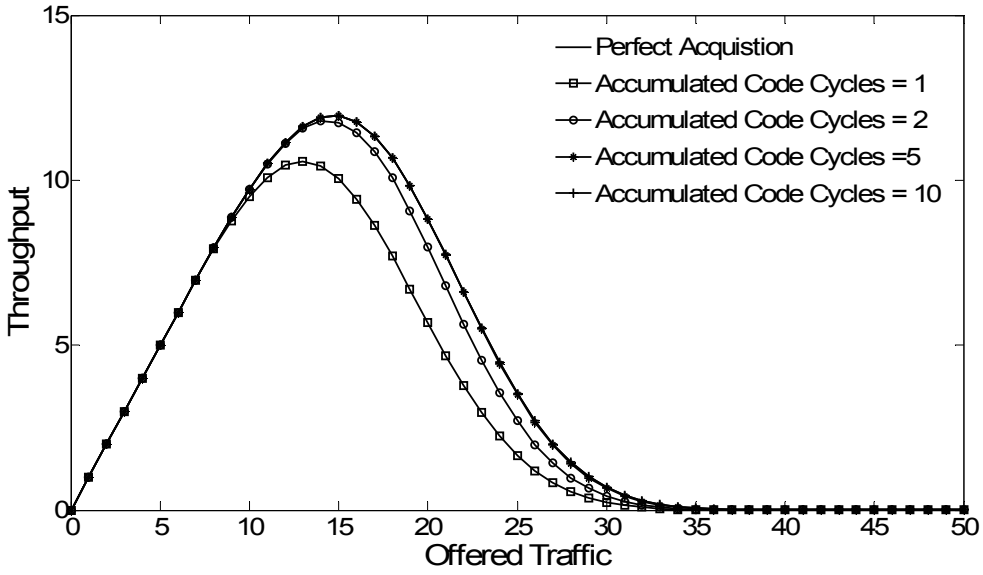

(a)

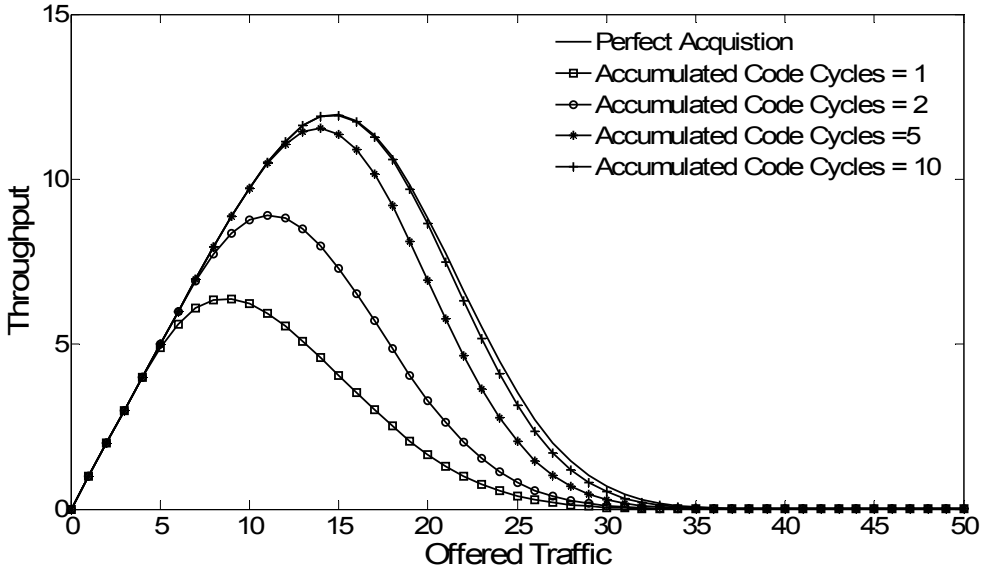

(b)

Figure 5.28 Throughput performance at (a) f_d = 0 kHz and (b) f_d = 10 kHz with t = 0.

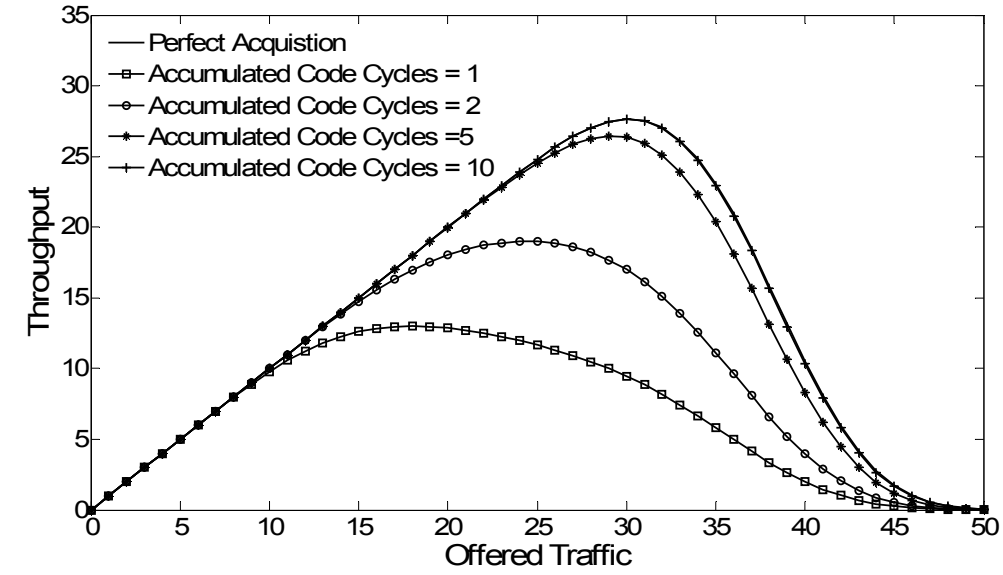

(a)

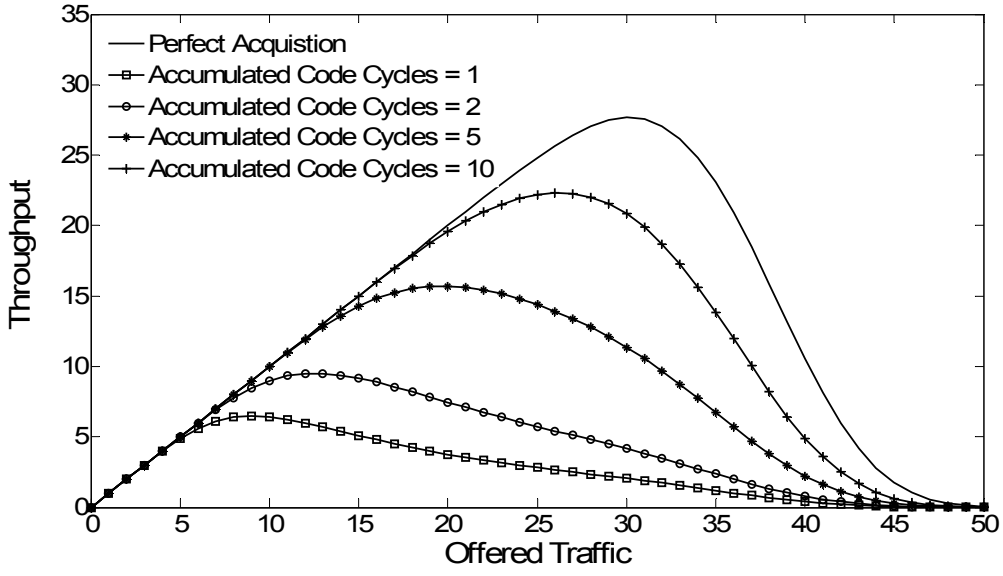

(b)

Figure 5.29 Throughput performance at (a) f_d = 0 kHz and (b) f_d = 10 kHz with t = 10.

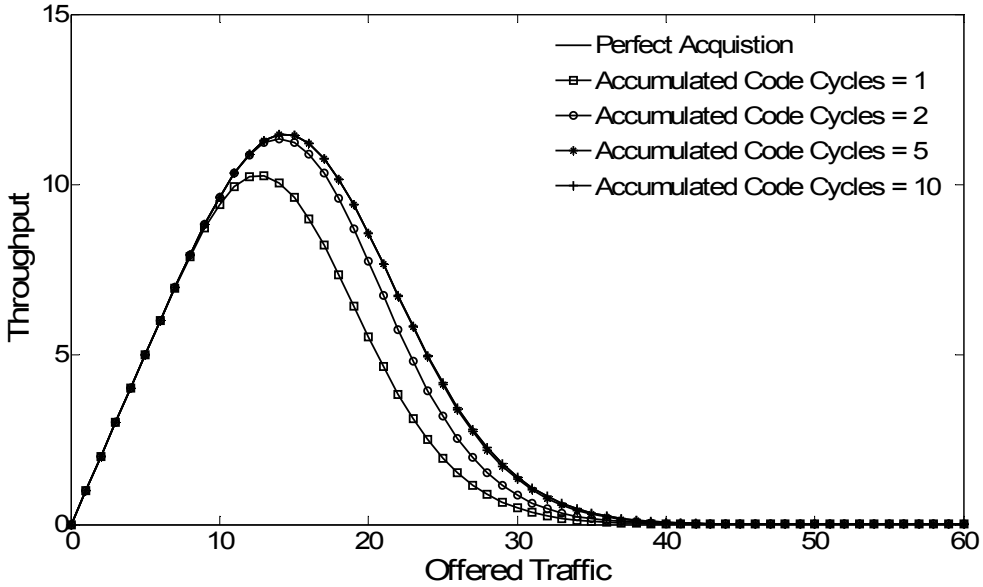

(a)

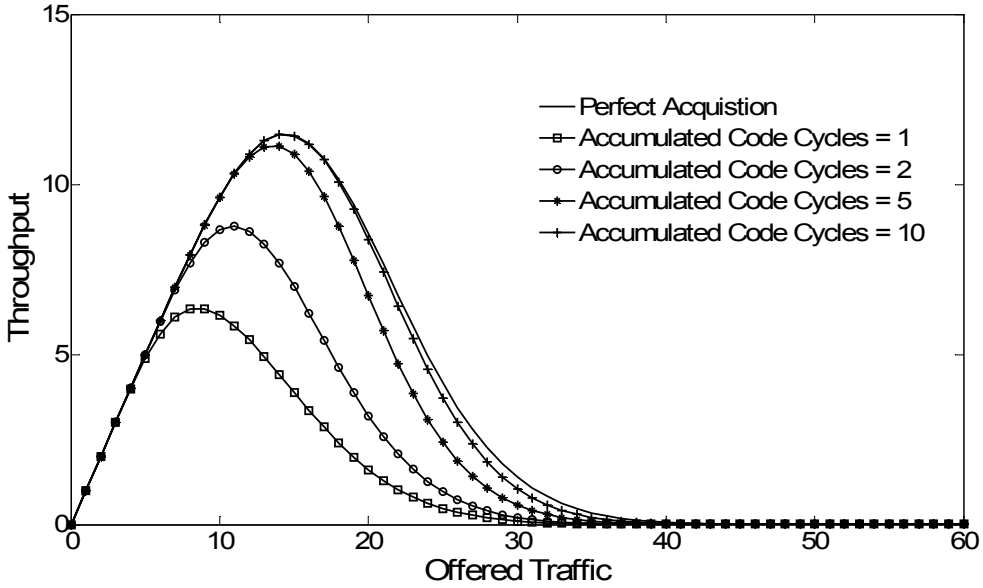

(b)

Figure 5.30 Throughput performance with Infinite-number of users at (a) f_d = 0 kHz and (b) f_d = 10 kHz with t = 0.

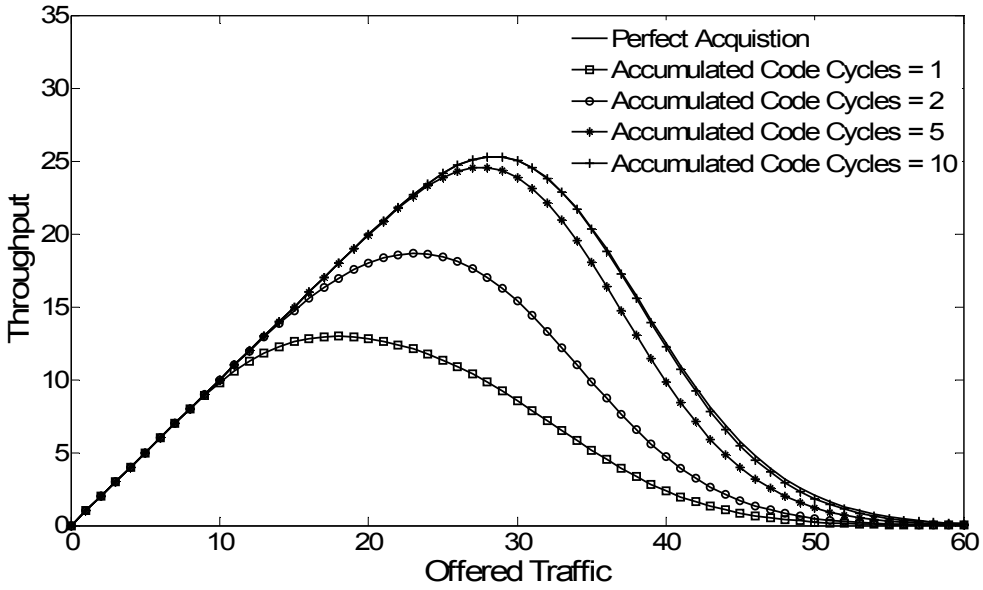

(a)

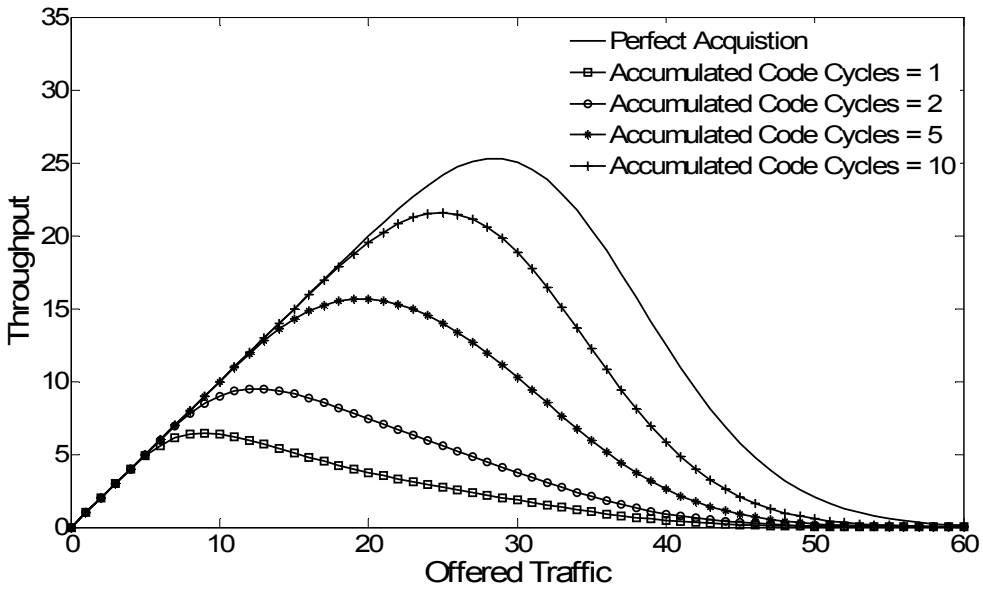

(b)

Figure 5.31 Throughput performance with Infinite-number of users at (a) f_d = 0 kHz and (b) f_d = 10 kHz with t = 10.

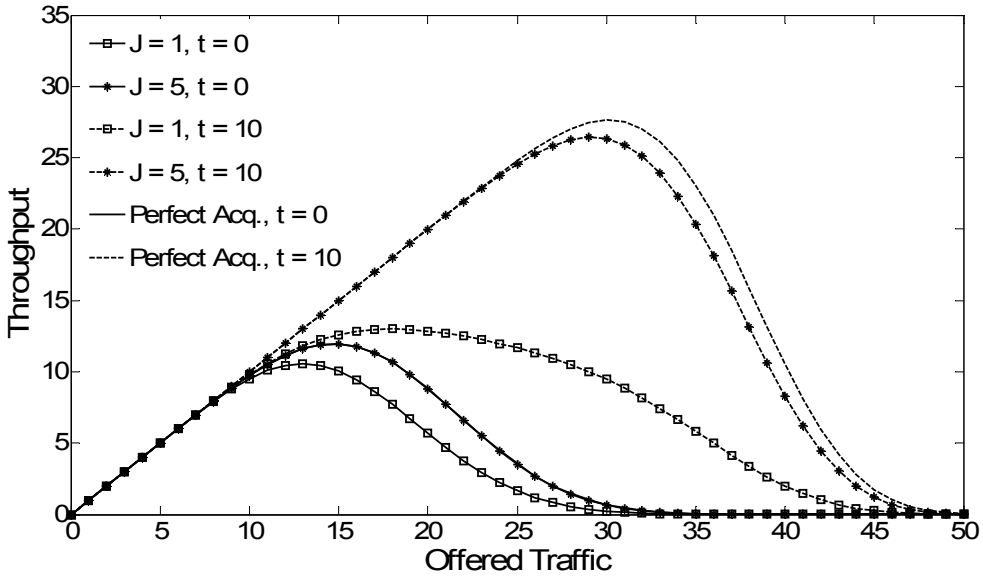

(a)

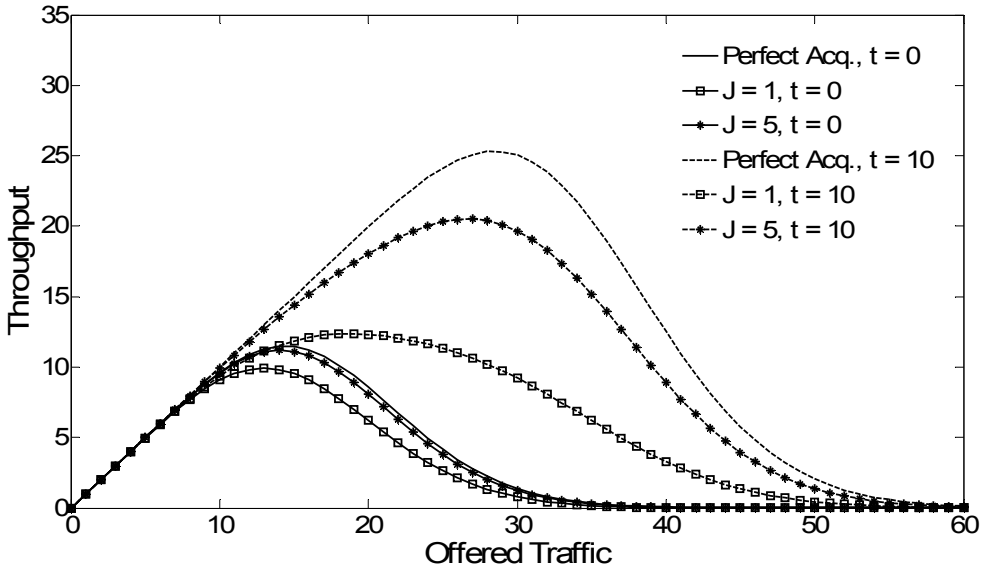

(b)

Figure 5.32 Throughput performance with (a) finite-number (b) Infinite-number of users at $f_d = 0$ kHz with $t = 0$ and $t = 10$.

In Figure 5.28, Figure 5.29, Figure 5.30, Figure 5.31, and Figure 5.32, the throughput performance of packet CDMA with accumulation and maximum likelihood detection are shown. Higher packet throughput is obtained when the number of accumulated code cycles is increased. In addition, higher value of error correction capability increases the packet throughput. When offered traffic is increased beyond the value for which maximum throughput is obtained, the reduction is due to the increased increase packet error rate and decreased probability of correct codephase detection. This is due to the fact that both chip and packet error rate are high and probability of acquisition is low at higher number of offered traffic. Throughput can also increased by increasing the spreading gain, N_c, however, this requires larger transmission bandwidth.

5.10 Chapter Summary

In this chapter two acquisition schemes (i.e. threshold detection and maximum likelihood and accumulation) have been described for application in packet CDMA systems. It has been shown that with the maximum likelihood and accumulation scheme, increased accumulated code cycles results in increased probability of correct codephase detection for a fixed number of co-users. As well, number of accumulated code cycles should be increased in the case of higher values of Doppler frequency and carrier frequency offset. For a packet transmission system, higher probability of detection increases packet throughput performance.

6. Conclusions and Future Research Directions

Packet CDMA has emerged as a strong candidate for third generation (3G) wireless systems. Several 3G wireless systems are based on direct-sequence code-division-multiple-access (DS-CDMA) technology. Leading 3G proposals are cdma2000 (an extension of IS-95B) and wideband CDMA (W-CDMA) [58]. Both depend on packet data communication services between the mobile terminals and the base stations. These systems will support a variety of services, such as voice, data, and fax and, in some services; each user will only send a short data packet occasionally. In this situation, it is most efficient to use discontinuous packet transmission. Application of code-division spread-spectrum concepts permits simultaneous transmission and successful reception of multiple packets.

6.1 Summary of the Results

The objective of the thesis is to examine the performance of SMF for codephase acquisition in the case the packet CDMA without preambles. Both analytical and simulation approaches were followed.

In this thesis, we search for the spreading sequence codephase using a segmented filter matched to the transmitter's spreading code. By segmenting the matched filter, the receiver is able to acquire codephase on signals that have both data modulation and Doppler frequency offset. Acquisition in the presence of data modulation eliminates the necessity of preambles at the beginning of the packet. Thus, packet communication without preamble is possible without significantly degrading the performance of the system.

The probability density functions for both aligned and non-aligned samples were calculated with no data modulation, random data modulation and alternate data modulations at various carrier frequency offsets. Theoretically derived pdfs closely match pdfs derived from the simulations.

The probability of correct codephase detection versus the number of simultaneous co-users at various carrier frequency offsets was shown using both threshold crossing and maximum likelihood and accumulation selection criteria.

In the case of threshold crossing criterion, the probability of correct codephase selection and the probability of false alarm vs. the threshold value were shown at various carrier frequency offsets. Threshold values were varied in order to show the effect of the threshold on the mean acquisition time.

In the case of maximum likelihood selection criterion, the probability of correct codephase selection is improved by accumulating matched filter outputs over several PN code cycles provided that the code Doppler rate is not significant. For a larger number of co-users, the improvement in the probability of correct codephase detection is obtained by increasing the number of accumulated code cycles.

One of the important performance measures of packet CDMA systems is throughput. Acquisition-dependent packet throughput performance has been described. The throughput of packet CDMA systems with the perfect acquisition assumption for both fixed capacity and infinite capacity are illustrated for reference. Increment in the maximum throughput is obtained by increasing the number of accumulated code cycles. As well, the effect of error correction capability on the throughput is also illustrated. At

high carrier frequency shifts, number of accumulated code cycles should be increased to increase packet throughput.

6.2 Future Research Directions

There are several possible research directions to extend the current research work. This work can be applied to an existing 3G CDMA system employing packet communications. Another issue of interest is the effect of the SMF parameters, such as the filter length, number of segments, and number of chips in a segment. Besides, performance at different spreading gains should be analyzed.

In this work, the channel is assumed to be a non-fading one. So, performance of the SMF in a fading channel can be measured. The effect of code Doppler along with carrier frequency offset on packet CDMA acquisition using SMF can also be evaluated. Another issue of interest is the performance of the SMF in acquisition for imperfect power-controlled environment.

Another important research direction might be frequency offset carrier synchronization using SMF. Frequency acquisition is followed by codephase acquisition and tracking in any CDMA system. Some work [59] has been done on this topic. Since, SMF has proven to be robust to carrier frequency offset; it should also be useful in acquiring carrier frequency.

LIST OF REFERENCES

[1] T.S. Rappaport, *Wireless Communications - Principles and Practice*, Prentice-Hall, New Jersey, 1996.

[2] CDMA Development Group, http://www.cdg.org.

[3] C.K.H. Deng, "Energy dissipation in pseudo-noise acquisition for auto-correlation based architectures", Ph.D. thesis, University Of California, Los Angeles, 2000.

[4] B. Persson, D.E. Dodds, and R.J. Bolton, "A segmented matched filter for CDMA code synchronization in systems with Doppler frequency offset," *Proceedings IEEE Globecom*, San Antonio, Texas, Nov 2001.

[5] K. Pahlavan, and P. Krishnamurthy, *Principles of Wireless Networks*, Pearson Education, Singapore, 2004.

[6] M.D. Austin, M.J. Ho, and G.L. Stuber, "Performance of switched-beam smart antenna systems," *IEEE Transactions on Vehicular Technology*, vol. 47, no. 1, pp. 10–19, January 1998.

[7] A. Jamalipour, T. Wada, and T. Yamazato, "A Tutorial on Multiple Access technologies for Beyond 3G Mobile Networks," *IEEE Communication Magazine*, February 2005.

[8] R.L. Peterson, R.E. Ziemer and D.E. Borth, *Introduction to Spread Spectrum Communications*

[9] The Bluetooth Special Interest Group (SIG), http://www.bluetooth.org.

[10] R.E. Ziemer and W.H. Tranter, *Principles of Communications – Systems, Modulation , and Noise*, 5th edition, John Wiley & Sons, Inc., New York, 2002.

[11] D.J. Torrieri, "Performance of Direct-Sequence Systems with Long Pseudorandom Sequences," *IEEE Journal on Selected Areas in Communications*, vol. 10, no. 4, pp. 770-781, May 1992.

[12] A.J. Viterbi, *CDMA Principles of Spread Spectrum Communication,* Addison-Wesley, MA, 1995.

[13] J.G. Proakis, *Digital Communications,* 4th ed., McGraw-Hill, New York, 2001.

[14] B. Yener, “Efficient Access and interference management for CDMA wireless systems,” Ph.D. thesis, Department of Electrical Engineering, Rutgers University, May 2000.

[15] S. Kumar, and S. Nanda, “High data-rate packet communications for cellular network using CDMA: algorithms and performance,’ *IEEE Journal on Selected Areas in Communications,* vol. 17, no. 3, pp. 472-492, March 1999.

[16] S. Haykin, *Communications Systems*, 5th edition, John Wiley & Sons, Inc., New York, 2001.

[17] H. Yin, and H. Liu, “Performance of Space-Division Multiple-Access (SDMA) With Scheduling,” *IEEE Transaction on Wireless Communications*, vol. 1, no. 4, pp. 611-618, October 2002.

[18] E.H. Dinan, and B. Jabbari, “Spreading Codes for Direct Sequence CDMA and Wideband CDMA Cellular Network,” *IEEE Communication Magazine*, September 1998.

[19] M.B. Pursley, "The role of spread spectrum in packet radio networks," *Proceedings of the IEEE* , vol. 75, no.1, pp. 116- 134, January 1987.

[20] M. Katz, “Code Acquisition in Advanced CDMA Networks,” Ph.D. Dissertation, University of Oulu, Finland, 2002.

[21] U. Madhow and M.B. Pursley, “Mathematical modeling and performance analysis for a two-stage acquisition scheme for direct-sequence spread-spectrum CDMA,” *IEEE Transaction on Communications*, vol. 43, no. 9, pp. 2511–2520, September 1995.

[22] M. Srinivasan and D.V. Sarwate, “Simple Schemes for parallel acquisition of spreading sequences in DS/SS systems,” *IEEE transaction on Vehicular technology*, vol. 45, no. 3, pp. 593-598, August 1996.

[23] K. Yu, and I.B. Collings, "Performance of low-complexity code acquisition for direct-sequence spread spectrum systems," *IEE Proceedings on Communications*, vol. 150, no. 6, pp. 453- 460, December 2003.

[24] B. Ai, Z. Yang, C. Pan, J. Ge, Y. Wang, and Z. Lu, "On the synchronization techniques for wireless OFDM systems," *IEEE Transactions on Broadcasting,*, vol. 52, no. 2, pp. 236-244, June 2006.

[25] W. Krzymien, A. Jalali, and P. Mermelstein, "An improved acquisition algorithm for the synchronization of CDMA personal wireless systems," *5th IEEE International Symposium on Wireless Networks - Catching the Mobile Future.*, September 1994.

[26] R.F. Ormondroyd, "PN code synchronisers for direct-sequence spread-spectrum systems - a comparative evaluation," *IEE Colloquium on New Synchronisation Techniques for Radio Systems*, November 1995.

[27] Y. Ikai, M. Katayama, T. Yamazato, and A. Ogawa, "An initial code acquisition scheme for indoor packet DS/SS systems with macro/micro antenna diversity," *IEICE Transaction on Fundamentals,* vol. E83-A, no. 11, November 2000.

[28] Y.T. Su, "Rapid Code Acquisition algorithms employing PN matched filters," *IEEE Transaction on Communications.*, vol. COM-36, no. 6, pp. 724–733, June 1988.

[29] V.M. Jovanovic, "Analysis of strategies for serial-search spread-spectrum code acquisition-direct approach," *IEEE Transaction on Communications*, vol.36, no. 11, pp. 1208-1220, November 1988.

[30] J.H.J. Iinatti, "On the threshold setting principles in code acquisition of DS-SS signals," *IEEE Journal on Selected Areas in Communications*, vol. 18, no. 1, January 2000.

[31] V.M. Jovanovic and E.S. Sousa, "Analysis of non-coherent correlation in DS/BPSK spread spectrum acquisition**,**" *IEEE Transaction on Communications*, vol. 43, No. 2/3/4, pp. 565-573, February/ March/ April, 1995.

[32] W. Zhuang, "Noncoherent hybrid parallel PN code acquisition for CDMA mobile communications," *IEEE Transaction on Vehicular Technology*, vol. 45, no. 4, pp. 643–656, November 1996.

[33] R. Rick and L. Milstein, "Noncoherent parallel acquisition in CDMA spread spectrum systems," in *Proc. ICC'94*, New Orleans, May 1994.

[34] E.A. Sourour and S.C. Gupta, "Direct-sequence spread-spectrum parallel acquisition in a fading mobile channel," *IEEE Transaction on Communications*, vol. 38, pp. 992–998, July 1990.

[35] D. Torrieri, *Principles of Spread-spectrum Communication Systems*, Springer, USA, 2004.

[36] M.K. Omura, J.K. Omura, R.A. scholtz, and B.K. Levitt, *Spread Spectrum Communication*s, Computer science Press, Inc., Rockville, Maryland, 1985.

[37] J.S. Yamamoto and R. Kohno, "Dynamic digital matched-filter acquisition of DS receiver," in *Proc. IEEE Int. Symp. Spread Spectrum Techniques, Applications*, 1996.

[38] U. Cheng, W.J. Hurd, and J.I. Statman, "Spread-Spectrum code acquisition in the presence of Doppler shift and data modulation," *IEEE Transaction on Communications*, vol. 38, no. 2, pp. 241–250, February 1990.

[39] J. Diez, C. Pantaleon, L. Vielva, I. Santamaria, and J. Ibanez, "A simple expression for the optimization of spread-spectrum code acquisition detectors operating in the presence of carrier-frequency offset," *IEEE Transaction on Communications*, vol. 52, no. 4, pp. 550-552, April 2004.

[40] U. Cheng, "Performance of a class of parallel spread-spectrum code acquisition schemes in the presence of data modulation," *IEEE Transaction on Communications*, vol. COM-36, no. 5, pp. 596–604, May 1988.

[41] R. Schmitz, "A segmented matched filter for spread spectrum codephase acquisition," M.Sc. thesis, Department of Electrical Engineering, University of Saskatchewan, SK, Canada. September 1998.

[42] B. Persson, "A mixed signal ASIC for CDMA code synchronization," M.Sc. thesis, Department of Electrical Engineering, University of Saskatchewan, SK, Canada. September 2001.

[43] B. Persson, D.E. Dodds, and R.J. Bolton, "A segmented matched filter for CDMA code synchronization in systems with Doppler frequency offset," *Global Telecommunications Conference, 2001.*

[44] TIA/EIA Interim Standard, *Mobile station-base station compatibility standard for dual-mode wideband spread spectrum cellular system.* Telecommunication Industry Association/ Electronics Industry Association, 1999.

[45] J.G. Proakis, and M. Salehi, *Communication Systems Engineering,* 2nd ed., Prentice-Hall, Upper saddle River, New Jersey, 2002.

[46] T. Kume, T. Yamazato, K. Ban, H. Okada, and M. Katayama, "CDMA packet recognition and signal acquisition using LMS-based adaptive receiver," *Wireless Communications and Networking Conference, 2002.*

[47] A. Papoulis, and S.M. Pillai, *Probability, Random variables and Stochastic Process*, 4th edition, McGraw Hill, New York, 2002.

[48] P.Z. Peebles, *Probability, random variables, and random Signal Principles,* 4th edition, McGraw-Hill, New York, 1997.

[49] H. Stark and J.W. Woods, *Probability, Random Processes, and Estimation Theory for Engineers,* 2nd edition, Prentice Hall, Englewood Cliffs, New Jersey, 1994.

[50] G. Corazza, "On the MAX/TC criterion for code acquisition and its application to in frequency-selective DS-SSMA systems," *IEEE Transaction on Communications*, vol. 12, pp. 1173–1182, September 1996.

[51] B. Persson, D.E. Dodds, J.E. Salt, and R.J. Bolton, "CDMA code synchronization using segmented matched filter with accumulation and best match selection," *MILCOM 2002. Proceedings*, October 2002.

[52] R.K. Morrow, and J.S. Lehnert, "Packet throughput in slotted ALOHA DS/SSMA radio systems with random signature sequences," *IEEE Transaction on Communications*, vol. 40, no. 7, pp.1223-1230, July 1992.

[53] J.S. Lehnert and M.B. Pursley, "Error probabilities for binary direct-sequence spread-spectrum communications with random signature sequences," *IEEE Transaction on Communications*, vol. 35, no. 1, pp. 87–97, October 1987.

[54] Y.K. Jeong, and J.S. Lehnert, "Acquisition of packets with a short preamble for direct-sequence spread-spectrum multiple-access packet communications," *MILCOM 2003.* October 2003.

[55] Y.K. Jeong, "Chip matched-filter receivers and packets acquisition for band-limited direct-sequence spread-spectrum multiple-access communications," Ph.D. Thesis, Purdue University, December 2003.

[56] D. Raychaudhuri, "Performance Analysis of Random Access Packet-Switched Code Division Multiple Access Systems," *IEEE Transaction on Communications*, vol. 29, no. 6, pp. 895- 901, June 1981.

[57] V.P. Ipatov, *Spread-Spectrum and CDMA-Principles and Applications,* John Wiley & Sons Inc., New Jersey, 2005.

[58] Z. Weigang, Y. Tingyan, W. Jinpei, and Z. Qishan, “Large frequency offset carrier synchronization in segmented matched filter DS/BPSK receiver,” *ISCIT 2005*.

A. SMF structure

As mentioned previously, the SMF is 512 chips long and consists of 16 cascaded segments. Each segment contains 32 chips. The signal register has one bit depth and, therefore, it receives only 'hard limited" signal samples. Each segment provides a measure of correlation between the code and the received signal samples. The measurement indicator shows the extent to which the number of matches outnumbers number of mismatches in a segment. This indicator is squared and since the segment size is fixed at 32 chips, then

$$M_X = 32 - M \tag{A.1}$$

and the resulting output characteristics for a segment is

$$\left(M - M_X\right)^2 = 4M^2 - 128M + 1024 = f(M) \tag{A.2}$$

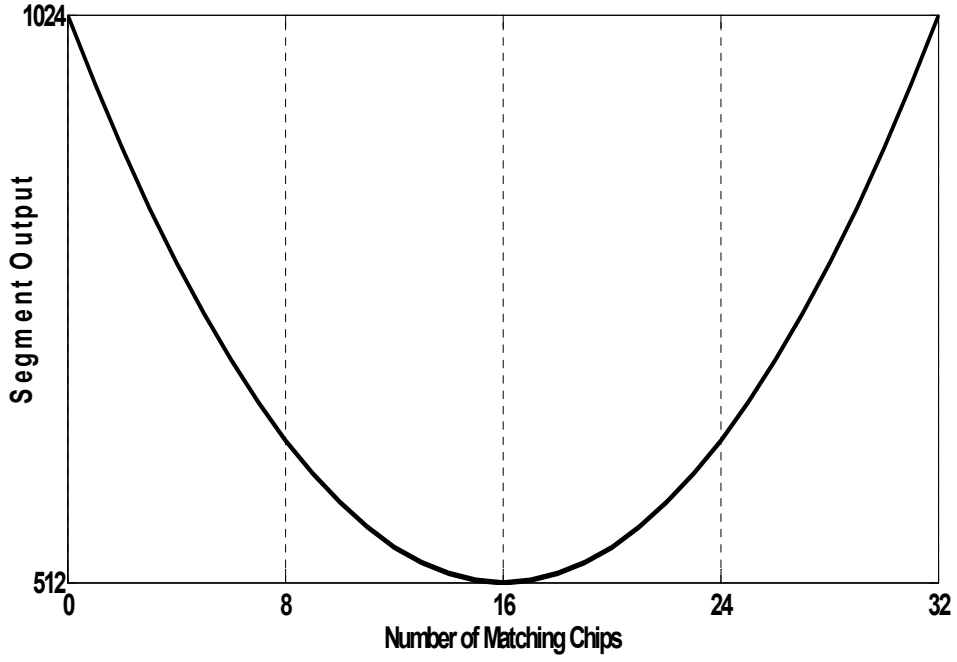

Figure A.1 Segment output vs matching Chips [42]

Figure A.2 shows a block diagram of SMF. This SMF was developed by B. Persson at the TRLabs, Saskatoon, SK. The received signal which is sampled at twice the chip rate is stored in the signal register. Every second sample is connected to perform interleaved processing as explained in Section. A PN reference code is preloaded in the code register before acquisition. The comparison between samples and code chips is performed by an XOR function. Both matches (XNOR) and matches (XOR) are generated. The number of matches and mismatches are then summed and squared separately. The results are then combined with the results from all other segments.

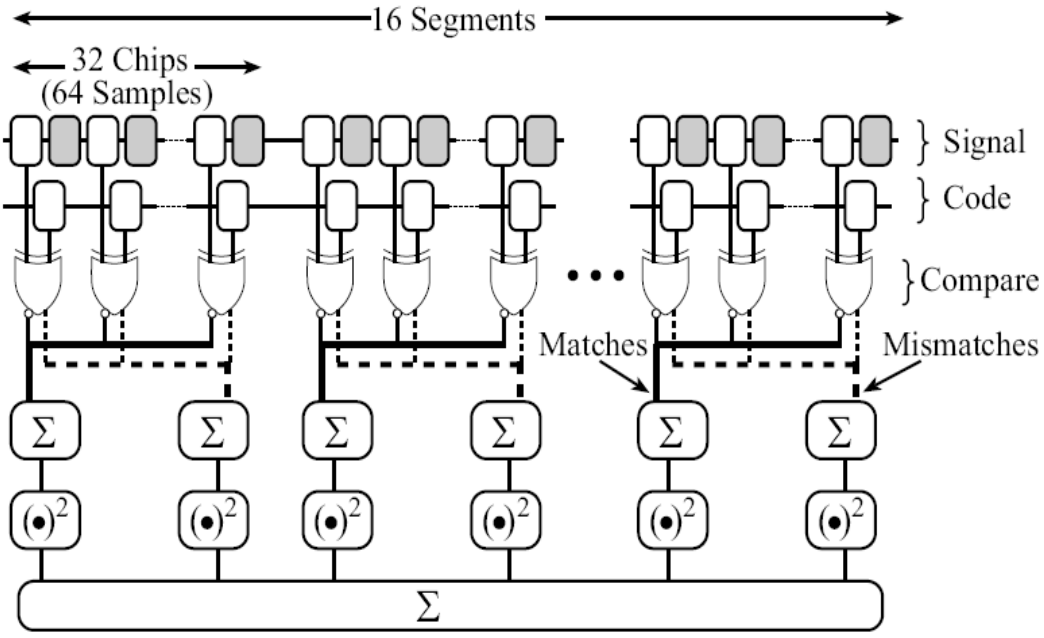

Figure A.2 Block Diagram of SMF. From [42].

B. Probability Density Function for Interfering Signal

Chip sequence is modeled as independent, identically distributed (i.i.d) sequence which has equal probabilities of having -1 and +1 respectively. The probability density function is given by,

$$f_X(x) = \frac{1}{2}\delta(x+1) + \frac{1}{2}\delta(x+1) \tag{B.1}$$

Figure B.1 pdf for discrete random variable X

Mean and variance of the above function are given by [41]

$$\mu_X = \sum_i x_i p_X(x_i) = 0, \tag{B.2}$$

$$\sigma_X^2 = \sum_i x_i^2 p_X(x_i) - \left(\sum_i x_i p_X(x_i) \right)^2 = 1. \tag{B.3}$$

Co-users' interfering signal exist in a CDMA system. It has been assumed that each user transmit signal with equal power P. Interfering signal will be a random variable with mean equals to the sum of the mean of K independent random variables and variance is equivalent to the summation of the variance of the K independent random variables [47]. Here, K is the number of active interfering users. So, the mean and variance for the interfering signal distribution are given by

$$\mu_{\text{interference}} = \sum_{i}^{K} \mu_i = 0, \tag{B.4}$$

$$\sigma^2_{\text{int erefernce}} = \sum_{i}^{K} \sigma_i^2 = K.1 = K. \tag{B.5}$$